ADVANCING ENVIRONMENTAL, SOCIAL, AND GOVERNANCE OUTCOMES THROUGH PROCESS OPTIMISATION AND CONTROL

by

John James Burchell

Submitted in partial fulfillment of the requirements for the degree
Philosophiae Doctor (Electronic Engineering)

in the

Department of Electrical, Electronic and Computer Engineering
Faculty of Engineering, Built Environment and Information Technology

UNIVERSITY OF PRETORIA

February 2024

SUMMARY

ADVANCING ENVIRONMENTAL, SOCIAL, AND GOVERNANCE OUTCOMES THROUGH PROCESS OPTIMISATION AND CONTROL

by

John James Burchell

Promoter:	Prof. J.D. le Roux
Co-promotor:	Prof. I.K. Craig
Department:	Electrical, Electronic and Computer Engineering
University:	University of Pretoria
Degree:	Philosophiae Doctor (Electronic Engineering)
Keywords:	Evolutionary algorithms, input blending, level averaging control, modeling, nonlinear model predictive control, optimisation, process control, refinery, simulation, tailings reprocessing

Organisations are compelled to integrate Environmental, Social, and Governance (ESG) considerations into their core strategy, with the tightening of regulatory requirements and the mounting pressure from stakeholders for sustainable practices driving a trend toward socially responsible investing. Advanced process optimisation and control provides innovative solutions to support ESG objectives. This thesis explores two case studies aimed at enhancing the consistency of material flow and composition into metallurgical operations to improve overall processing efficiency.

The first case study introduces a $(\mu + \lambda)$-Evolutionary Strategy (ES) to solve the input blending problem for a base metal refinery (BMR), where variability in the feed of contaminants to the operation impact negatively on plant throughput, product quality, and harmful emissions. The algorithm outperforms baseline blending strategies demonstrating a significant improvement in the blended consistency of contaminant feed.

In the second case study, a nonlinear Model Predictive Controller (NMPC) is developed and implemented on a surge tank for level averaging control in an industrial tailings reprocessing circuit. A rigorous dynamic model is derived to describe the rate of change of both the volume and density in these surge tanks. By simulation with industrial data it is demonstrated that the significant input disturbances typical to tailings reprocessing circuits drive a gain inversion in the density model of the surge tank. This gain inversion and the multivariable objectives of both density and flow disturbance attenuation motivates for a NMPC solution. Results presented show significant improvements in both the water recovery and the stability of mass flow of tailings in the circuit.

These advanced optimisation and control solutions support ESG objectives across multiple dimensions. Improved input stability with the $(\mu + \lambda)$-ES enhances the efficiency of downstream processes where contaminants are extracted, resulting in lower emissions, especially when hazardous reagents are involved in the extraction process. By improving the efficiency of contaminant extraction the need for rework of product that fail to meet specifications is minimised, which leads to a reduction in waste generation, conservation of resources, and lower energy consumption. Improved water recovery with the NMPC lowers the overall environmental footprint of the tailings reprocessing circuit by reducing water consumption and energy usage, while stability improvements positively impact recoveries, thereby reducing waste and supporting responsible resource management.

OPSOMMING

BEVORDERING VAN OMGEWINGS-, SOSIALE, EN BESTUURSRESULTATE DEUR PROSESOPTIMERING EN PROSESBEHEER

deur

John James Burchell

Promotor:	Prof. J.D. le Roux
Medepromotor:	Prof. I.K. Craig
Departement:	Elektriese, Elektroniese en Rekenaar-Ingenieurswese
Universiteit:	Universiteit van Pretoria
Graad:	Philosophiae Doctor (Elektroniese Ingenieurswese)
Sleutelwoorde:	Evolusionêre algoritmes, invoermenging, modellering, nie-lineêre modelvoorspellende beheer, prosesoptimering, prosesbeheer, raffinadery, simulasie, uitskot herverwerking, vlakgemiddelde beheer

Met die verstramming van regulatoriese vereistes en die toenemende druk van belanghebbers vir volhoubare praktyke wat 'n neiging na sosiaal verantwoordelike belegging aanwakker, word organisasies gedwing om Omgewings-, Sosiale, en Bestuurs- (OSB) oorwegings in hul kernstrategie te integreer. Hierdie proefskrif bied 'n studie oor die toepassing van gevorderde prosesoptimerings- en beheertegnieke om operasionele doeltreffendheid en OSB-doelwitte in industriële verwerkingsbedrywighede te verbeter. Hierdie tesis ondersoek twee gevallestudies wat daarop gemik is om die konsekwentheid van materiaalvloei en samestelling na metallurgiese operasies te verbeter om algehele verwerkingsdoeltreffendheid te verbeter.

Die eerste gevallestudie stel 'n $(\mu + \lambda)$-Evolusionêre Strategie (ES) voor om die invoermengprobleem vir 'n basismetale raffinadery op te los, waar die variasie van besoedelstowwe in die voer die aanlegdeurset, produkgehalte, en vrystelling van skadelike emissies negatief beïnvloed. Die algoritme presteer

beter as basislynmengstrategieë en toon ’n beduidende verbetering in die gemengde konsekwentheid van besoedelstofvoer.

In die tweede gevallestudie is ’n nie-lineêre Model Voorspellende Beheerder (NMVB) ontwikkel en geïmplementeer op ’n stuwingsbak vir vlakgemiddelde beheer in ’n industriële uitskot herverwerkings kring. ’n Volledige dinamiese model word afgelei om die tempo van verandering van beide die volume en digtheid in hierdie stuwingsbak te beskryf. Deur simulasie met industriële data word hier gedemonstreer dat die beduidende insetversteurings tipies aan uitskotherprosessering die versterkingsverhouding in die digtheidsmodel van die stuwingsbak omkeer. Die omkeer van die versterking en die multiveranderlike doelwitte om beide digtheid en vloeiversteuring te verwerp motiveer vir ’n NMVB-oplossing. Resultate wat aangebied word toon beduidende verbeteringe in beide die waterherwinning en die stabiliteit van massa vloei vir die uitskot herverwerking bedrywighede.

Hierdie gevorderde optimering- en beheeroplossings ondersteun ESG-doelwitte oor veelvuldige dimensies. Verbeterde insetstabiliteit met die $(\mu + \lambda)$-ES verhoog die doeltreffendheid van stroomaf prosesse waar besoedelstowwe onttrek word, wat lei tot laer emissies, veral wanneer gevaarlike reagense in die onttrekkingsproses betrokke is. Deur die doeltreffendheid van besoedelstofonttrekking te verbeter, word die behoefte aan herwerk van produkte wat nie aan spesifikasies voldoen nie, geminimaliseer, wat lei tot ’n vermindering in afvalgenerasie, bewaring van hulpbronne en laer energieverbruik. Verbeterde waterherwinning met die NMPC verlaag die algehele omgewingsvoetspoor van die stertverwerkingskring deur waterverbruik en energiegebruik te verminder, terwyl stabiliteitsverbeterings positief op herwinnings inwerk, wat afval verminder en verantwoordelike hulpbronbestuur ondersteun.

ACKNOWLEDGEMENTS

This work is dedicated to my mother, Lucy, whose wholehearted commitment to her family and passion for the arts have deeply influenced us, and to my father, Henry, whose example taught us the value of hard work.

To my love, Zelda, for the many weekends and nights you assumed the role of a single parent, allowing me the space and time to pursue my work. Your patience and support have been invaluable throughout this academic journey.

To my colleagues, Manja Horne and Neale McCulloch, our conversations and your insights were instrumental in shaping the ideas presented in this thesis.

Lastly, my sincere gratitude goes to Prof. Ian Craig and Prof. Derik le Roux for your guidance throughout the development of this thesis. And beyond, you continue to inspire a deeper understanding into process control and optimisation.

LIST OF ABBREVIATIONS

AS/RS	automated storage and retrieval system
BTT	bulk tailings treatment
EA	evolutionary algorithm
ES	evolutionary strategy
GCP	general control problem
IRR	internal rate of return
LP	linear programming
MHE	material handling equipment
MILP	mixed integer linear programming
MIMO	multiple input multiple output
ML	machine learning
MPC	model predictive controller
NLP	nonlinear programming
NMPC	nonlinear model predictive controller
NP	nondeterministic polynomial-time
PGMs	platinum group metals
PI	proportional integral
PID	proportional integral derivative
PSD	particle size distribution
PSO	particle swarm optimisation
RO	robust optimisation
SA	simulated annealing
SO	stochastic optimisation

TABLE OF CONTENTS

LIST OF FIGURES

LIST OF TABLES

CHAPTER 1 INTRODUCTION

1.1 ESG, PROCESS OPTIMISATION AND CONTROL

Environmental, Social, and Governance (ESG) criteria represent a broad set of operating standards, increasingly influencing socially conscious investment (Murad, 2017) and have thus become integral to corporate strategic planning. Factors driving an increase in ESG influence include growing concerns about climate change and the introduction of stricter regulations globally to address environmental and social challenges.

Process optimisation and control refer to the application of algorithms and technologies to enhance the efficiency of industrial processes, and advance all components of ESG. For instance, effective process optimisation and control ensures efficient use of resources, and sustainably reduces waste and emissions. Adherence to increasingly stringent regulatory standards is unattainable without enhanced optimisation and control.

This thesis presents two applications of optimisation and control, to enhance the consistency of material flow and composition into processing operations, and considers their impact on ESG objectives. In the first application, an evolutionary algorithm is developed to optimise the input blend into a base metals refinery. In the second application, a nonlinear model predictive controller is developed to improve the feed stability of a tailings reprocessing circuit. The following subsections present a background on base metal refining and tailings reprocessing, with a focus on these processing operations' ESG considerations.

1.1.1 Base metal refining

Base metal refineries are critical processing operations dedicated to the production of base metals such as copper, nickel, zinc, lead, tin, or aluminum. These refineries operate in the latter stages of the metals

processing value chain, succeeding initial mining and tailings reprocessing, mineral concentration, and smelting activities (Rosenqvist, 2004).

A base metal refinery (BMR) typically processes a converter matte received from smelting operations. During processing metals are extracted and refined by removing impurities. The choice among pyrometallurgy, hydrometallurgy, or electrometallurgy as refining techniques is determined by the specific metals and impurities involved in the process.

Compared to tailings reprocessing, the literature on the ESG and sustainability considerations for base metal refining is lacking. This is to be expected, as these refinery operations can be considered a more traditional and established part of the metals processing value chain. Unlike tailings reprocessing, they are not directly enabling key ESG themes like waste management and the concept of the circular economy. However, as with tailings management, there are general advances in ESG objectives to be obtained by improving the efficiency with which a base metals refinery is operated. These are discussed in Section 1.1.3.

1.1.2 Tailings reprocessing

Waste material from mining operations are referred to as mine tailings. The most common method for tailings storage, is behind dammed impoundments commonly referred to as *tailings ponds* or *tailings dams* (Kossoff et al., 2014). The materials used in the construction of tailings dams are often waste rock and the tailings itself. To accommodate more tailings as mining operations continue, the retaining embankment of a tailings dam is raised at an angle for structural support, resulting in the dam taking on a trapezoidal shape.

Tailings consists of a fine particle slurry, which when deposited in a tailings dam settles to the bottom and with the water recycled back to operations. To accommodate more waste the height of the dam is increased by extending the crest of the embankment over time (Martin and McRoberts, 1999).

The reprocessing of mine tailings supports ESG objectives in a number of ways. It introduces a necessary loop that enables circular economic models in mining, to reduce primary resource consumption - a key objective for sustainable development (Blomsma and Brennan, 2017; Lèbre et al., 2017; Zeng et al., 2021). Tailings reprocessing, having already been subject to primary processing, significantly

reduced the need for mining, crushing and milling, thus reducing energy costs, water consumption, and CO_2 emissions (Curry et al., 2014; Hann, 2022; Marín et al., 2022).

Beside supporting ESG objectives, mine tailings dams are also processed to recover discarded or unexploited minerals. The presence of economic value in tailing deposits stems from the superior grade of historical original ores and inefficiencies in previous processing methodologies. Given diminishing ore grades and the increase in metal prices due to sustained demand, tailings deposits are increasingly being economically exploited through reprocessing (Alcalde et al., 2018; Falagán et al., 2017; Hann, 2022).

The reprocessing of tailings is also undertaken to mitigate safety and environmental risks. In light of recent catastrophic structural failures of tailings dams (Roche et al., 2017; Santamarina et al., 2019), mining operations are under increased pressure to reprocess dams at risk. The storage of tailings often results in long term harmful interactions with the environment, such as the outflow of acidic water from sulphide containing tailings deposits referred to as acid mine drainage (McCarthy, 2014; Park et al., 2019; Wang et al., 2014). Reprocessing of tailings, to produce for example construction materials, is an acid mine drainage management strategy that is gaining attention (Park et al., 2019; Xu et al., 2019).

1.1.3 The impact of process efficiency on ESG objectives

Process efficiency refers to the effectiveness with which a process delivers its specified objectives. Key ESG objectives benefiting from improved process efficiency include:

- **Environmental Stewardship:** Reducing water and energy use, or the decrease in greenhouse gas or pollutant emissions, supports sustainability goals by minimising the overall environmental footprint of operations.
- **Resource Efficiency:** Enhancing the metal recovery efficiency reduces the dependence on primary resource extraction, which contributes to the preservation of natural resources and reduces the ecological footprint of mining activities.
- **Social Impact and Community Engagement:** The improved efficiency of a processing operation can have significant social implications, such as the mitigation of harmful emissions that affect the health and safety of workers and local communities.

- **Governance and Compliance:** Improved efficiency is critical for complying with increasingly stringent environmental and social regulations.

Process optimisation and control are technologies used primarily to enhance process efficiency. Innovative use of these technologies contributes to sustainable development and strengthens an organisation's reputation, assisting in securing its long-term position in a market that is increasingly valuing responsible environmental and social practices.

1.2 PROBLEM STATEMENT

With the tightening of regulatory requirements and the mounting pressure from stakeholders for sustainable practices driving a trend toward socially responsible investing, organisations are compelled to integrate ESG considerations into their core strategy. Advanced process optimisation and control provides a pivotal solution to meet these challenges. The application of these technologies has demonstrated benefits for operational efficiency, and can be specifically applied to reduce resource consumption, harmful emissions, and other factors to minimise an organisation's environmental footprint. Innovation with a focus on ESG objectives, and not solely for improved profitability, is crucial for building stakeholder trust, as it demonstrates a commitment towards sustainable, ethical, and responsible business practices. Robust process optimisation and control serve as key enablers for businesses to effectively address the growing demands of ESG imperatives.

1.3 RESEARCH OBJECTIVES AND HYPOTHESES

The primary objective of this thesis is to demonstrate the potential for process optimisation and control to improve ESG objectives at processing operations. Two industrial operations are investigated, a base metal refinery in a platinum group metals value chain and a tailings reprocessing circuit for chrome recovery. For both operations feed instabilities negatively impact ESG objectives, including environmental stewardship, resource efficiency, and social impact.

The variance in mass flow of impurities into the base metal refinery contributes to inefficiencies in contaminant extraction through the operation. These inefficiencies negatively impact product quality, energy consumption when product rework is required, and harmful emissions from the refinery with sulfur dioxide, an air pollutant, used as the reagent for contaminant extraction. The hypothesis is that an optimisation algorithm can significantly improve the blending of impurities into the refinery. An improved blend leads to a more consistent contaminant feed into downstream circuits tasked with contaminant extraction, which improves the efficiency of these circuits.

A significant variance in observed massflow into a tailings reprocessing circuit, which relies on hydromining for slurrying and transport, contributes to inefficiencies throughout the reprocessing circuit. These inefficiencies include lower separation and classification effectiveness from equipment like hydrocyclones and thickeners, which negatively impact water and product recovery, as well as energy consumption due to an increased recirculating load of solids back to the tailings dam via the process water supplied for hydromining activities. The hypothesis is that significant instabilities into the reprocessing circuit drives a gain inversion, where the relationship between the tailings feed rate and downstream density undergoes a change in sign. This gain inversion necessitates a non-linear control strategy to stabilise the massflow into the circuit and improve separation and classification efficiencies throughout.

1.4 RESEARCH CONTRIBUTION

This thesis investigates two process optimisation and control problems in processing operations not studied before. The first considers the optimisation of the input blend to a base metal refinery (BMR) that processes a converter matte. This blending problem represents a discrete scheduling task not solvable with traditional linear programming approaches. This study proposes the use of a $(\mu + \lambda)$-evolutionary algorithm (EA) to solve this and other similar discrete blending problems found in processing operations. The application of EA in this context requires novel considerations that define the evolutionary operators used and developed here. The application of EA as a solution to discrete blending problems in processing is novel, as are the considerations that define the strategy and the operators developed here.

The second problem considers the control of surge tanks in a hydromining based tailings reprocessing circuit. The literature on surge tank control mainly considers only flow disturbance rejection and where mass flow stability is considered, constant density is assumed. It is demonstrated that the input density disturbances common to these tailings reprocessing circuits are significant enough to drive a model gain inversion. In this thesis, a non-linear model predictive controller (NMPC) is developed to improve surge tank control for hydromining circuits. The rigorous dynamic modelling and closed-loop simulations, used to demonstrate model gain inversion and for controller design, and the industrial implementation of the proposed NMPC solution are all novel contributions.

1.5 RESEARCH OUTPUTS

A top-down control structure for the base metal refinery presented in Section 2.2 was developed to investigate its optimal steady state operation in:

- Burchell, J. J., le Roux, J. D. and Craig, I. K.(2017). Plant-wide control of a base metal refinery: Top-down analysis, *IFAC-PapersOnLine*, **50**(2): 59–64.

A heuristic optimisation approach for solving the BMR input blending problem described in Section 4.2, together with simulated results, is presented in:

- Burchell, J. J., le Roux, J. D. and Craig, I. K.(2018). Optimised blending of a base metal refinery feed using evolutionary programming, *IFAC-PapersOnLine*, **51**(21): 268–272.

The rigorous dynamic model for the tailings reprocessing surge tank developed in Section 4.3 was used as a case study to demonstrate how an access economy platform with competing controllers may offer superior process control over the established single vendor-controller approaches:

- Rokebrand, L. L., Burchell, J. J., Olivier, L. E. and Craig, I. K.(2020). Competing advanced process control via an industrial automation cloud platform. ArXiv, arXiv:2011.13184.

- Rokebrand, L. L., Burchell, J. J., Olivier, L. E. and Craig, I. K.(2021). Towards an Access Economy Model for Industrial Process Control: A Bulk Tailings Treatment Plant Case Study, *IFAC-PapersOnLine*, **54**(21): 121–126.

The derivation of a rigorous dynamic model for surge tanks in water-intensive tailings reprocessing operations, and the implementation of a NMPC on an industrial circuit was published in:

- Burchell, J. J., le Roux, J. D., and Craig, I. K.(2023). Nonlinear model predictive control for improved water recovery and throughput stability for tailings reprocessing, *Control Engineering Practice*, **131**: 105–185.

1.6 OVERVIEW OF THE STUDY

This thesis follows the general control problem (GCP) framework for developing model-based controllers (Craig, 1997; Craig and Henning, 2000) outlined in Figure 1.1. Chapter 2 investigates the two processing operations and identifies the optimisation and control objectives addressed in this thesis. Chapter 3 presents a review of literature related to the identified objectives. The optimisation and control problems are formulated in Chapter 4, with algorithm and controller design presented in Chapter 5. Chapter 6 presents details on the implementation and results obtained.

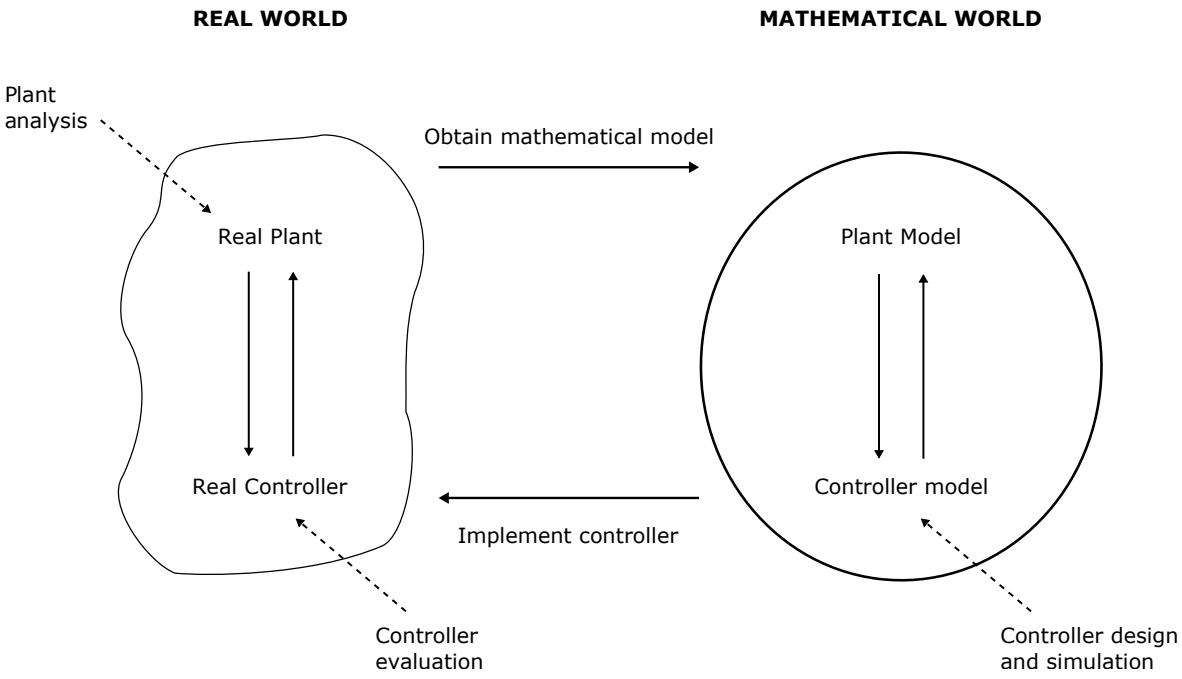

Figure 1.1. The general control framework for developing advanced control systems, taken with permission from Craig and Henning (2000).

The thesis presents two case studies focused on optimisation and control. Figure 1.2 presents an overview of the thesis layout, providing coloured references to guide the reader along the individual case study tracks. The first track (■) details the development and implementation of an optimisation algorithm to solve the input blending problem for the BMR. The second track (♦) explores the development of an advanced control solution to improve surge control in chrome tailings reprocessing circuits.

CHAPTER 1
INTRODUCTION

CHAPTER 2
PROCESS OVERVIEW

■ Section 2.2
Base Metal Refinery

♦ Section 2.3
Chrome tailings reprocessing

CHAPTER 3
LITERATURE REVIEW

■ Section 3.2
Input blending to processing operations

♦ Section 3.3
Surge tank control for processing operations

CHAPTER 4
MODEL DEVELOPMENT AND PROBLEM FORMULATION

■ Section 4.2
BMR input blending problem formulation

♦ Section 4.3
Surge tank dynamic modeling

CHAPTER 5
ALGORITHM AND CONTROLLER DESIGN

■ Section 5.2
Evolutionary algorithm (EA) for BMR input blending

♦ Section 5.3
Nonlinear model predictive (NMPC) control for level averaging control

CHAPTER 6
IMPLEMENTATION

■ Section 6.2
BMR input blending using a (μ + λ)-EA

♦ Section 6.3
Level averaging control using NMPC

Figure 1.2. Layout of the thesis demonstrating the two case study tracks. BMR input blending optimisation track (■) and surge control in chrome tailings reprocessing track (♦).

CHAPTER 2 PROCESS OVERVIEW

2.1 INTRODUCTION

Sibanye-Stillwater is one of the largest primary platinum producers in the world. Its platinum group metals (PGMs) operations in South Africa is situated in the North West province near the towns of Rustenburg and Marikana. It is one of few PGM producers in South Africa with a complete mine to market value chain, which include ore extraction, processing and concentration, smelting and refining. This chapter offers an overview of two processing operations within this value chain, which are central to this thesis: the base metal refinery and a specific chrome tailings reprocessing circuit. An overview is provided of the main processing activities in these operations to provide context, and motivate the specific optimisation and control objectives addressed in the chapters that follow.

2.2 BASE METAL REFINERY

The BMR produces a PGM concentrate, copper cathodes, and nickel sulphate crystals. It treats a converter matte that contains approximately 30 % Cu, 50 % Ni, and less than 1 % PGMs (Eksteen et al., 2011). The matte also contain small amounts of iron (Fe), selenium (Se), tellurium (Te), and silica (SiO_2). The base metals and other impurities are extracted in a series of solid-liquid separation steps, with the PGMs ideally remaining in a solid phase, moving along the primary product stream through the plant. After base metal extraction and impurities are removed from the matte, a PGM concentrate is produced in excess of 70 % grade. An overview of its main processing activities is presented in Figure 2.1.

The matte is processed in a milling circuit to increase surface area, which improves leach efficiencies throughout the plant. Converter matte is received at approximately 2mm in diameter and the target particle size for the milling circuit's product is 80 % passing 75 µm.

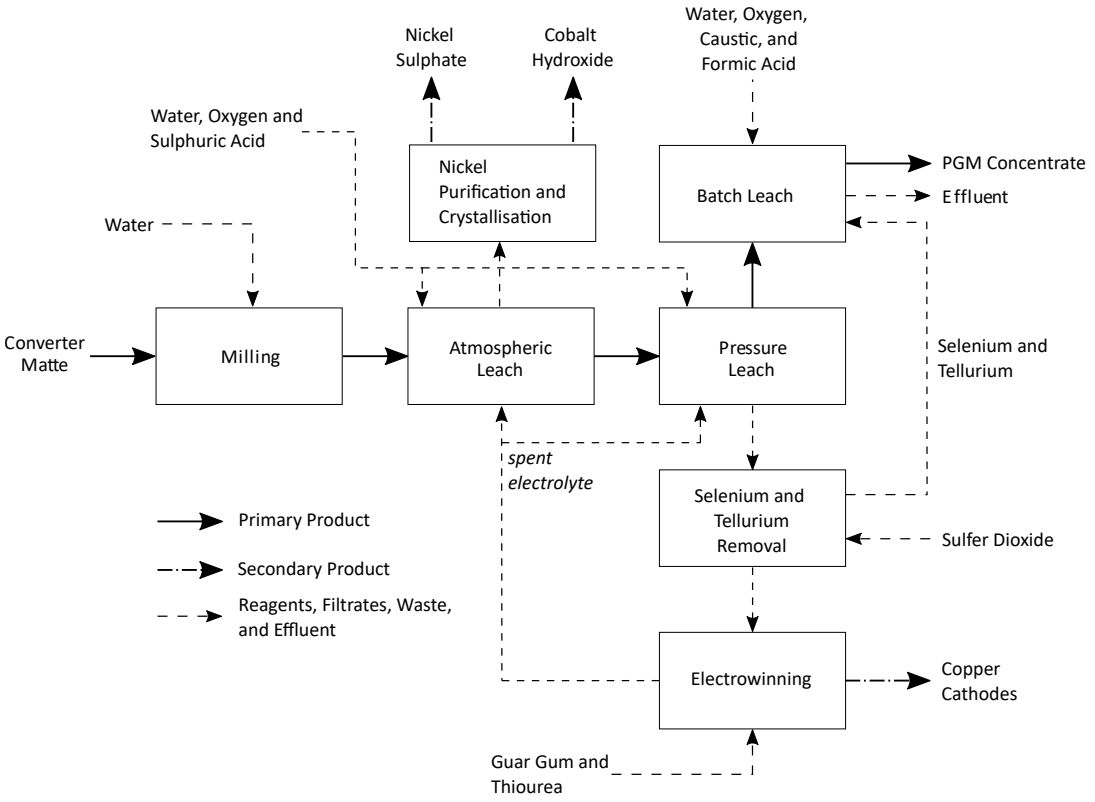

Figure 2.1. An overview of Sibanye-Stillwater's base metal refinery.

The continuous leach circuit comprises an atmospheric leach and a pressure leach. In the atmospheric leach the nickel is dissolved and separated from the primary solid stream, which contains the PGMs, through a filtration process. Similarly, the pressure leach circuit extracts copper from the primary solid stream by dissolving it and then removing it through filtration. This continuous leach circuit employs the established processing route for nickel matte containing high concentrations of copper and PGMs that relies on copper sulphate media (spent electrolyte) and oxygen as the oxidising agent, and where the emphasis is on PGM recovery (Dorfling, 2012; Muir and Ho, 2006).

Downstream from the BMR, the capacity and processing costs require that the PGM concentrate contains less than a specified amount of copper and nickel. Consequently, the efficiency of the continuous leach circuit must provide for sufficient base metal extraction. Since the atmospheric leach capacity exceeds that of the pressure leach, under normal conditions, the pressure leach determines the throughput capacity of the plant.

The nickel purification and crystallisation circuit purifies the filtrate received from the atmospheric leach, producing a battery grade nickel sulphate with cobalt hydroxide as a byproduct. This circuit also crystallises the nickel sulfate for bagging and transportation.

The electrowinning circuit processes the filtrate from the pressure leach to extract copper from the plant via a cathode product. The spent electrolyte from this circuit is used as a leach reagent in both the atmospheric and pressure leaches. Prior to electrowinning, sulfur dioxide is used as a reagent to precipitate selenium and tellurium so that it can be removed from the circuit through filtration.

After passing through the continuous leach section the volume of the primary product is significantly reduced allowing for batch treatment. A series of batch leaches follows to further purify the PGM concentrate by extracting more selenium, tellurium, iron, and nickel, as well as other impurities.

2.2.1 Base metal refinery revenue

The filtration circuit, through which the pressure leach discharges, represents the interface between the continuous and batch leach sections of the plant. This filtration circuit has sufficient capacity to allow for uninterrupted batch accumulation. As such the batch leach section has no influence on the throughput of the continuous section. Furthermore, any PGMs lost to the batch leach section's effluent stream occurs independently from operations in the continuous leach section. The two portions of the plant are, from a control perspective, essentially independent.

At steady state the mass balance of the continuous section of the plant is given by

$$m_{\text{in}} + m_{\text{reagents}} + m_{\text{w}} = m_{\text{out}} + m_{\text{Cu}} + m_{\text{NiSO}_4} + m_{\text{Fe}} + m_{\text{Co(OH)}_2}. \tag{2.1}$$

The mass flow of the inputs, the converter matte, reagents, and water, are represented by m_{in}, m_{reagents}, and m_{w} respectively. Here the reagents include oxygen, sulphuric acid, guar gum, and thiourea. The mass flow of the outputs, comprises the concentrate to the batch leach section, the copper and nickel sulfate secondary products, and the iron and cobalt hydroxide waste streams, represented by m_{out}, m_{Cu}, m_{NiSO_4}, m_{Fe}, and $m_{\text{Co(OH)}_2}$ respectively.

By introducing a coefficient ω_{x} that represents the mass fraction of PGMs in each of these streams the PGM balance is given by

$$\omega_{\text{in}} m_{\text{in}} = \omega_{\text{out}} m_{\text{out}} + \omega_{\text{Cu}} m_{\text{Cu}} + \omega_{\text{NiSO}_4} m_{\text{NiSO}_4} + \omega_{\text{Fe}} m_{\text{Fe}} + \omega_{\text{Co(OH)}_2} m_{\text{Co(OH)}_2}. \tag{2.2}$$

Note that the nickel and copper terms, $\omega_{Cu}m_{Cu}$ and $\omega_{NiSO_4}m_{NiSO_4}$ respectively, represent PGM losses with the nickel sulphate and copper streams.

The BMR's revenue is the difference between sales and operating costs

$$\text{Revenue} = \text{Sales} - \text{Costs}. \tag{2.3}$$

Where Sales are determined by the mass flow of the primary and secondary products, and their market prices:

$$\text{Sales} = \alpha\omega_{out}m_{out}P_{\$PGM} + m_{Cu}P_{\$Cu} + m_{NiSO_4}P_{\$NiSO_4}. \tag{2.4}$$

The recovery of the batch leach section is accounted for by α, taken as a constant value that can be derived from historical performance, $P_{\$PGM}$ represents the basket price for the PGM product, which takes into account the market price for the individual platinum group elements, transportation, and downstream processing costs. The price received for the copper product is represented by $P_{\$Cu}$, which depends on the achieved copper grade and market price. Similarly, $P_{\$NiSO_4}$ represents the price received for the nickel sulphate product, again, dependent on achieved grade and market price.

Costs are divided into fixed and variable components. Fixed costs include, for example, labour, insurance, and a component of the utility costs. Variable costs include the costs that vary with the production rate, which include the costs of reagents, logistics, packaging, consumables like filter clothes, and a variable component of the utility costs. Costs can therefore be expressed as a function of the production rate, represented by m_{in}, as follows:

$$\text{Costs} = f_{costs}(m_{in}). \tag{2.5}$$

This relationship can be fitted to historical data.

Using (2.2) to (2.5) the BMR revenue can be expressed as

$$\begin{aligned}\text{Revenue} =& \alpha P_{\$PGM}(\omega_{in}m_{in} - \omega_{Cu}m_{Cu} - \omega_{NiSO_4}m_{NiSO_4} - \omega_{Fe}m_{Fe} - \omega_{Co(OH)_2}m_{Co(OH)_2}) \\ &+ m_{Cu}P_{\$Cu} + m_{NiSO_4}P_{\$NiSO_4} - f_{costs}(m_{in}).\end{aligned} \tag{2.6}$$

2.2.2 Blending challenges

The converter matte from the smelter is received in individual blows. Each blow comprises a number of bags that are identical in their mineralogical composition but vary in weight. A stockpile of blows are accumulated at the input of the plant, which allows for a matte stock buffer to blend and to absorb disruptions in the supply of matte from the smelter. When the BMR is not in operation, for example

during an extended maintenance shut, it is possible for a large matte stockpile to accumulate. The BMR implements a matte blending plan that considers the mass and composition of each bag in the matte stockpile and determines the sequence in which the individual matte bags are loaded into the mill hopper.

The optimal sequence, or blending plan, minimises sudden changes in the mass flow of impurities into the operation. The BMR input blend strategy specifically aims to minimise variations in the mass flow of silica, iron, selenium, and tellurium into the plant. These impurities contaminate downstream products and as such require control actions to minimise their impact.

Inefficiencies in the atmospheric leach circuit can lead to instances of excessive iron sludge precipitation (Coetzee, 2016), which negatively impacts the filtration operations that separate the nickel containing filtrate from the primary PGM containing solid stream. Under these abnormal conditions of high iron sludge formation, the plant feed rate must be reduced to allow for the removal of sludge from the filtration circuit. The rate of sludge formation is primarily influenced by the pH in the atmospheric leach circuit and mass flow of iron into the BMR. Moreover, the iron concentration in the input feed to the BMR is related to differences in the nickel mineralogy of the converter matte (Thyse et al., 2011). The BMR has historically experienced lower nickel leach efficiencies when processing converter matte with low iron concentrations. Consequently, blending of the iron feed helps with filtration operations in the atmospheric leach, and to ensure that the nickel concentration in the final concentrate is within specification.

Silica is not extracted from the primary product stream and operations downstream from the BMR has limited capacity to deal with large amount of silica. The BMR also potentially introduce silica through housekeeping operations. Blending of the silica feed helps to ensure that the silica concentration in the final concentrate is within specification.

The plant's revenue is directly impacted by the grade of its copper, which is determined by the concentrations of impurities like selenium and tellurium. Retention time in the selenium and tellurium removal circuit is increased, by lowering the feed rate to the circuit, to promote the extraction of these impurities. Operations can only increase the retention time in this circuit for short periods of time, since at steady-state the circuit's feed rate must align to the matte feed rate. Blending the selenium and tellurium in the matte assists with dampening sudden changes in the concentration of these impurities,

which assists with establishing a more consistent retention time in the removal circuit. Moreover, the measurements of the selenium and tellurium concentrations in the input to this circuit relies on sample and analysis with a turnaround time that can exceed multiple shifts. Therefore, blending also reduces the risk that a sudden increase in impurity concentration is not identified in time to make and adjustment to reagent addition rates, thus improving the efficiency of impurity extraction.

2.2.3 ESG considerations

The composition specifications for the PGM concentrate produced by the BMR stipulate that nickel and silica levels must remain below certain thresholds. Exceeding these thresholds necessitates the reworking of concentrate batches. As with first pass efficiency challenges, rework inevitably results in product losses to waste and secondary product streams. This negatively impacts the overall PGM recovery by the organisation, reducing the value derived from each ton of ore processed.

Furthermore, the reworking of product batches imposes extra costs on the BMR, notably additional water, energy, and reagent consumption. By improving the blending of silica and iron, which enhances nickel leach efficiencies, the likelihood of needing to rework PGM concentrate is reduced. This reduces the overall environmental footprint of the operations.

The reagent used in the extraction of selenium and tellurium is sulfur dioxide, which is an air pollutant harmful to the employees and surrounding communities. Inefficient reagent addition not only results in insufficient impurity extraction, but may lead to excessive reagent dosing and additional emissions from the operations. Enhanced blending of selenium and tellurium improves overall efficiency of sulfur dioxide usage, lowering the risk of exposure, and reducing the social impact of the operations.

2.3 CHROME TAILINGS REPROCESSING

Figure 2.2 presents an overview of the industrial circuit used to recover chrome from a tailings dam. A bulk tailings treatment (BTT) plant dewaters and stabilises the tailings before it is fed to a chrome concentrator plant. This concentrator plant produces chrome using spiral separators to sort the tailings into different chrome grades and a waste product.

The commercial considerations for a tailings reprocessing project include:

- The total amount of chrome in the dam, which is estimated from a geological survey.

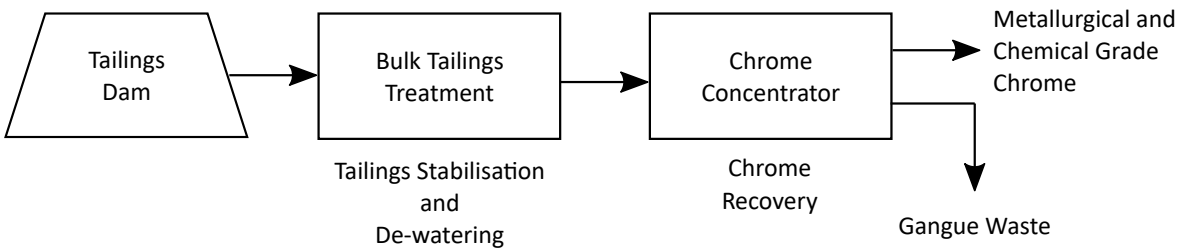

Figure 2.2. Chrome recovery circuit.

- Characteristics of the tailings, such as its particle size distribution (PSD), also estimated by a geological survey.
- The expected chrome recovery or yield from the circuit, influenced by tailings characteristics such as the PSD, which would affect the efficiency of hydrocyclones and spiral separators.
- The throughput from the circuit, which would largely be influenced by design considerations such as the sizing of pumps, spirals, thickeners, etc.
- The chrome price.
- The circuit operating costs.

Of the listed factors influencing the internal rate of return (IRR), a measure of the profitability and efficiency of investment, for the tailings reprocessing project, recovery is affected the most by improving the efficiency of operation for the circuit. The total amount of chrome in the dam, the tailings characteristics, and chrome price can not be influenced, while operating cost and throughput are largely influenced by circuit design. The key performance indicator for the chrome retreatment circuit is therefore its recovery. During the lifetime of the project, operations are under pressure to achieve the expected recovery used to establish the business case for the project. Any improvements on this recovery is celebrated as a realisation of the upside potential for the project.

Ultimately, the recovery of the circuit depends on the spiral efficiencies of the chrome concentrator. The process variables influencing spiral efficiency include feed density and flow rate (Russell, 2020; Umadevi et al., 2021). The key control objective for the circuit must therefore be to supply the chrome concentrator with consistent feed as highly variable feed characteristics would negatively effect the efficiency of the spiral separators.

Figure 2.3 presents an overview of the typical tailings dam operations using hydromining for tailings recovery and transport. High pressure water is pumped from the BTT plant and used to erode the dam into a tailings slurry. The tailings runs through naturally formed channels into a sump. This sump contains a floating barge and a vertical pump.

Two operators oversee key re-mining operations at the tailings dam. The first operator manages the positioning of a high pressure hose that targets the tailings dam face, and tries to cut the face at a steady rate in a first attempt to produce a consistent tailings density. The second operator manages sump operations, agitating the sump with high pressure water to avoid excessive settling of solids in an attempt to improve the consistency of the tailings density to the BTT plant. The density of the tailings to the BTT plant is monitored by the BTT control room. Requests for density adjustment are communicated via hand radio to the tailings dam operators.

From an automatic control perspective, operations at the tailings dam are largely unregulated, lacking automated systems to control and maintain a stable feed to the BTT operations. The only feedback in the system relies on radio communication between the operations and are largely triggered to correct severe density challenges, i.e. the density and flow control to the BTT plant is effectively open-loop.

2.3.1 Tailings stabilisation and dewatering

The flowsheet for the BTT plant is presented in Figure 2.4. It uses a large vibrating screen to remove vegitation debris that unavoidably makes its way into the tailings feed. A surge tank is used to reduce both the variability of tailings density and flow. The hydrocyclone, thickener, and holding tank provides for dewatering and to further improve the stability of feed to the downstream chrome concentrator.

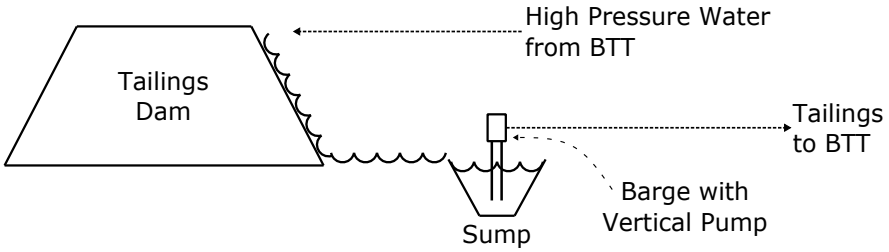

Figure 2.3. Overview of the tailings dam operations.

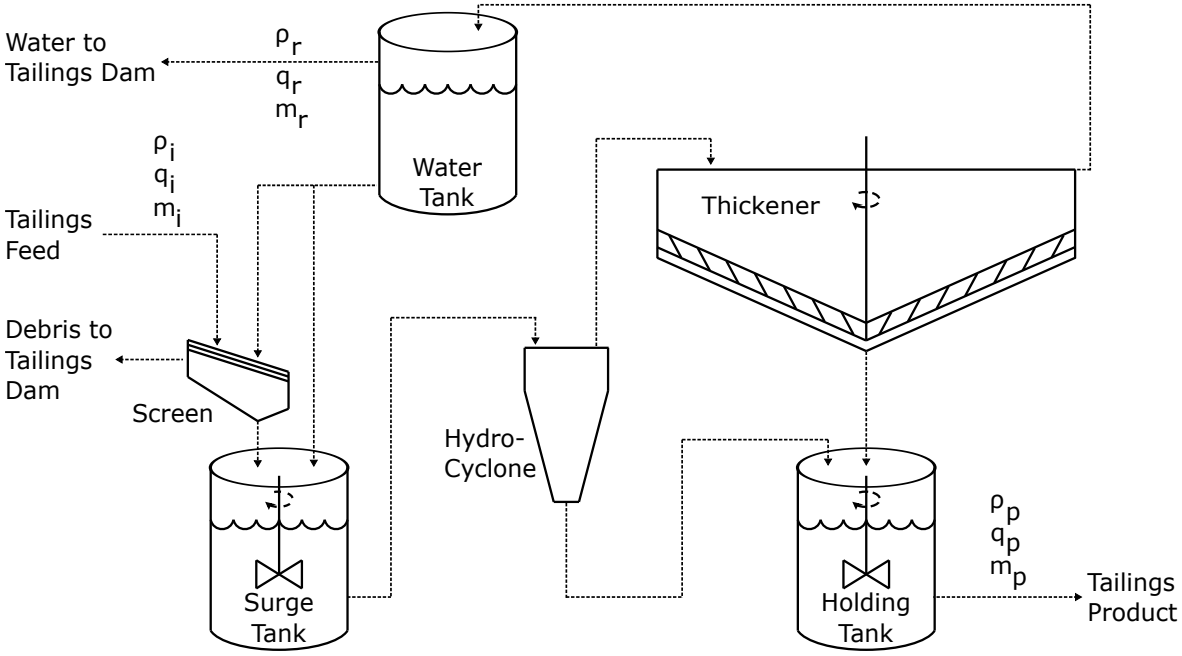

Figure 2.4. Flowsheet of the BTT plant.

The performance of the plant is measured on its ability to dewater the tailings fed to it and on the variability of the tailings it supplies to the chrome concentrator. Since the feed density to a hydrocyclone and the pressure drop across it both affect hydrocyclone efficiency (Ghodrat et al., 2016; Ntengwe and Witika, 2011), compounding improvements in hydrocyclone and thickener efficiencies can be expected by stabilising the surge tank density and output flow.

2.3.2 ESG considerations

The dewatering ability of the BTT plant refers to its capacity to remove solids from the thickener overflow, which is primarily influenced by hydrocyclone and thickener efficiencies. The plant supplies the tailings dam with the water it requires for its operations, thus any solids remaining in the thickener overflow is recycled back to the tailings dam resulting in wasteful rework. Rework not only increases the per ton processing cost of operations, but directly impacts ESG by increasing water and energy consumption. The increase in processing time related to rework results in wasteful water consumption due to inevitable evaporation losses, while a higher recirculating solids load requires additional power to maintain the needed flow rates for hydrominning activities.

2.4 CHAPTER CONCLUSION

This chapter provides an overview of two critical processing operations at Sibanye-Stillwater, a BMR and a chrome tailings reprocessing circuit, and emphasises the significance of maintaining consistent

feed quality in both operations. The BMR section highlights the importance of input blending strategies to improve product quality, maintain a consistent throughput, and reduce harmful emissions from the plant. The chrome tailings reprocessing section underscores the circuit's reliance on surge control to improve the consistency in input density and flow rates into the circuit, which benefits chrome recovery, energy usage, and water recovery.

CHAPTER 3 LITERATURE REVIEW

3.1 INTRODUCTION

Surge control and input blending, while distinct process optimisation and control approaches, are related in their roles in optimising the efficiency and stability of processing operations. Both surge control and input blending are employed to enhance the consistency of feed into operations, with surge control maintaining physical parameters like flow rate or density and input blending maintaining chemical or mineralogical parameters such as the feed composition.

Surge tanks or buffering tanks are units employed in surge control to attenuate the propagation of disturbances within processing circuits like the chrome reprocessing circuit studied here. Variations in feed disturb downstream processes, which are generally not in a position to manipulate their incoming flow rates and, therefore, depend on the buffering capacity of surge tanks to dampen incoming surges.

Input blending is fundamentally concerned with finding the optimal combination of raw materials, or the optimal sequence of available inputs, to achieve a desired feed composition into a process. While surge tanks can be used to provide a more consistent flow to continuous blending operations, they do not actively participate in the blending strategy.

This chapter reviews the literature on level averaging control and input blending. Both topics are applicable and relevant to a wide range of industries, for which their specific implementation and the criticality of their role can vary widely. The focus here is on their different implementation approaches and use cases in specifically processing operations.

3.2 INPUT BLENDING TO PROCESSING OPERATIONS

The algorithmic optimisation approach to input blending for processing operations depends on specific considerations of the problem category. For dynamic problems where the system state changes over time, such as the level averaging control problem, dynamic optimisation and control theory is required to adapt to these changes. When the relationships in the process variables or constraints are linear, linear programming (LP) (Vanderbei, 2014) or mixed integer linear programming (MILP) (Nemhauser and Wolsey, 1999) are used, with LP suitable for problems with continuous variables and MILP for those with discrete or mixed variable scenarios. When the problem considers non-linear relationships, nonlinear programming (NLP) (Rugenstein and Kupferschmid, 2004), mixed integer nonlinear programming (MINLP) (Bonami et al., 2008; Vinel and Krokhmal, 2017), or heuristic methods are required. Some problems have high degrees of uncertainty, which can be addressed through stochastic optimisation (SO) (Sepúlveda et al., 2020) or robust optimisation (RO) (Liu et al., 2023).

Heuristic methods are required for complex problems, where the solution or search space is high in dimensionality and computationally complex. These algorithms provide solutions to complex problems that are not guaranteed globally optimal, but pseudo-optimal or "good enough" to be implemented within a practical time frame. Heuristic methods include particle swarm optimisation (PSO) (Mohammad Nezhad and Mahlooji, 2011), simulated annealing (SA) (Franzin and Stützle, 2019), and evolutionary algorithms (EA) (Eiben and Smit, 2011).

The BMR blending problem, presented in Section 2.2.2, requires the blending of a matte stockpile that consists of a collection of bags. For each bag there is a recorded mass and composition vector. The search space for this optimisation problem, which solves for the optimal sequence to introduce matte bags into the operation to minimise sudden changes in input impurity, expands factorially. For a stockpile with m matte bags, there are m choices for the first bag in the sequence, $m-1$ for the second with the first bag no longer available for selection, $m-2$ for the third, and so on. Hence, the search space is factorial in size, corresponding to the number of possible arrangements of m bags in a matte stockpile.

This factorial growth means that even for a relatively small number of bags, the total number of possible sequences becomes very large, presenting a significant computational challenge due to an exponential growth in the search space. The BMR blending problem can generally be considered a combinatorial

optimisation or sequencing and scheduling problem, both of which are well studied in operations research. These problem types are proven to be nondeterministic polynomial-time(NP)-hard, which implies that for all known algorithms there is no guarantee of finding in polynomial time an optimal solution for every instance of the problem (Mazyavkina et al., 2021; Zheng et al., 2023).

Various operations and processes receive input material in discrete containers–such as bags, shipping containers, tanker trucks, etc.–with known mass and composition, and require arranging the sequence of these containers to satisfy blend requirements. These operations include matte processing refineries, such as nickel refineries that receive matte via shipping containers (Moskalyk and Alfantazi, 2002), and smelting operations that receive concentrate from several processing facilities via tanker trucks. The smelting operation that supplies the BMR, for example, receives concentrate via tankers from different operations, with each operation able to disptach several tankers at a time. This smelter's input blend requires the composition of base metals (Cu + Ni) to be within maximum and minimum limits, and the chrome composition (in the form of Cr_2O_3) to be below a specified limit (Eksteen et al., 2011). Operators schedule tanker deliveries to achieve blending, considering the availability of material and estimated composition at each upstream facility. Discrete input blending problems are therefore quite common in processing operations.

3.2.1 Methods for input blending optimisation in processing operations

This section reviews algorithmic blending approaches for processing operations to assess the spectrum of problems addressed in the literature and to identify potential solutions to the blending problem at the BMR. Chanda and Dagdelen (1995) considers the general problem of input blending of run of mine (ROM) ore into concentrator operations, and link it to mine planning, for which the objective is to mine an ore body, with known composition, such that the resulting mix of ROM ore from the mine meets the quality specifications of the concentrator operations product. They present a case study for coal processing, where environmental and economic considerations require the blending of ROM ore to ensure concentrator production meets strict limits on ash, sulphur, and thermal content. They propose a linear goal programming (LGP) model for the blending problem in short term mine planning, which is a variation on traditional LP, to solve multi objective optimisation problems. The authors demonstrate the usefulness of their approach by comparing it to traditional interactive trial-and-error, for which mine planning does not guarantee optimal solutions.

Singh et al. (2016) investigates input blending of ferromanganese ore to a smelting operation, not only considering ore composition, but also geometallurgical properties such as particle size distribution, porosity, and reducibility, all of which significantly affect furnace efficiency. An EA was used to maximise the overall manganese while satisfying constraints on geometallurgical properties. Industrial trails were performed, which demonstrated a consistent reduction in coke and energy consumption under normal operating conditions.

Amini et al. (2022) investigates the input blending problem at coal blending operations. They provide a rigorous MINLP formulation of the economic objective of coal blending operations, and augment this model using robust optimisation (RO) to deal with uncertainty in input coal quality attributes. This MINLP formulation of the economic object defines the blending problem and is solved to maximise profit. The authors additionally investigate the relationship between uncertainty and the potential profitability of these operations, quantifying the expected increase in profit that can be obtained by reducing uncertainty by different levels.

Eom and Kim (2023) investigate the blending scheduling problem common to steelworks operations, where melted material is transported using container trains from preprocessing plants, to blending plants where paired containers decant into pots to produce steel according to strict product specifications. The problem is formulated into two separate optimisation tasks. The first (transfer planning) solves for optimal container pairs and container assignment to blending plants, the second (blending scheduling) solves for logistic considerations at the blending operations to minimise employee and machine workloads. The authors formulate the integrated problem into a MILP model, and proposes a novel three-stage hierarchical approach to solve it. The approach involves first solving a relaxed version of the transfer planning planning problem, and then resolving the transfer planning problem with fixed variables, after which the blending scheduling problem is solved using a combinatorial benders decomposition algorithm (Rahmaniani et al., 2017), which is a method for solving large scale MILP problems that involve combinatorial decision making. The authors demonstrate that their three-stage approach outperforms an industry standard dispatching heuristic approach, by producing solutions faster and results closer to chemical composition specifications.

Yang et al. (2009) investigates the input blending problem of a raw slurry feed to an alumina sintering process. The problem requires solving for the relative proportions of input materials that are continuously fed from silos and tanks and combined to produce a raw slurry, the quality of which

significantly impacts alumina quality and the energy consumption of the process. The authors combine a mass-balance model with an artifical neural network (ANN) to predict the quality of the raw slurry. These model predictions are used together with expert knowledge to implement a hierarchical inference strategy, an expert system, to blend the raw material input for improved slurry quality. The authors compare the results obtained from this approach to those obtained by human operators at an industrial plant, demonstrating significant improvement in the consistency of raw slurry quality.

3.3 SURGE TANK CONTROL FOR PROCESSING OPERATIONS

Surge tank control considers a trade-off between two competing objectives. The first is the attenuation of incoming disturbances and the second is the maintenance of the tank level within minimum and maximum constraints. While the attenuation of disturbances is important to ensure, for example, a stable feed rate to a chemical reactor, the priority must be placed on ensuring the level constraints are not violated as this may lead to a loss in containment or damage to equipment such as agitator assemblies, which experience excessive stresses when a tank is operated at or below blade level, or pumps, which require sufficient liquid level to avoid cavitation. To maintain the level within its constraints, the control strategy must on average ensure equal incoming and outgoing flow rates. Consequently, the surge tank control problem is generally referred to as *level averaging control*.

3.3.1 Level averaging control in processing operations

Level averaging control is a topic extensively addressed in literature as a control strategy for specifically rejecting flow disturbances. The problem was studied as a proportional-integral-derivative (PID) tuning problem (Luyben, 2020; Reyes-Lúa et al., 2018; Rosander et al., 2012) and an optimal control problem (Lee and Shin, 2009; Lakerveld et al., 2013). Gous et al. (2023) investigates three advanced regulatory control techniques to address this problem, Sanchis et al. (2011) proposes a nonlinear control solution, and Rosander et al. (2011) a robust MPC solution. Although the literature on averaging level control mainly considers single surge tank processes, some investigations extend to multiple tank processes (Khan and Spurgeon, 2006; Sbarbaro and Ortega, 2007).

There are several applied industrial case studies investigating flow disturbance rejection using level averaging control. Crisafulli and Peirce (1999) presents a gain scheduled feed forward controller on a surge tank in a raw cane sugar factory to attenuate flow disturbances and improve clarification of cane juice. Lambooy (2011), demonstrates a reduction in the production of off-spec material from a tubular reactor by reducing input flow variations using optimal-averaging level control. A novel nonlinear level averaging controller presented in Sanchis et al. (2011) was implemented on a surge tank in an

oil refinery, demonstrating improved input flow disturbance rejection without discussing benefit to downstream processing.

Sbarbaro and Ortega (2007) presents a mass balance approach to the level averaging control problem for multi tank systems. The control problem is treated using the energy-based approach of Ortega et al. (2001), where the energy function for the overall system, which includes the controller, is shaped to provide the desired dynamic response.

3.4 CONCLUDING REMARKS

The literature on blending or scheduling for processing operations is vast, and covers all potential variations of problem classifications, including linear and nonlinear, stochastic and deterministic, continuous and discrete variables, etc. It is clear from the literature reviewed, that the key contribution to solving an input blending problem lies in the formulation of the problem, which includes development of models to accurately represent the operational challenges. While the use of heuristic methods to solve input blending problems to processing operations is not unique, their application, which includes the formulation of the scheduling problem and optimisation objectives, for the problem at the BMR could not be identified in the literature reviewed.

With regards to level averaging control for tailings reprocessing, due to the open-loop, unregulated nature of hydromining operations described in Section 2.3.1, the feed into a tailings reprocessing circuits are subject to significant disturbances in both flow and density. The control challenge in these circuits require the attenuation of both flow and density disturbances while maintaining tank levels within constraints, for which no literature could be found. All literature reviewed address level averaging control for flow disturbance rejection only. While some literature rely on a mass balance to model the system, either constant density is assumed, like in Sbarbaro and Ortega (2007), or density is not considered at all, like in Rosander et al. (2011). The surge tank in the BTT flowsheet described in Section 2.3.1 deviates from reviewed surge tank systems, as it includes a line for water addition. This water line allows for an extra degree of freedom to address the additional density control variable.

CHAPTER 4 MODEL DEVELOPMENT AND PROBLEM FORMULATION

4.1 CHAPTER OVERVIEW

This chapter develops the models used to explore and formulate the problem for both the heuristic approach to input blending optimisation of the base metal refinery and the level averaging control in the tailings reprocessing circuit. Model based optimisation and control often necessitates the trade-off between model simplicity and accuracy. Altough the success of model based approaches is intuitively dependent on the accuracy of the process models, simple models are often favoured for their computational efficiency and comparative ease of development.

A significant advantage of heuristic optimisation methods lies in their flexibility regarding both model construction and problem formulation. These approaches allow for a more adaptable and less rigid structure compared to traditional optimisation methods. It is, for example, possible that the heuristic formulation of the BMR problem as it is presented in this chapter can be approached differently. In contrast, a rigorous approach is necessary for modeling the dynamics of the level averaging control problem. This chapter explores the process considerations for both problems to motivate for specific optimisation and control approaches.

4.2 BASE METAL REFINERY INPUT BLENDING PROBLEM FORMULATION

The blending objective at the BMR is to minimise short term changes in the concentrations of contaminants fed to the plant. The ideal blend would result in the matte feed to contain the average concentration of the contaminants in the matte stockpile, i.e. the ideal blend would be obtained by processing the complete matte stockpile in a large stirred vessel. This ideal is of course not practical and blending occurs when smaller volumes of matte mixes when a bag sequence is loaded into the mill hopper, and as the matte makes its way through the various stirred vessels throughout the plant.

To model the blending that the matte experiences a moving average filter (Proakis and Manolakis, 2007) over the sequence in which bags are fed to the plant is used. Specifically, the blend of contaminant $X \in \{Silica, Iron, Selennium, Tellurium\}$ for a particular arrangement of matte bags is taken as the n bag moving average over the contaminant concentration in the bag sequence as shown in Algorithm 1.

Algorithm 1 The moving average $\widetilde{\boldsymbol{c}}_X$ of contaminant X

given n and $\boldsymbol{c}_X$
for $i \in \{n, ..., m\}$ **do**
  if $i == n$ **then**
    $\widetilde{\boldsymbol{c}}_X^n = \frac{1}{n}\sum_{k=1}^{n} \boldsymbol{c}_X^k$
  else
    $\widetilde{\boldsymbol{c}}_X^i = \widetilde{\boldsymbol{c}}_X^{i-1} + \boldsymbol{c}_X^i - \widetilde{\boldsymbol{c}}_X^{i-n}$
  end if
end for

Here, $n \in \{2, 3, 4, ..., m\}$ is the moving average window size, and $i \in \{n, n+1, ..., m\}$ is the bag index for the sequence in which the m bags in the matte stockpile are fed into the plant. The moving average concentration at index i for contaminant X is $\widetilde{\boldsymbol{c}}_X^i$, and $\boldsymbol{c}_X^i$ is the specific concentration of contaminant X in bag i.

The window size n determines the amount of smoothing for a moving average filter. In Algorithm 1 a larger n will simulate a greater amount of blending due to, for example, a greater amount of mixing of the matte in the milling circuit. The ideal blend is obtained with a window size of $n = m$, when the contaminant input into the plant is the average of the contaminant composition in the total matte stockpile. This is of course impractical, as it simulates the perfect mixing of all the matte in the stockpile. A arbitrary window size of $n = 4$ is used here, since it corresponds to the typical number of bags loaded into the milling circuit during a shift, and this relatively small window size exposes significant short term dynamics.

A measure of the deviation from the ideal blend is used here, to score the quality of blending achieved by different bag sequences. Specifically, the overall measure of the blend for a contaminant X is taken as the sum of squares difference SS_X between the contaminant's blended concentration $\widetilde{\boldsymbol{c}}_X$ and the

average concentration of the contaminant in the matte stockpile $\bar{c}_X$

$$SS_X = \sum_{i=1}^{m-n} (\widetilde{\boldsymbol{c}}_X^i - \bar{c}_X)^2$$
$$\bar{c}_X = \frac{1}{m} \sum_{k=1}^{m} \boldsymbol{c}_X^k. \tag{4.1}$$

4.2.1 Heuristic optimisation strategy selection

There are several heuristic optimisation strategies available; SA (van Laarhoven and Aarts, 1987), PSO (Eberhart and Shi, 2001), and EA (Bäck, 1996) are considered in this section. SA relies on iteratively improving a single candidate solution and may be less efficient given the vast search space of all possible bag sequences.

PSO leverages the behavior of multiple solutions (particles), allowing for exploration of a broader search space. The sharing of information among particles in PSO can accelerate convergence to optimal or near-optimal solutions. However, while adaptable to discrete problems (Kennedy and Eberhart, 1999), PSO is traditionally more suited for continuous optimisation.

Finally, EAs maintain a population of candidate solutions, enabling broad exploration of the search space without needing specific adaptation for discrete problems. Although evaluating a population of solutions can be computationally expensive, leading to longer solution times, this is not a significant concern for the blending problem at the BMR. Operations typically require a solution only once per 8-hour shift, making time a less critical factor. Therefore, an EA is a reasonable choice for this optimisation problem.

4.3 SURGE TANK DYNAMIC MODELING

A nonlinear model of the surge tank was developed to assess how effective different control strategies are at rejecting the typical input density and flow disturbances from the tailing dam. Figure 4.1 presents a simplified schematic diagram of the surge tank with all relevant process variables labelled. The nomenclature for the key surge and holding tank variables is shown in Table 4.1. The input flow rate, water flow rate, and output flow rate are respectively q_i, q_w, and q_o. The tank volume, derived from a tank geometry and level measurement, is v, and the input density, the density in the tank, and the output density are respectively ρ_i, ρ, and ρ_o.

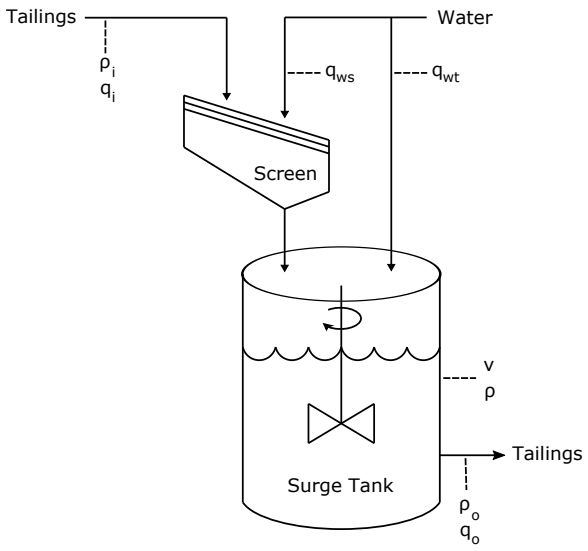

Figure 4.1. BTT surge tank.

Assuming perfect mixing, i.e. $\rho = \rho_o$, and conservation of mass the rate of accumulation of mass in the surge tank is

$$\frac{d\rho v}{dt} = \rho_i q_i + q_w - \rho q_o. \tag{4.2}$$

The derivative term on the left is expanded using the chain rule

$$v\frac{d\rho}{dt} + \rho\frac{dv}{dt} = \rho_i q_i + q_w - \rho q_o. \tag{4.3}$$

Assuming no volume change during mixing, which is a reasonable assumption when modelling slurry dynamics (Dontsov and Perice, 2014), the volume in the surge tank will be conserved and the rate of change of volume in the surge tank can be expressed as

$$\frac{dv}{dt} = q_i + q_w - q_o. \tag{4.4}$$

Substituting (4.4) into (4.3) gives the rate of accumulation of density independent of the rate of change in volume

$$\frac{d\rho}{dt} = \frac{q_i\rho_i - \rho(q_i + q_w) + q_w}{v}. \tag{4.5}$$

The nonlinear model of the surge tank follows from (4.4) and (4.5)

$$\begin{bmatrix} \dot{v} \\ \dot{\rho} \end{bmatrix} = \begin{bmatrix} q_i + q_w - q_o \\ \frac{1}{v}(q_i\rho_i - \rho(q_i + q_w) + q_w) \end{bmatrix}. \tag{4.6}$$

In subsequent sections, the following functional form of the nonlinear model in (4.6) is used

$$\begin{aligned} \dot{\mathbf{x}} &= \mathbf{f}(\mathbf{x}, \mathbf{u}, \mathbf{d}), \\ \mathbf{y} &= \mathbf{h}(\mathbf{x}). \end{aligned} \tag{4.7}$$

Table 4.1. A description of key surge tank and holding tank process variables.

Surge Tank Variables	Units	Description
q_i	m^3/h	Feed rate from tailings dam
ρ_i	t/m^3	Density from tailings dam
m_i	t/h	Mass flow from tailings dam
ρ	t/m^3	Density in surge tank
v	m^3	Volume in surge tank
l	%	Surge tank level
q_w	m^3/h	Surge tank water addition rate
q_o	m^3/h	Feed rate from surge tank
ρ_o	t/m^3	Density from surge tank
ψ_o	bar	Pressure surge tank output line
Holding Tank Variables	**Units**	**Description**
q_p	m^3/h	Plant output flow
ρ_p	t/m^3	Plant output density
m_p	t/h	Plant output mass flow
Water Tank Variables	**Units**	**Description**
q_r	m^3/h	Flow to tailings dam
ρ_r	t/m^3	Density to tailings dam
m_r	t/h	Mass flow to tailings dam

The elements of the state vector is $\mathbf{x} = \begin{bmatrix} v & \rho \end{bmatrix}^\top$, the input is $\mathbf{u} = \begin{bmatrix} q_i & q_w \end{bmatrix}^\top$, and the disturbance vector is $\mathbf{d} = \begin{bmatrix} \rho_i & q_o \end{bmatrix}^\top$. Since the tank volume is not directly measured, an output vector $\mathbf{y}$ is specified that defines a mapping between the measurable outputs, tank level l and tank density ρ, and $\mathbf{x}$

$$\mathbf{y} = \begin{bmatrix} l \\ \rho \end{bmatrix} = \begin{bmatrix} \frac{100}{v_t} & 0 \\ 0 & 1 \end{bmatrix} \mathbf{x}, \tag{4.8}$$

with v_t the total volume of the surge tank.

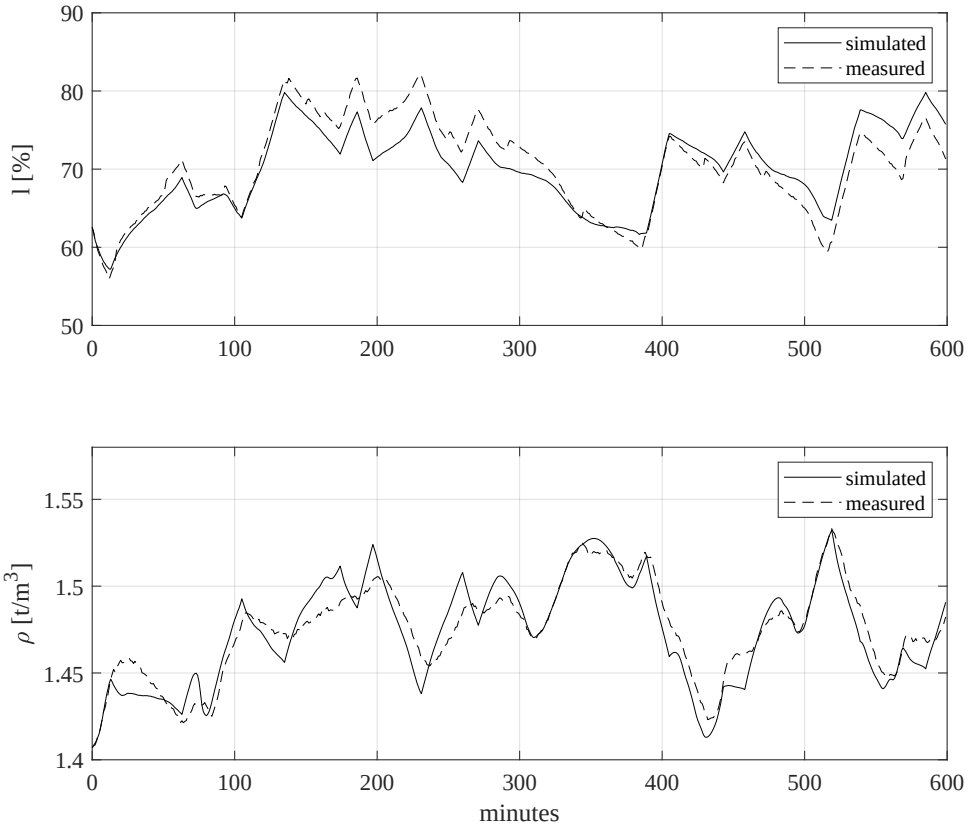

Figure 4.2. Validation of the nonlinear model.

4.3.1 Model validation

The model in (4.6) is validated using an industrial dataset, which is described in more detail in Section 5.3.3. The tank level and tank density was initialised with the tank level and density measured at $t = 0$, and the simulated outputs was obtained by subjecting the model to measured inputs $\mathbf{u}$ and disturbances $\mathbf{d}$. The simulated and measured tank density and level are shown in Figure 4.2. Table 4.2 presents a summary of the model validation results, comparing the difference between simulated and measured tank level and density using the mean absolute error (MAE) and coefficient of determination (R^2).

The model validation results show good correspondence between the measured and simulated values. An R^2 of 0.796 for the tank level suggests that approximately 80 % of the variance is explained by the simulated level, while an MAE of 2.237 % represents a small deviation between the measured and simulated tank levels. Similarly, with an R^2 of 0.837 and an MAE of 0.009 t/m^2 there is good correspondence between the simulated and measured tank density. Small deviations in the model

accuracy may be due to inaccuracies in the measurements, e.g. imperfect instrumentation calibration, while deviation between specifically the simulated and measured tank density may be due to imperfect mixing.

Table 4.2. Model validation results, comparing differences between the simulated and measured tank level and density using the mean absolute error (MAE) and coefficient of determination (R^2).

Variable	MAE	R^2
l	2.237 %	0.796
ρ	0.009 t/m^3	0.837

4.3.2 Linear approximation

A linear approximation of a system is generally useful as it allows the application of the well developed theory on linear systems to explore the dynamic behaviour of a system (Skogestad and Postlethwaite, 2005). An in-depth model analysis and exploration of the dynamic behaviour of this surge tank are not presented here, however, the interested reader is referred to Rokebrand et al. (2020, 2021) and Rokebrand (2022).

With the expression for the accumulation of volume in (4.4) already linear, a linear approximation of the surge tank requires only the Taylor series expansion of (4.5). Taking the functional form

$$\frac{d\rho}{dt} = f_\rho(q_i, q_w, q_o, \rho_i, \rho, v), \tag{4.9}$$

and applying a multivariate Taylor series expansion about the nominal steady-state operating point $\bar{x} = [\bar{q}_i, \bar{q}_w, \bar{\rho}_i, \bar{\rho}, \bar{v}]^\top$, and ignoring the higher order terms gives

$$\begin{aligned} f_\rho(q_i, q_w, q_o, \rho_i, \rho, v) \cong f_\rho(\bar{x}) &+ \left.\frac{\partial f_\rho}{\partial q_i}\right|_{\bar{x}} \delta q_i + \left.\frac{\partial f_\rho}{\partial q_w}\right|_{\bar{x}} \delta q_w + \\ &\left.\frac{\partial f_\rho}{\partial q_o}\right|_{\bar{x}} \delta q_o + \left.\frac{\partial f_\rho}{\partial \rho_i}\right|_{\bar{x}} \delta \rho_i + \\ &\left.\frac{\partial f_\rho}{\partial \rho}\right|_{\bar{x}} \delta \rho + \left.\frac{\partial f_\rho}{\partial v}\right|_{\bar{x}} \delta v \end{aligned} \tag{4.10}$$

$$\begin{aligned} \cong f_\rho(\bar{x}) &+ \frac{\bar{\rho}_i - \bar{\rho}}{\bar{v}} \delta q_i + \frac{1 - \bar{\rho}}{\bar{v}} \delta q_w + \\ &\frac{\bar{q}_i}{\bar{v}} \delta \rho_i - \frac{\bar{q}_i + \bar{q}_w}{\bar{v}} \delta \rho - \\ &\frac{\bar{q}_i \bar{\rho}_i + \bar{q}_w - (\bar{q}_i + \bar{q}_w)\bar{\rho}}{\bar{v}^2} \delta v. \end{aligned}$$

By definition, at steady-state $\bar{q}_i + \bar{q}_w - \bar{q}_o = 0$ and $\bar{q}_i\bar{\rho}_i + \bar{q}_w - \bar{q}_o\bar{\rho} = 0$ such that (4.10) reduces to

$$f_\rho(q_i, q_w, q_o, \rho_i, \rho, v) \cong f_\rho(\bar{x}) + \frac{\bar{\rho}_i - \bar{\rho}}{\bar{v}}\delta q_i + \frac{1-\bar{\rho}}{\bar{v}}\delta q_w + \frac{\bar{q}_i}{\bar{v}}\delta\rho_i - \frac{\bar{q}_o}{\bar{v}}\delta\rho. \tag{4.11}$$

The continuous state-space representation of a linear system with N_x states, N_u manipulated inputs, N_d disturbance inputs, and N_y outputs is

$$\begin{aligned} \frac{d\mathbf{x}(t)}{dt} &= \mathbf{A}\mathbf{x}(t) + \mathbf{B}\mathbf{u}(t) + \mathbf{E}\mathbf{d}(t) \\ \mathbf{y}(t) &= \mathbf{C}\mathbf{x}(t), \end{aligned} \tag{4.12}$$

where $\mathbf{x}(k) \in \mathbb{R}^{N_x \times 1}$ is the state vector, $\mathbf{u}(k) \in \mathbb{R}^{N_u \times 1}$ is the input vector, $\mathbf{d}(k) \in \mathbb{R}^{N_d \times 1}$ is the disturbance vector, $\mathbf{y}(k) \in \mathbb{R}^{N_y \times 1}$ is the output vector, $\mathbf{A} \in \mathbb{R}^{N_x \times N_x}$ is the state matrix, $\mathbf{B} \in \mathbb{R}^{N_x \times N_u}$ is the input matrix, $\mathbf{E} \in \mathbb{R}^{N_x \times N_d}$ is the disturbance matrix, and $\mathbf{C} \in \mathbb{R}^{N_y \times N_x}$ is the output matrix.

The linear model of the surge tank follows from (4.4), (4.8), and (4.11):

$$\begin{aligned} N_x = N_y = 2, N_d = N_u = 2, \\ \mathbf{A} = \begin{bmatrix} 0 & 0 \\ 0 & -\frac{\bar{q}_o}{\bar{v}} \end{bmatrix}, \mathbf{B} = \begin{bmatrix} 1 & 1 \\ \frac{\bar{\rho}_i - \bar{\rho}}{\bar{v}} & \frac{1-\bar{\rho}}{\bar{v}} \end{bmatrix}, \\ \mathbf{E} = \begin{bmatrix} -1 & 0 \\ 0 & \frac{\bar{q}_o}{\bar{v}} \end{bmatrix}, \text{ and } \mathbf{C} = \begin{bmatrix} \frac{100}{v_t} & 0 \\ 0 & 1 \end{bmatrix}. \end{aligned} \tag{4.13}$$

4.3.3 Linear vs nonlinear model based control

The linear model in (4.13) was derived on the assumption that higher order terms in the Taylor series expansion can be disregarded, since close to the nominal operating point $\bar{x}$ higher order terms will be approximately zero. Processes, of course, continuously deviate from their nominal operating points and plant-model mismatch, in the form of inaccuracies between the true system dynamics and the linear model predictions, cannot be avoided (Olivier and Craig, 2015).

Considering that, for example, the vast majority of industrial model predictive control (MPC) solutions rely on linear models to control nonlinear processes (Qin and Badgwell, 2003), plant-model mismatch is often disregarded. This can be explained by noting that it is comparatively cheap to develop linear models, typically by assuming that the dynamic responses of the system follow first-order-plus-time delay (FOPTD) transients, and by fitting FOPTD models to data obtained from step testing. Compared to a first principles approach to obtain a nonlinear process model, a linear model obtained from step tests is markedly less complicated and time consuming.

Generally, linear approximations are at least accurate to the direction of relationships between model inputs and outputs. This is often considered *good enough* for control since the system can be driven towards a desired operating point. Moreover, feedback control has a linearising effect as it keeps the plant close to an operating point (Skogestad and Postlethwaite, 2005). Ultimately, the negative effects of some model mismatch is likely never considered when a linear MPC achieves noteworthy improvements compared to a baseline control system.

A linear approximation for this surge tank model is not sufficient, however, since the observed deviation of input density from the tailings dam cause inversion of the direction of the relationship between input flow q_i and tank density ρ. For the linear approximation of the surge tank model the term in the input matrix **B** in (4.12) associated with the input flow q_i will always be positive. The constant flow of water q_w to maintain the screen dilutes the incoming tailings, and guarantees that:

$$\frac{\bar{\rho}_i - \bar{\rho}}{\bar{v}} > 0. \tag{4.14}$$

A linear MPC relying on the model in (4.12) would therefore always use q_i to increase ρ. However, the re-mining process followed at the tailings dam, described in Section 2.3, relies on manual operations and is exposed to various environmental factors that results in an input density ρ_i that varies over a large range. This high degree of variation often results in a scenario where the direction of the relationship between q_i and ρ would be negative, i.e. an inversely proportional relationship where an increase in q_i would result in a decrease in ρ.

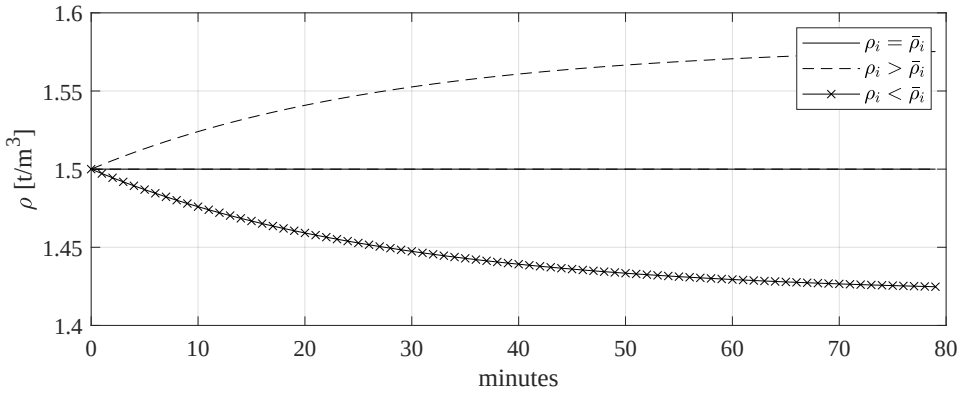

Figure 4.3. Gain inversion in the relationship between input flow q_i and tank density ρ as a result of significant variance in the instantaneous input density ρ_i.

This *gain inversion* is demonstrated in Figure 4.3 for a fictitious, although reasonably likely, steady-state operating point. The steady-state operating point considered is:

$\bar{q}_i = 600$ m^3/h, $\bar{q}_w = 150$ m^3/h, $\bar{q}_o = 750$ m^3/h,
$\bar{\rho}_i = 1.625$ t/m^3, $\bar{\rho} = 1.5$ t/m^3, and
$v = 350$ m^3/h.

Figure 4.3 simulates three scenarios using the nonlinear model in (4.6). For all three the instantaneous input flow q_i remains constant and equal to the steady-state input flow $\bar{q}_i$. In the first scenario $(-)$, representing the case with no model mismatch, the instantaneous input density ρ_i remains constant and equal to the steady-state input density $\bar{\rho}_i$. In the second scenario $(--)$ $\rho_i = \bar{\rho}_i + 0.1$. In the third scenario $(-\times)$, $\rho_i = \bar{\rho}_i - 0.1$.

Therefore, for the particular scenario where a controller is tasked to maintain ρ at a target density ρ_{target}, with $\rho_i < \bar{\rho}_i$ and $\rho < \rho_{target}$, a linear model based controller would increase q_i, further driving ρ away from ρ_{target}. It is therefore important to account for the demonstrated gain inversion in the controller design, which necessitates a nonlinear model based control strategy.

4.3.4 Nonlinear level averaging control strategy selection

There are several nonlinear model based control approaches for nonlinear multiple-input, multiple-output systems like the tailings surge tank problem presented here. Adaptive MPC (Adetola et al., 2009) modifies the model parameters in real time using recent observations from the system, and derives a linear model that is valid around the current system operating point. Gain scheduled MPC (Ilka and Veseleý, 2015; Wiid et al., 2021) relies on a set of models to cover different operating points and selects among these models an active model based on real time observations.

NMPC relies on a nonlinear model of the system and solves a nonlinear optimisation problem at each time step. The main drawback of NMPC control is the computational burden associated with solving its non-convex optimisation problem. However, generally speaking this is not much of a concern in the process industry, where the dynamics of systems are relatively slow allowing for more computationally intensive control approaches (Allgöwer et al., 2004). While there are non-standard NMPC approaches to solve computational complexity concerns (Gros et al., 2020), the comparatively slow dynamics

expected from this system should not present challenges with computational complexity. Hence, a standard NMPC strategy is motivated for application here.

4.4 CONCLUDING REMARKS

This chapter presents the modelling and formulation for both the BMR input blend and the tailings reprocessing level averaging control problems. For the input blending problem a heuristic optimisation strategy using an evolutionary algorithm was found to be most suitable. This decision was informed by an analysis of heuristic optimisation strategies including SA and PSO. The choice of EA was primarily due to its ability to handle the vast search space efficiently without the need for specific adaptation to the discrete nature of the problem. Additionally, the operational requirements of the BMR, which demand solutions once per 8-hour shift, rendered the computational intensity of EAs acceptable. An EA is developed for the BMR blending problem in Chapter 5, and tested on an industrial dataset in Chapter 6.

In the case of the tailings reprocessing circuit, this chapter introduced a nonlinear model of the surge tank dynamics. The model was validated against real-world data, demonstrating its accuracy and reliability. The nonlinear nature of the process and the significant variance in input density necessitated an NMPC strategy. The NMPC approach is preferred over other control strategies due to its robustness and ability to handle the complexities inherent in the surge tank system. The slow dynamics of the system further justified the choice of NMPC, despite its computational demands. The NMPC will be designed in Chapter 5 and applied on an industrial plant in Chapter 6.

CHAPTER 5 EA ALGORITHM AND NMPC CONTROLLER DESIGN

5.1 CHAPTER OVERVIEW

An EA is motivated as a fit for purpose heuristic approach for the BMR input blending optimisation problem, and NMPC for a nonlinear multivariable control strategy to treat the level averaging control problem in tailings reprocessing. This chapter presents a detailed algorithmic design for a $(\mu + \lambda)$-evolutionary strategy (ES), a type of EA, as well as controller design for the NMPC and the baseline control strategy used for level averaging control in an industrial circuit.

5.2 EVOLUTIONARY STRATEGY FOR BMR INPUT BLENDING

ESs (Schewefel, 1995), a subset of EAs sometimes referred to as evolutionary programming (Fogel et al., 1966), are search paradigms that mimic the principles of biological evolution. Hansen et al. (2015) presents a thorough overview of the principles of ESs. This section presents a description of the $(\mu + \lambda)$-ES (Ramos-Figueroa et al., 2020), used to solve the BMR blending problem.

ESs assume a population of individuals, P. Each individual represents a potential solution to the problem at hand and consists of a solution vector, $\boldsymbol{x}$, and an associated fitness value, $f(\boldsymbol{x})$. An input blend solution vector for the BMR blending problem represents a specific arrangement of the bags in the BMR matte stockpile. The blend solution vector is of length m and each entry denotes the blow number associated with a particular bag, recalling from Section 2.2.2 that the converter matte from the smelter is received in individual blows, with each blow comprising a number of bags that are identical in their mineralogical composition but vary in weight.

Instead of uniquely identifying each bag in the solution vector, only the blow associated with each bag is identified. This is done to accommodate logistical constraints at the BMR, where access to individual

bags is not guaranteed, but where access to individual blows is possible. Hence, this approach assume equal weights and devise an input blend solution vector that will only recommend the order in which individual bags from blows are fed to the plant.

Two examples of blend solution vectors are presented in Figure 5.1. The top solution vector is the as received, or unblended, arrangement of three blows containing eleven bags. The bottom solution vector is a blend obtained by random permutation of the unblended solution vector.

1	1	1	2	2	2	2	3	3	3	3

1	2	3	2	3	2	3	1	1	2	3

Figure 5.1. Two examples of solution vectors. An unblended BMR matte stockpile (top) containing three blows and eleven bags ($m = 11$), and a blend obtained by random permutation (bottom).

Pseudo code for the $(\mu + \lambda)$-ES algorithm is presented in Algorithm 2. A population P of size μ is initialised through μ random permutations of the unblended solution vector. For each of n_{gen} generations, a set O of size λ offspring individuals is created by applying either the mutation, crossover, or reproduction operators to P.

At the end of each generation, the offspring set O is added to the population set P to create a combined set C. Only μ individuals are selected from C using a *select* operator function to survive to the next generation. Tournament selection (Blickle and Thiele, 1995) is used, which repeats the following procedure μ times: sample at random t_{sel} individuals from C and copy only the fittest of these sampled individuals into the new population set P.

The fitness value $f(\boldsymbol{x}_k)$ of an individual is determined by a weighted sum for each contaminant's sum of squares deviation presented in (4.1):

$$f(\boldsymbol{x}_k) = \omega_{SiO_2} SS_{SiO_2} + \omega_{Fe} SS_{Fe} + \omega_{Se} SS_{Se} + \omega_{Te} SS_{Te}. \tag{5.1}$$

The contaminant weights ω_X are chosen to assign relative importance to each contaminant. Since the $(\mu + \lambda)$-ES algorithm minimises the fitness of the population, a larger weight will assign a greater importance to the contaminant in question. Moreover, the concentrations of the contaminants in the matte are not equal, with Fe for example ten times more abundant in the matte compared to Se. To

Algorithm 2 The $(\mu+\lambda)$-Evolutionary Strategy

given $\mu, \lambda \in \mathbb{N}_+$ and $\rho_{cross}, \rho_{mut} \in \mathbb{R}$
initialize $P = \{\boldsymbol{x}, f(\boldsymbol{x})\}$ with μ individuals
for $g \in \{1, ..., n_{gen}\}$ **do**
  $O = \{\}$ {Initialize offspring set}
  for $k \in \{1, ..., \lambda\}$ **do**
    Sample parent(s) from P at random
    Initialise offspring solution vector $\boldsymbol{x}_k$ as a copy of the selected parent(s)
    With probability ρ_{cross}, apply *crossover*
    With probability ρ_{mut}, apply *mutation*
    With probability $1 - (\rho_{cross} + \rho_{mut})$, apply *reproduction*
    Evaluate $f(\boldsymbol{x}_k)$
    Add $(\boldsymbol{x}_k, f(\boldsymbol{x}_k))$ to O
  end for
  $C \leftarrow P \cup O$ {Combine parents and offspring}
  $P \leftarrow select(C, \mu)$ {Select μ individuals for the next generation}
end for

avoid biasing the outcome of the blending strategy, the contaminant concentrations are standardised, i.e. normalised to zero mean and unit standard deviation. For the BMR, SiO_2 contamination is regarded as more severe, with Fe considered to have the second most severe impact. Consequently the contaminant weights in (5.1) are ranked $\omega_{SiO_2} \geq \omega_{Fe} \geq \omega_{Se} = \omega_{Te}$.

EA problems can be formulated as general nonlinear constrained optimisation problems, where the objective is to minimise the fitness function $f(\boldsymbol{x})$ subject to both linear or nonlinear equality and inequality constraints, represented by $h(\mathbf{x})$ and $g(\mathbf{x})$ respectively:

$$\min_{\mathbf{x}} f(\mathbf{x}) \quad \text{subject to}: \quad g(\mathbf{x}) \leq 0, \quad h(\mathbf{x}) = 0. \tag{5.2}$$

The challenge of handling constraints in EAs is well-studied; Coello Coello (2002) presents a comprehensive survey of different approaches, which include penalty approaches, where the fitness function is modified to penalise constraint violations, or the use of tailored representations and operators to ensure that feasibility is preserved. In this work, the latter approach is adopted by defining operators that ensure sequencing constraints – such as the requirement that all bags in the stockpile be used exactly once in a solution vector – are met.

The *mutation* operator is selected to produce offspring with probability ρ_{mut}, and the *crossover* operator with probability ρ_{cross}. The sum of ρ_{cross} and ρ_{mut} must be in range $[0,1]$, and the probability of selecting the *reproduction* operator is $1-(\rho_{cross}+\rho_{mut})$. For crossover, the ordered crossover procedure in

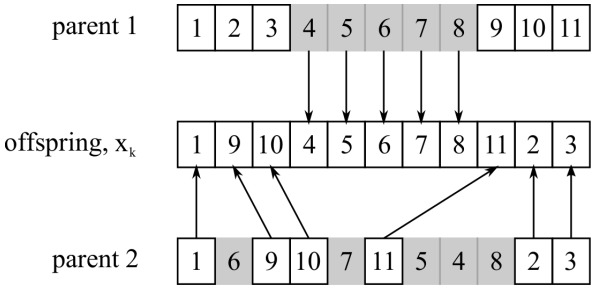

Figure 5.2. An illustration of the ordered crossover procedure.

Davis (1985), illustrated in Figure 5.2, is used. Two parent individuals are selected at random from P. A sub-string from parent 1 is selected at random and copied to the corresponding position in the offspring. All entries from the selected sub-string are deleted from parent 2, and the remaining parent 2 entries are copied in sequence to the missing positions in the offspring. For mutation, an individual is selected at random from P. Each element in this individual's solution vector $\boldsymbol{x}_k$ is moved to a new random index within the solution vector at probability ρ^i_{mut}. For reproduction, an individual is simply selected at random from P and its solution vector is cloned. Table 5.1 presents a description for each of the $(\mu+\lambda)$-ES algorithm parameters.

Table 5.1. Description of the $(\mu+\lambda)$-ES algorithm parameters.

Parameter	Description
P	Population of individuals
$\boldsymbol{x}$	Solution vector stipulating a blow order
$f(\boldsymbol{x})$	Fitness value for solution vector $\boldsymbol{x}$
μ and λ	Population size and number of offspring per generations
ρ_{cross} and ρ_{mut}	Probabilities for crossover and mutation
ρ^i_{mut}	Probability of moving element i in the solution vector during mutation
t_{sel}	Number of individuals sampled for tournament selection
n_{gen}	The number of generations
ω_{SiO_2} and ω_{Fe}	Contaminant importance weighting for SiO_2 and Fe
ω_{Se} and ω_{Te}	Contaminant importance weighting for Se and Te

Note that in addition to the choice of operator functions, several hyperparameters determine the convergence behavior of the algorithm. Ineffective selection of these parameters and functions will hinder the algorithm's ability to converge, result in inconsistent convergence towards near-optimal solutions, or cause convergence to require an excessive amount of time. Figure 5.3 presents a convergence plot with crossover and mutation probabilities set to 0.9 and 0.01 respectively. The difference between the population mean fitness and the fittest individual provides a measure of diversity in the population. After generation 300 of the algorithm, the difference between mean and fittest individual becomes indistinguishable, indicating low diversity in the population. This hampers the algorithm's ability to explore the solution space, leading to a poor solution.

In contrast, Figure 5.4 displays a convergence plot with adjusted crossover and mutation probabilities of 0.8 and 0.1, respectively, while keeping all other parameters the same. By increasing the mutation probability tenfold from its initial value, population diversity is substantially improved, which prevents premature plateauing and results in a significantly improved solution.

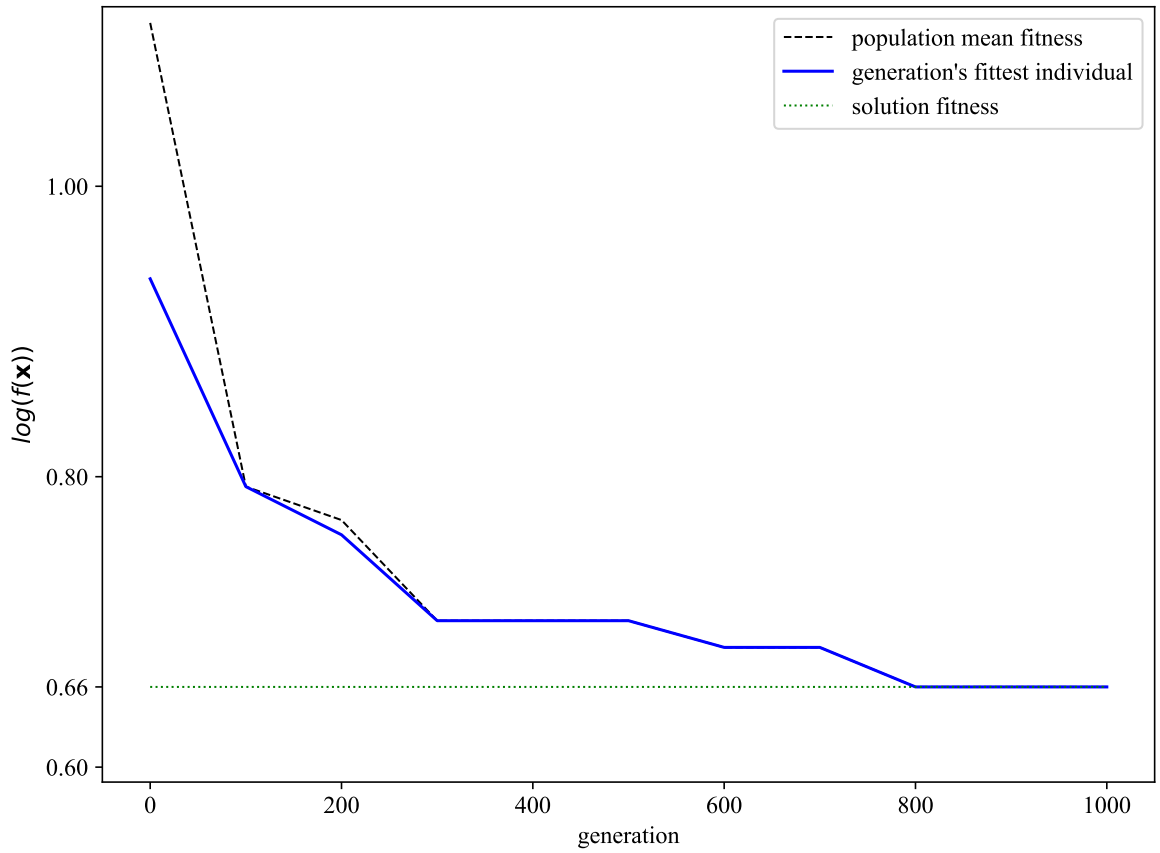

Figure 5.3. Convergence plot for the $(\mu + \lambda)$-ES blending strategy using $\rho_{cross} = 0.9$ and $\rho_{mut} = 0.01$.

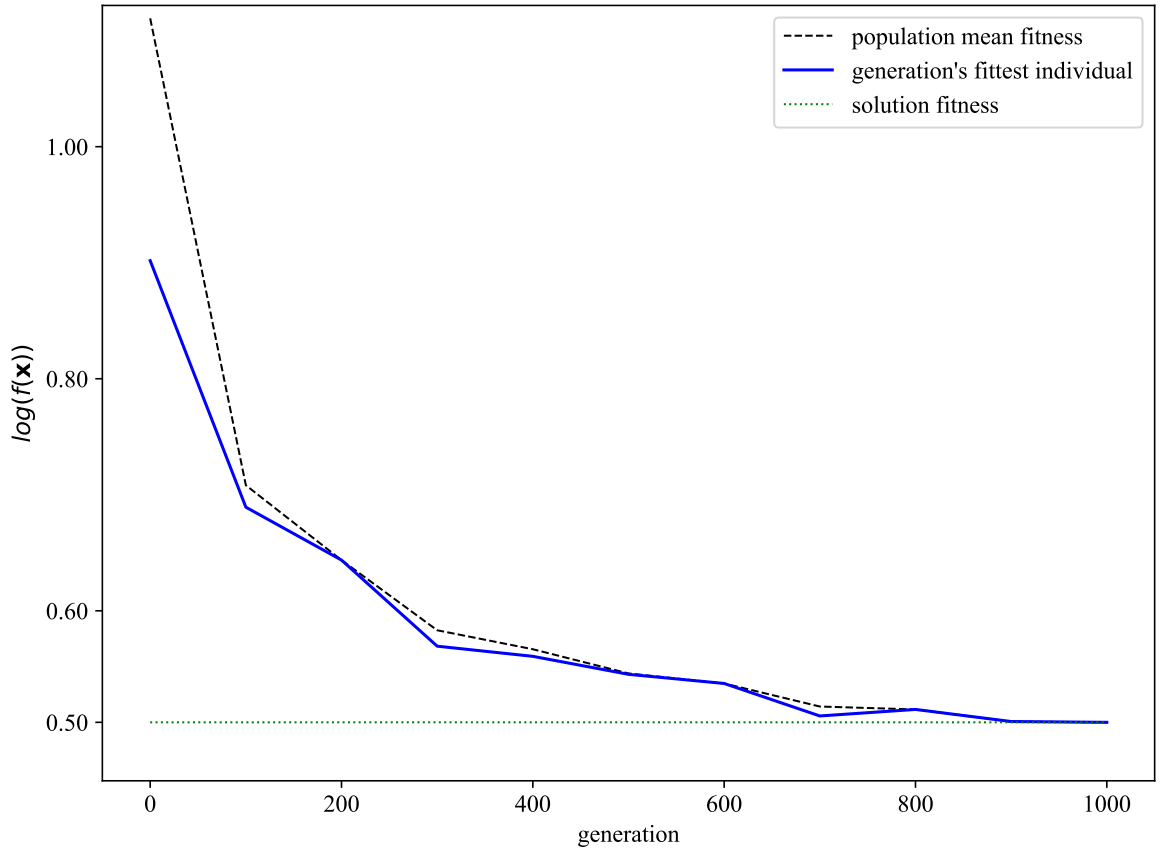

Figure 5.4. Convergence plot for the $(\mu + \lambda)$-ES blending strategy using $\rho_{cross} = 0.8$ and $\rho_{mut} = 0.1$.

5.3 NONLINEAR MODEL PREDICTIVE CONTROL FOR LEVEL AVERAGING CONTROL

This section presents a detailed design for the NMPC used for level averaging control in the tailings reprocessing circuit. Different control objectives are evaluated via closed loop simulation to identify a preferred NMPC strategy. The baseline control strategy is also identified to assist with NMPC design considerations and for reference during implementation discussions to follow.

5.3.1 Model predictive control

Model predictive control (MPC) refers to a class of advanced control algorithms that have been shown to be effective in the process industry in dealing with multivariable constrained control problems (Meyer et al., 2019; Qin and Badgwell, 2003). MPC relies on a model to predict the state and output responses of a system over a finite prediction horizon N_p.

At each control interval k the MPC solves for a set of control actions over a control horizon N_c

by minimising an objective function $J(.)$, given estimates of the initial state of the system $\mathbf{x}(k)$, measurements of the initial system manipulated inputs $\mathbf{u}(k)$, disturbance inputs $\mathbf{d}(k)$, outputs $\mathbf{y}(k)$, and a desired reference trajectory for the system output $\mathbf{y}_{ref}$. The measured disturbance inputs are assumed to remain constant over the prediction horizon N_p.

Only the first control action is implemented, and at the subsequent control interval, the prediction horizon shifts, leading to the derivation of a new set of control actions. This shifting or "receding" nature of the prediction horizon is why MPC is sometimes referred to as Receding Horizon Control (Ma et al., 2021).

This constrained optimisation problem solved at each control interval can be expressed as follows:

$$
\begin{aligned}
&\min_{\mathbf{u}(k+1|k),\ldots,\mathbf{u}(N_c+1|k)} \quad J\left(\mathbf{u},\mathbf{d}(k),\mathbf{x}(k),\mathbf{y}_{ref}\right)\\
&\text{subject to:}\\
&\mathbf{x}\in\mathbb{R}^{N_x\times N_p}, \quad \mathbf{x}_l\leq\mathbf{x}\leq\mathbf{x}_h;\\
&\mathbf{u}\in\mathbb{R}^{N_u\times N_c}, \quad \mathbf{u}_l\leq\mathbf{u}\leq\mathbf{u}_h;\\
&\mathbf{y}\in\mathbb{R}^{N_y\times N_p}, \quad \mathbf{y}_l\leq\mathbf{y}\leq\mathbf{y}_h;\\
&\mathbf{x}(k+i+1|k) \quad = \mathbf{f}_k(\mathbf{x}(k+i|k),\mathbf{u}(k+i|k),\mathbf{d}(k)),\\
&\mathbf{y}(k+i|k) \quad = \mathbf{h}_k(\mathbf{x}(k+i|k)),\forall\ i=1,2,\ldots,N_c;\\
&\mathbf{x}(k+j+1|k) \quad = \mathbf{f}_k(\mathbf{x}(k+j|k),\mathbf{u}(k+N_c|k),\mathbf{d}(k)),\\
&\mathbf{y}(k+j|k) \quad = \mathbf{h}_k(\mathbf{x}(k+j|k)),\forall\ j=N_c+1,N_c+2,\ldots,N_p.
\end{aligned}
\tag{5.3}
$$

The system state $\mathbf{x}$ is constrained to operate within upper and lower bounds, $\mathbf{x}_h$ and $\mathbf{x}_l$ respectively, as are the system inputs and outputs, $\mathbf{u}$ and $\mathbf{y}$. These are referred to as *hard constraints*, which must be satisfied for the solution to be considered feasible. Note that the optimisation procedure solves for only N_c control vectors, with the input vector kept constant at $\mathbf{u}(k+N_c)$ for the remainder of time intervals in the prediction horizon N_p.

The cost function in (5.3) is defined as:

$$
J(\mathbf{u},\mathbf{d}(k),\mathbf{x}(k),\mathbf{y}_{ref}(k)) = \sum_{i=1}^{N_p}\left\|\mathbf{y}_{ref}(k+i)-\mathbf{y}(k+i|k)\right\|_{\mathbf{Q}}^2 + \sum_{i=1}^{N_c}\left\|\Delta\mathbf{u}(k+i|k)\right\|_{\mathbf{S}}^2, \tag{5.4}
$$

with $\mathbf{y}_{ref}\in\mathbb{R}^{N_y\times N_p}$ and $\Delta\mathbf{u}(k+i|k)=\mathbf{u}(k+i|k)-\mathbf{u}(k+i-1|k)$. Here $\mathbf{Q}$ and $\mathbf{S}$ are diagonal matrices used to weight the controlled and manipulated variables respectively. These weights specify the relative importance of the systems states and control actions.

At each control interval k the MPC solves for N_c control vectors and implements the first control move $\mathbf{u}(k+1)$. At the following interval new measurements are obtained from the system and the optimisation procedure is repeated.

The cost function above represents a standard formulation of the MPC optimisation problem, where the controller solves for a minimum squared error between the predicted and reference outputs and penalises control effort. For NMPC the state transition or output functions $\mathbf{f}_k$ and $\mathbf{u}_k$, or the hard constraints, or the cost function includes a nonlinear function. The NMPC used in the simulations in Section 5.3.3 and implemented in Chapter 6 uses the nonlinear state transition function (4.7) derived in Chapter 4.

5.3.2 Baseline level averaging control strategy for the BTT surge tank

An example of the industrial BTT surge tank's dynamics while under the baseline control strategy is presented in the 10-hour long dataset shown in Figures 5.5 to 5.7. This dataset was recorded while the plant was under normal operation, i.e. while the plant was not under start-up or shut-down conditions.

The input density varies at times rapidly and generally over a large range. This is expected due to the highly manual operation of the process at the tailing dam, as described in Section 2.3.

The input flow is seemingly inversely proportional to the input density. This is expected as the baseline control strategy did not manipulate the input flow directly but maintained a fixed pump speed. Consequently, flow dynamics are dominated by density fluctuations.

The baseline control strategy clearly implements steps in water addition and output flow rate to maintain tank level and tank density within acceptable ranges. The output flow rate is not directly adjusted to maintain the tank level, instead there is a pressure controller on the output line to keep the pressure across the hydro-cyclone constant, as shown in Figure 5.8. The set-point to this pressure controller is stepped to affect a change in output flow so as to maintain the tank level within a range.

5.3.3 Controller simulations

The aim is to maintain the surge tank density at a target density ρ_{target}. This target density is likely to change slowly over time due to changes in the nominal input density ρ_i, which in turn is due to slow changes in equipment condition and tailings characteristics. A strategy for operations can be to set

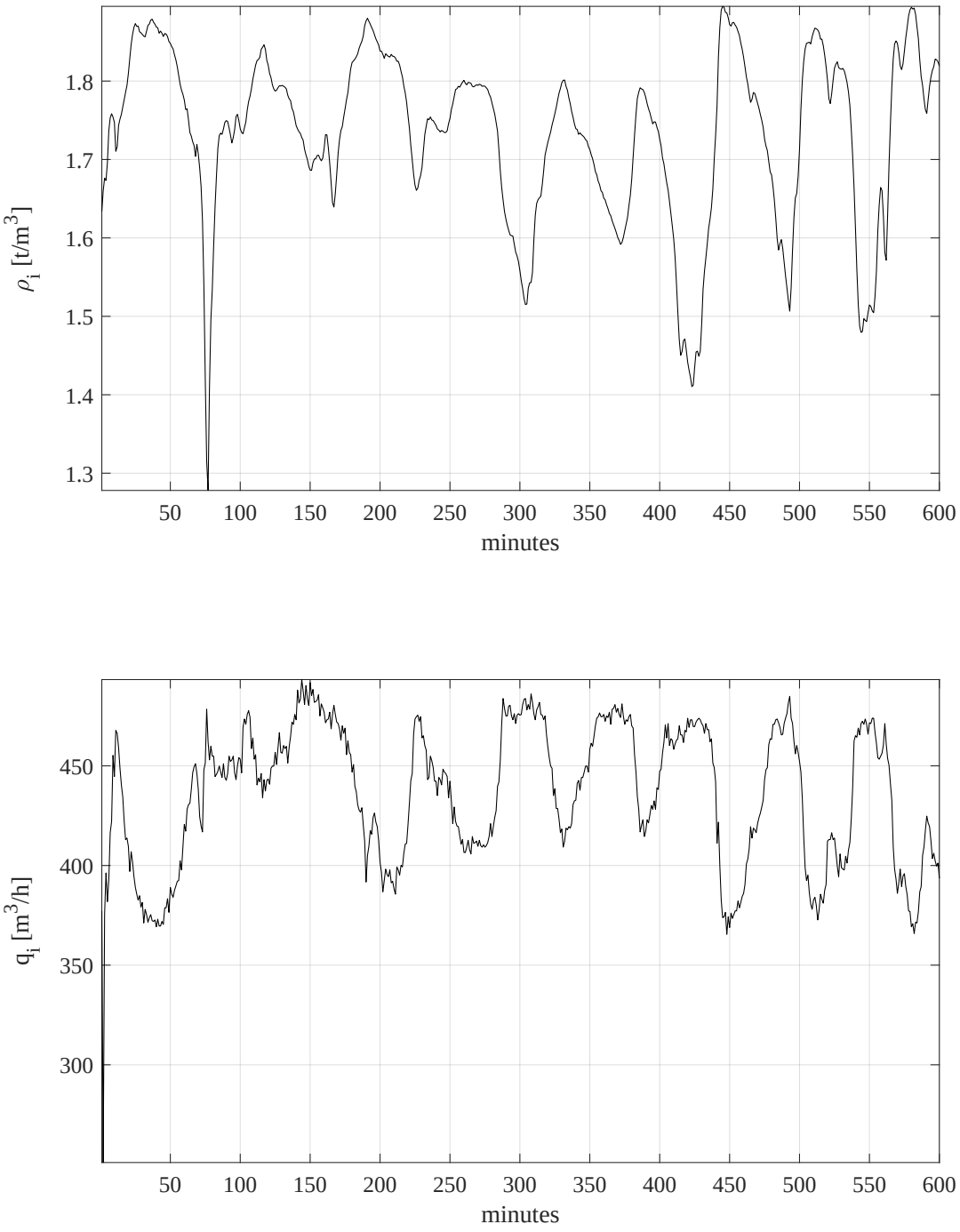

Figure 5.5. Density and flow rate into the BTT surge tank while operated under the baseline surge control strategy.

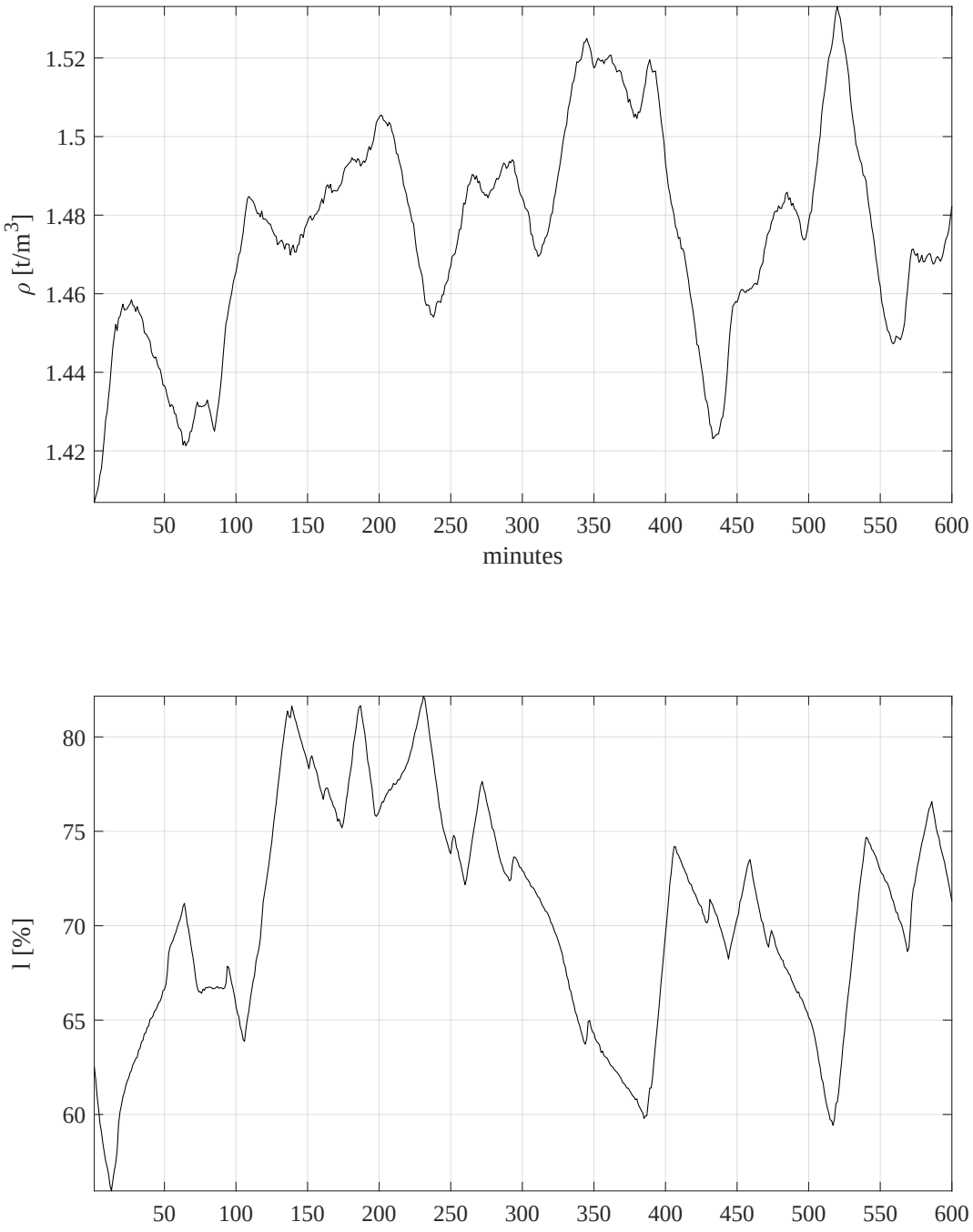

Figure 5.6. Density out of and level of BTT surge tank while operated under the baseline surge control strategy.

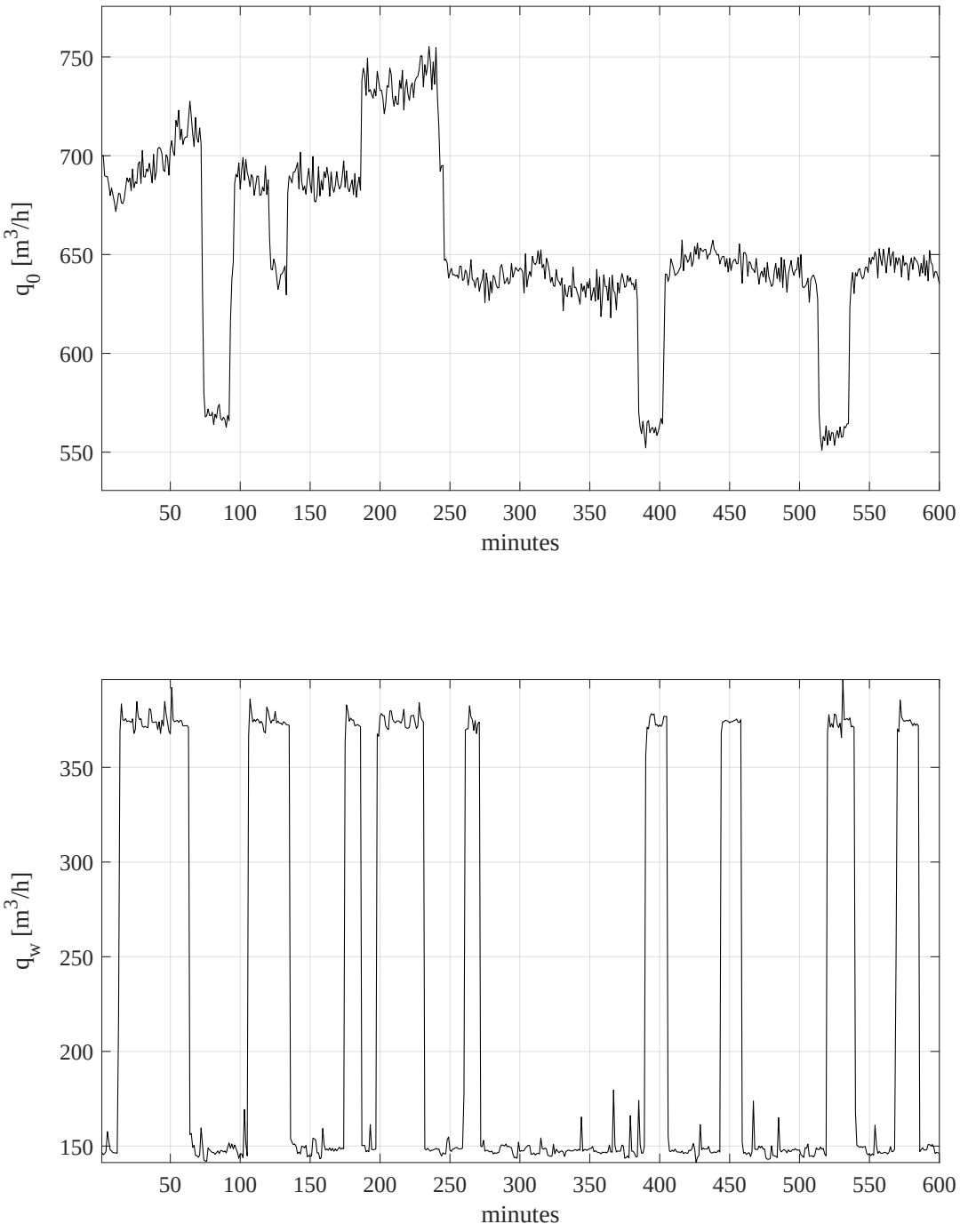

Figure 5.7. Waster addition to and flow out of the BTT surge tank while operated under the baseline surge control strategy.

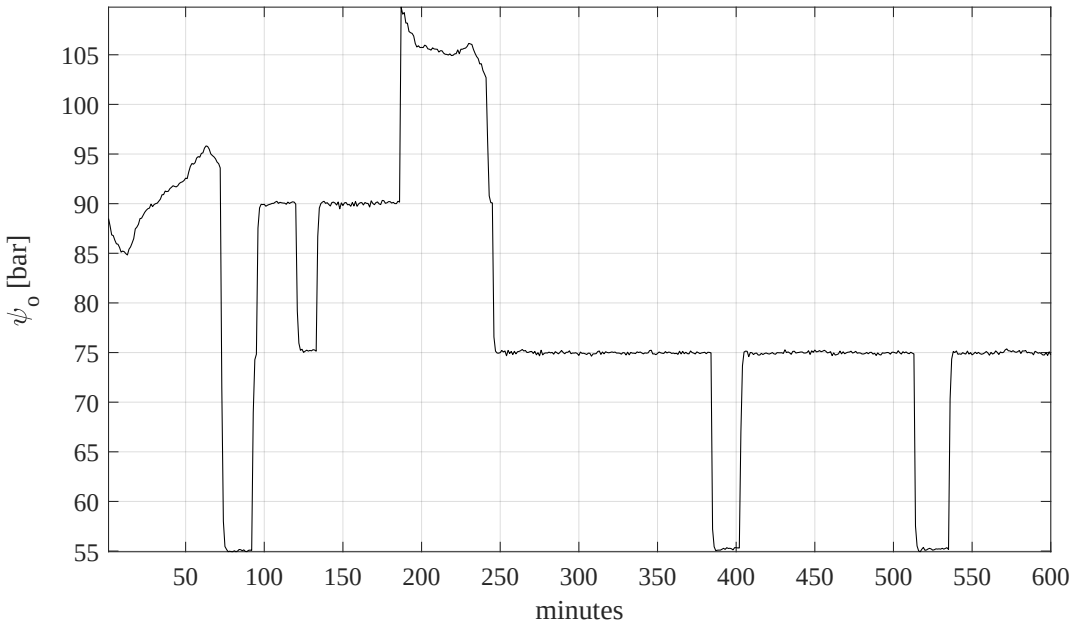

Figure 5.8. Output lines pressure and flow rate out of the BTT surge tank while operated under the baseline surge control strategy.

ρ_{target} to the nominal tank density $\bar{\rho}$ achieved during the previous day. Note, the nominal output flow $\bar{q}_o$ and tank density $\bar{\rho}$ sets the throughput of the chrome recovery circuit as a whole. Hence, operations need to maintain ρ_{target} within an acceptable range to deliver on the assumptions that motivated the business case discussed in Section 2.3.

Two controller simulations were performed. In the first simulation the surge tank level was allowed to move freely within upper and lower limits of 90 % and 40 % respectively. In practice a lower limit is chosen to protect the agitator assembly, which would get damaged if it was allowed to operate under no load. An upper limit is chosen to avoid overflow should there be inaccuracies in the level measurement and/or an unmeasured input into the tank. By allowing the tank level to move freely within these limits, the NMPC can absorb short term disturbances in for example input density ρ_i by reducing the input flow q_i.

Because of the settling of solids in the tailings dam sump ρ_i can decrease significantly. The tailings dam operators implement measures to alleviate these settling issues, but for the duration of the low input density the controller could decrease the input flow q_i to dampen the impact on ρ.

In the second simulation the surge tank level was maintained at a set point of 90 %. Note that in (4.5), the expression for the rate of accumulation of density, the volume appears in the denominator. Therefore, the tank volume acts as a buffer and maintaining the surge tank at a high volume will provide improved disturbance rejection.

A summary of the process variable targets and constraints used in the simulations is presented in Table 5.2. Apart for the level all targets and constraints were identical in both simulations.

Table 5.2. A summary of the process variable targets and constraints used in the controller simulations.

Process Variable	Target or Range Constraint
Level in simulation 1 l_1	$40 \leq l_a \leq 90$ %
Level in simulation 2 l_2	90 %
Tank density ρ_{target}	1.475 t/m^3
Input flow q_i	$250 \leq q_i \leq 500$ m^3/h
Total water addition q_w	$100 \leq q_w \leq 400$ m^3/h
Input flow step size Δq_i	$\Delta q_i \leq 150$ m^3/h
Water step size Δq_w	$\Delta q_w \leq 50$ m^3/h

The input flow is constrained to operate within upper and lower limits of 250 m^3/h and 500 m^3/h respectively. Plant knowledge dictates that the minimum input flow must be 250 m^3/h to avoid solids settling in the input line, which can result in the line choking. The maximum input flow is set to the maximum observed flow in the dataset used for model validation, as presented in Figure 5.5.

The input water is constrained to operate within upper and lower limits of 100 m^3/h and 400 m^3/h respectively. The minimum flow of water to the surge tank is set as the flow required to operate the screen. The maximum water addition is set as the maximum flow observed in the validation dataset.

A small cost is assigned to avoid overly aggressive moves in the input variables in order to minimise equipment wear. By simulation on the validation dataset it can be shown that setting both diagonal elements in S to 5×10^{-6} ensures that $\Delta q_i \leq 150$ m^3/h and $\Delta q_w \leq 50$ m^3/h.

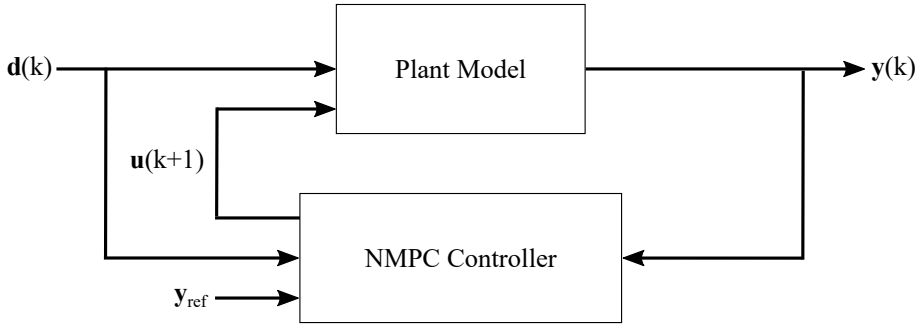

Figure 5.9. Block diagram of the NMPC controller and plant model configuration used to obtain the simulated results.

The design of the NMPC can be summarised as the constrained optimisation problem in (5.3) and (5.4) with:

$$N_p = 20,\ N_C = 10,\ \mathbf{y}_{ref} = \rho_{target},$$
$$\mathbf{Q} = 1, \text{ and } \mathbf{S} = \begin{bmatrix} 5 \times 10^{-6} & 0 \\ 0 & 5 \times 10^{-6} \end{bmatrix}. \tag{5.5}$$

The model is descretised using the 4th order Runge-Kutta method, with a step size of 1 minute. The simulated model outputs are initialised to the measured initial conditions of the system. Figure 5.9 presents a block diagram of the NMPC and the plant model configuration used to obtain the simulated results.

Figure 5.10 and Figure 5.11 present the results for simulations 1 and 2 respectively. In both simulations the plant model was subjected to the measured input flow and output flow disturbances shown in Figure 5.5.

In both simulations the NMPC maintains the tank level within the specified level range or at set point. The NMPC is able to reject much of the input density disturbances, however, it is unable to maintain the tank density ρ at the target density ρ_{target} at very low input densities.

Figure 5.12 compares the tank density ρ *measured*, obtained from the plant under baseline control, to the simulated tank densities, ρ *simulation 1* and ρ *simulation 2*, under NMPC control. The simulated NMPC performance improves on the baseline performance in both simulations. The standard deviation of the surge tank density in simulation 1 was 54 % lower compared to the measured density, while the standard deviation of the surge tank density for simulation 2 was 33 % lower. Therefore, by simulation

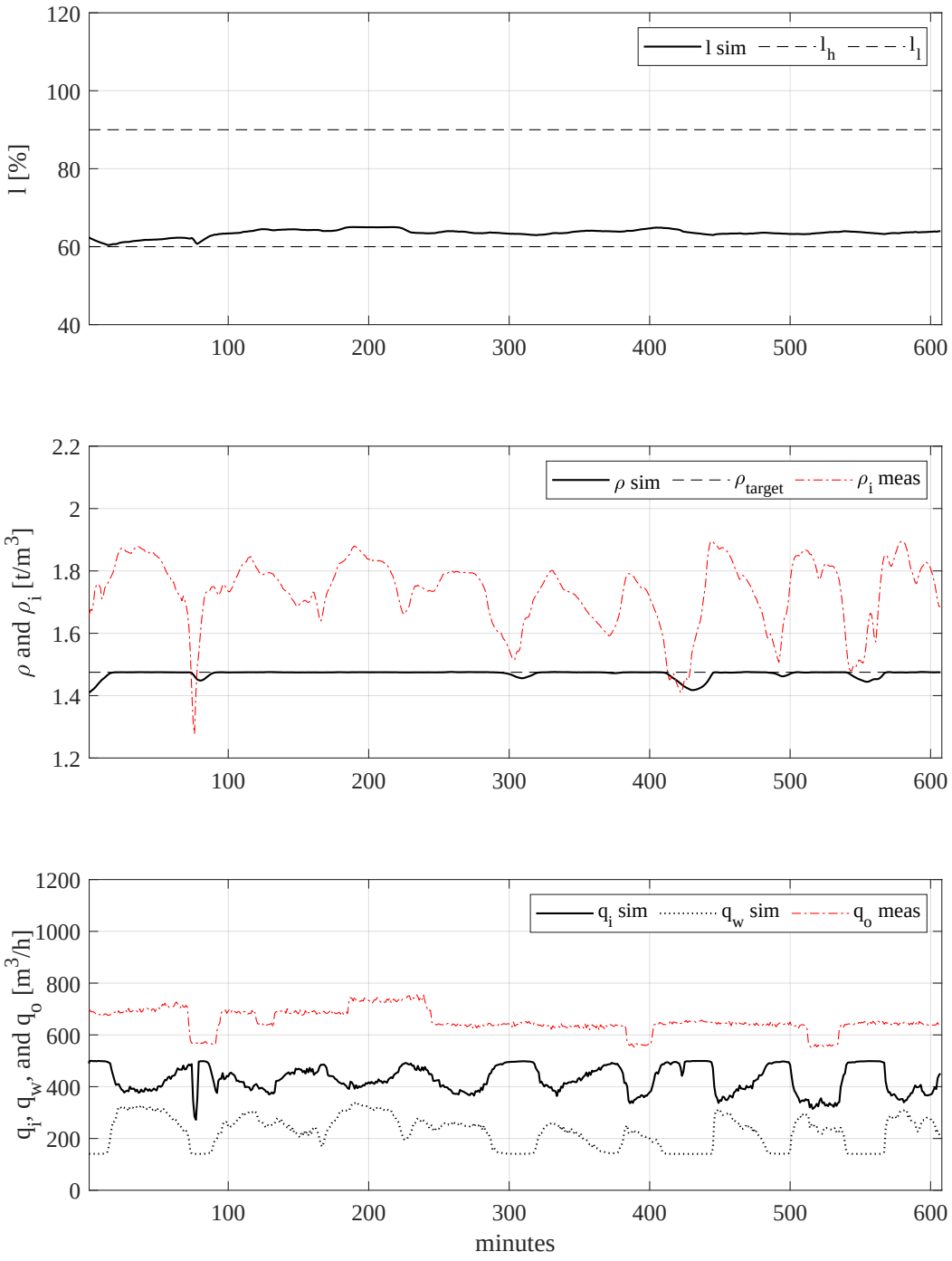

Figure 5.10. Simulation 1: NMPC control of the surge tank under measured input density and output flow disturbances, with the tank level allowed to travel within a specified range.

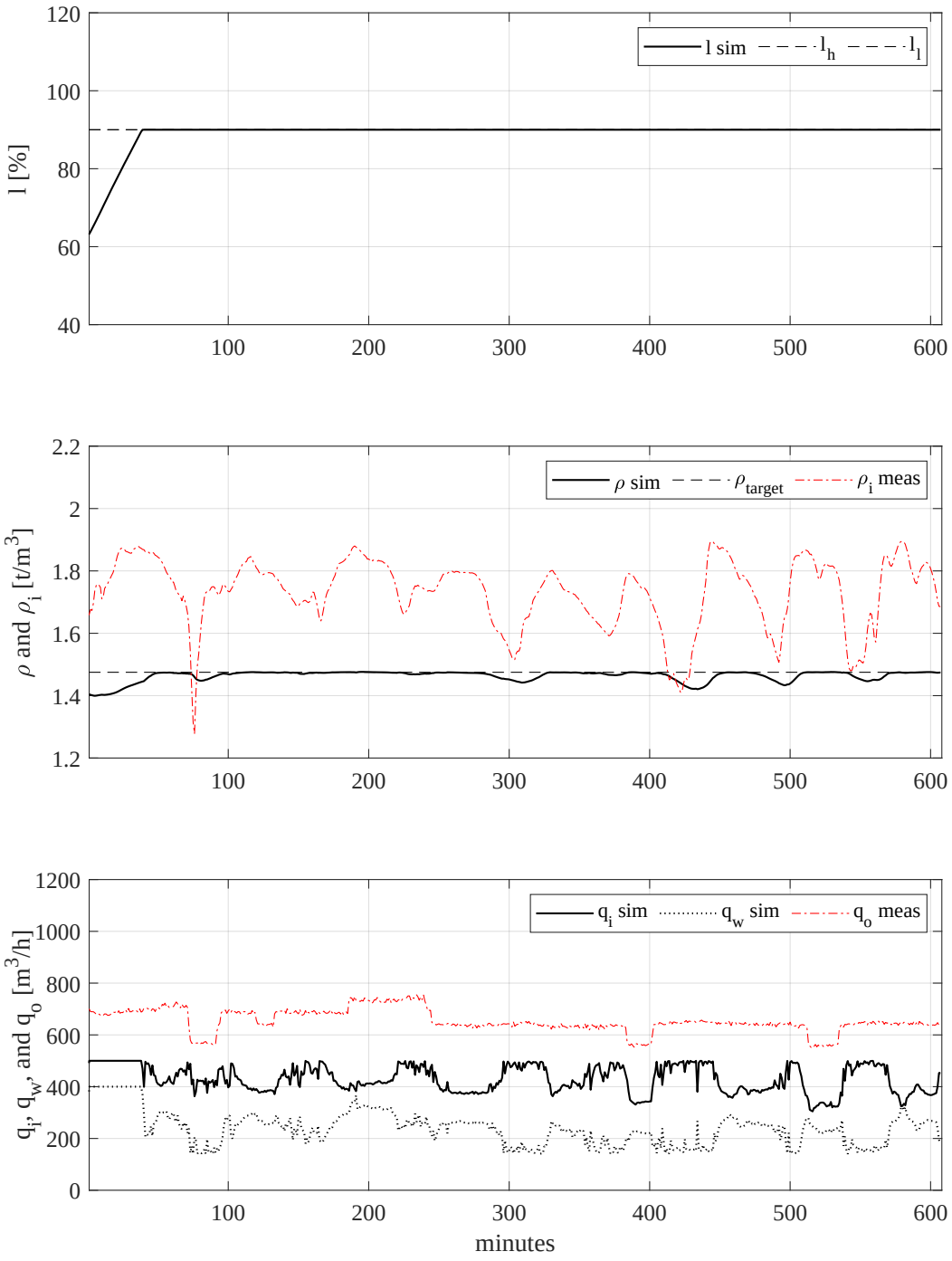

Figure 5.11. Simulation 2: NMPC control of the surge tank under measured input density and output flow disturbances, with the tank level maintained at set point.

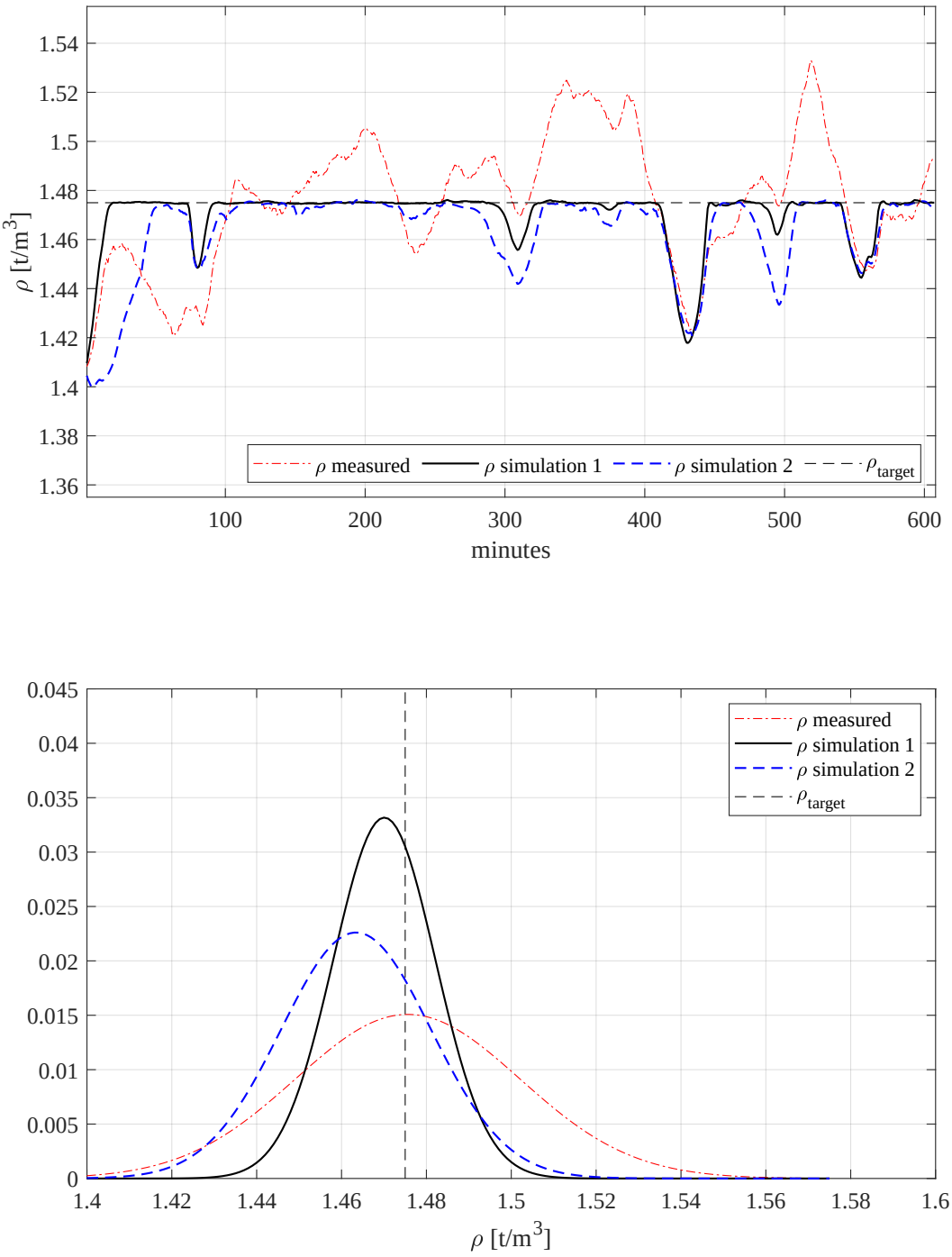

Figure 5.12. A comparison between the measured tank density under baseline control and the simulated tank density under NMPC control. In simulation 1 the tank level was allowed to travel within a specified range, while in simulation 2 the tank level was maintained at set point.

it is shown that an NMPC control strategy that maintains the tank level within a specified range is the superior control strategy.

5.4 CHAPTER CONCLUSION

This chapter focused on algorithm and controller design. A $(\mu + \lambda)$-evolutionary strategy was introduced to solve the BMR blending problem and nonlinear model predictive control (NMPC) for level averaging control of the surge tank in the tailings reprocessing circuit. The baseline control strategy for the industrial surge tank at the BTT plant was assessed using real operational data, which highlighted the strategy's response to variations in input density and flow rates. Two simulation tests were performed to identify an NMPC strategy: one allowed the surge tank level to fluctuate within limits, and the other maintained a constant level. The results demonstrate the NMPC's effectiveness in stabilising tank density, particularly when the tank level is allowed to vary within a range.

CHAPTER 6 CONTROLLER IMPLEMENTATION

6.1 CHAPTER OVERVIEW

The $(\mu+\lambda)$-EA developed in 5.2 was used to solve the input blending problem for the base metal refinery and the NMPC controller used in simulation 2 in Section 5.3.3 was implemented on the industrial BTT plant. This chapter presents details on algorithm and controller implementation, together with the results obtained.

6.2 BMR INPUT BLENDING USING AN $(\mu+\lambda)$-EA

The $(\mu+\lambda)$-EA was implemented using the Distributed Evolutionary Algorithms in Python (DEAP) (Fortin et al., 2012) package, which is a reproduction of the algorithm presented in Back et al. (2000). The effectiveness of the $(\mu+\lambda)$-ES is assessed using historical data from the BMR, and compared to the unblended feed and a purely randomised blend strategy. A dataset was obtained from the BMR that records the concentrations of contaminants in a matte stockpile containing 60 bags. Figure 6.1 presents the contaminant concentrations for each contaminant in this dataset.

Table 6.1. Hyperparameter selection for the $(\mu+\lambda)$-ES.

Parameter	μ	λ	ρ_{cross}	ρ_{mut}	ρ^{i}_{mut}	t_{sel}	n_{gen}	ω_{SiO_2}	ω_{Fe}	ω_{Se}	ω_{Te}
Value	500	300	0.5	0.4	0.03	2	1000	4	3	2	2

Unblended and randomised blending strategies are used as baseline strategies to evaluate the $(\mu+\lambda)$-ES's performance. For the unblended feed strategy the matte stock is arranged in the bag sequence in which it is received from the smelter. A random blend strategy would shuffle all bags in a random order, noting that during initialisation of the $(\mu+\lambda)$-ES algorithm, each individual in the population is created by shuffling the unblended bag sequence, and hence the best individual in the initial population represents the baseline random blend strategy performance.

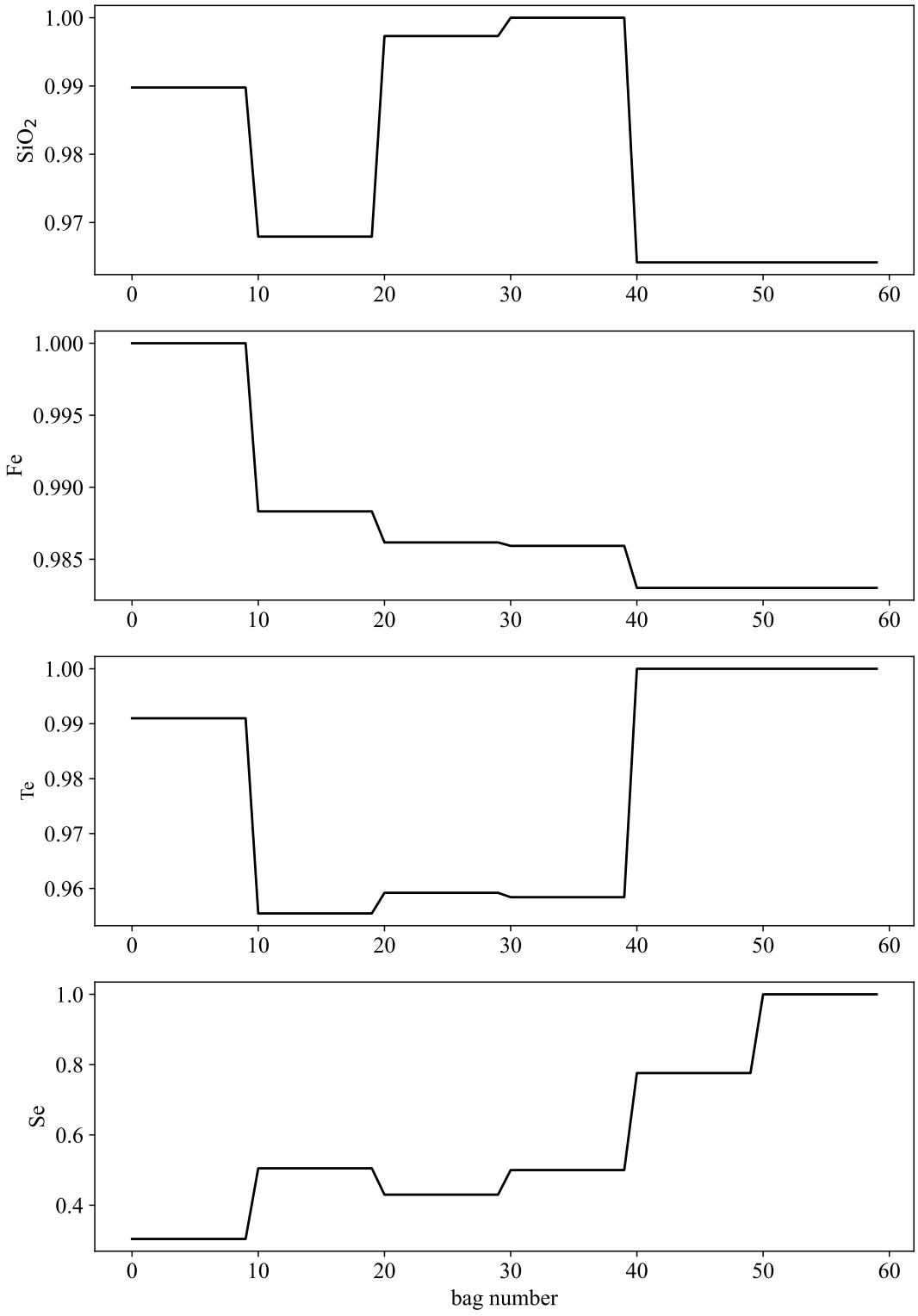

Figure 6.1. Normalised contaminant concentrations in the BMR matte stockpile.

Figure 6.2 presents the convergence plot for the $(\mu + \lambda)$-ES using the hyperparameters presented in Table 6.1. These hyperparameters were selected through manual tuning by iteratively adjusting

parameter settings and observing convergence behaviour. With the hyperparameters selected the algorithm repeatably converged to a good solution within a reasonable time frame and maintained sufficient population diversity to prevent premature plateauing. Eiben and Smit (2011) presents a thorough survey of different tuning approaches for EAs, which include sampling, screening, and model based methods.

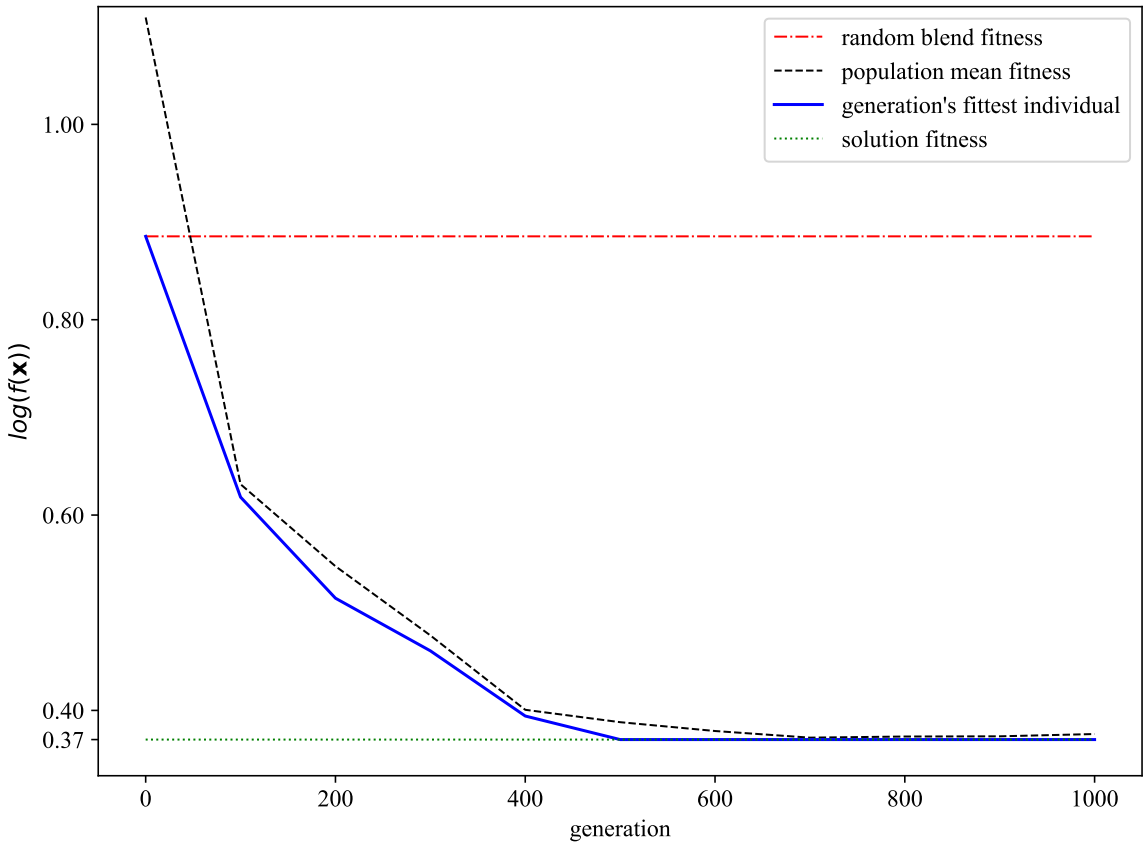

Figure 6.2. Progress and performance of the $(\mu + \lambda)$-ES blending strategy compared to an unblended and randomised blend.

The unblended sequence has a fitness of 26.63, the randomised blend fitness is 7.67, and the best individual in the final generation for the $(\mu + \lambda)$-ES has a fitness of 2.3. These fitness values do not hold absolute significance, but allows for a relative performance assessment. The $(\mu + \lambda)$-ES achieves an 91.2% improvement on the unblended strategy and an 69.5% improvement on the randomised blend strategy.

Figure 6.3 presents a visualisation of the SiO_2 blend achieved by the $(\mu + \lambda)$-ES compared to the unblended and random blend strategies. The SiO_2 blend for each approach is superimposed on the

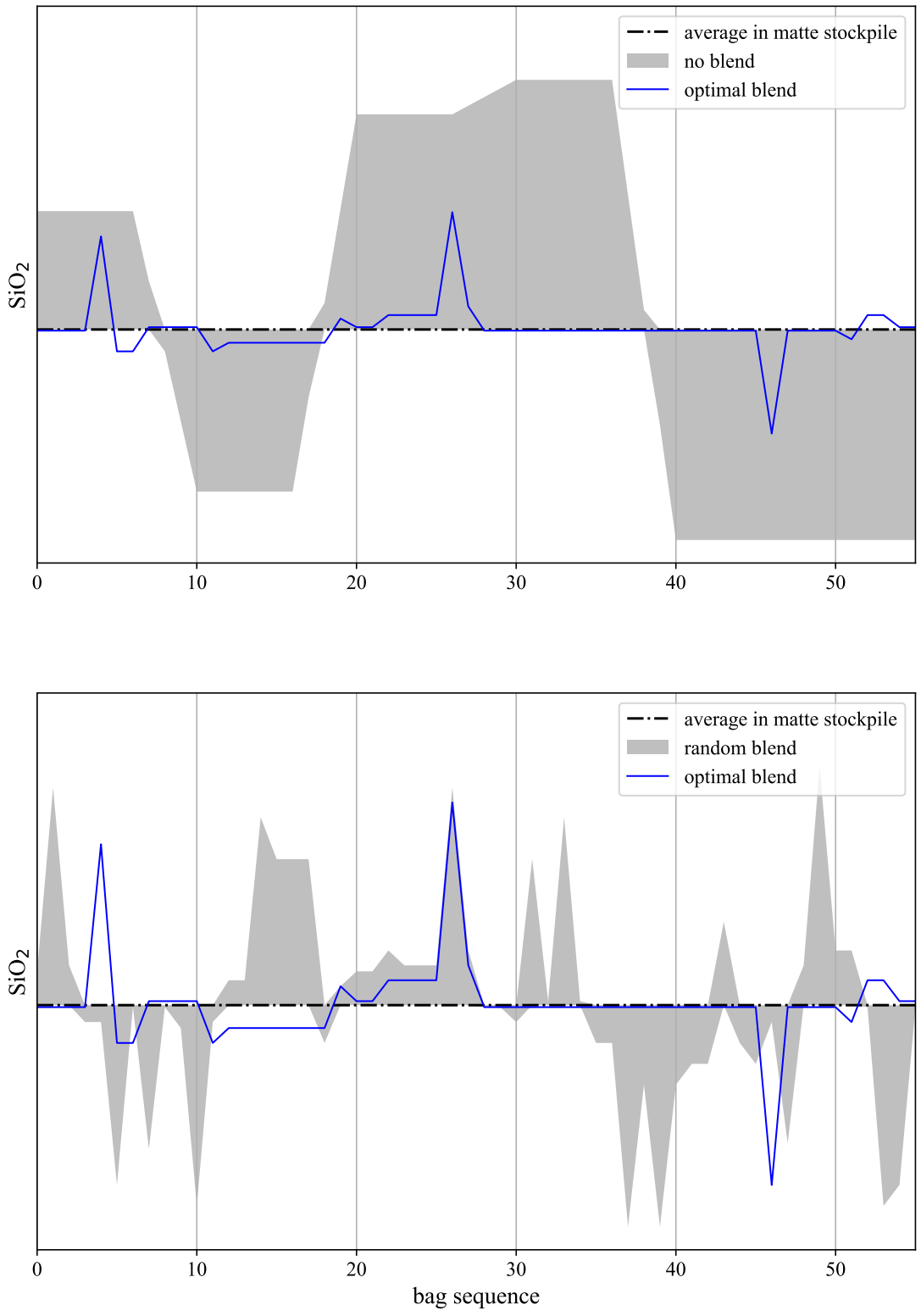

Figure 6.3. Four bag moving average of the SiO_2 optimal blend achieved with the $(\mu + \lambda)$-ES compared to the unblended feed (top) and randomised feed (bottom) strategies.

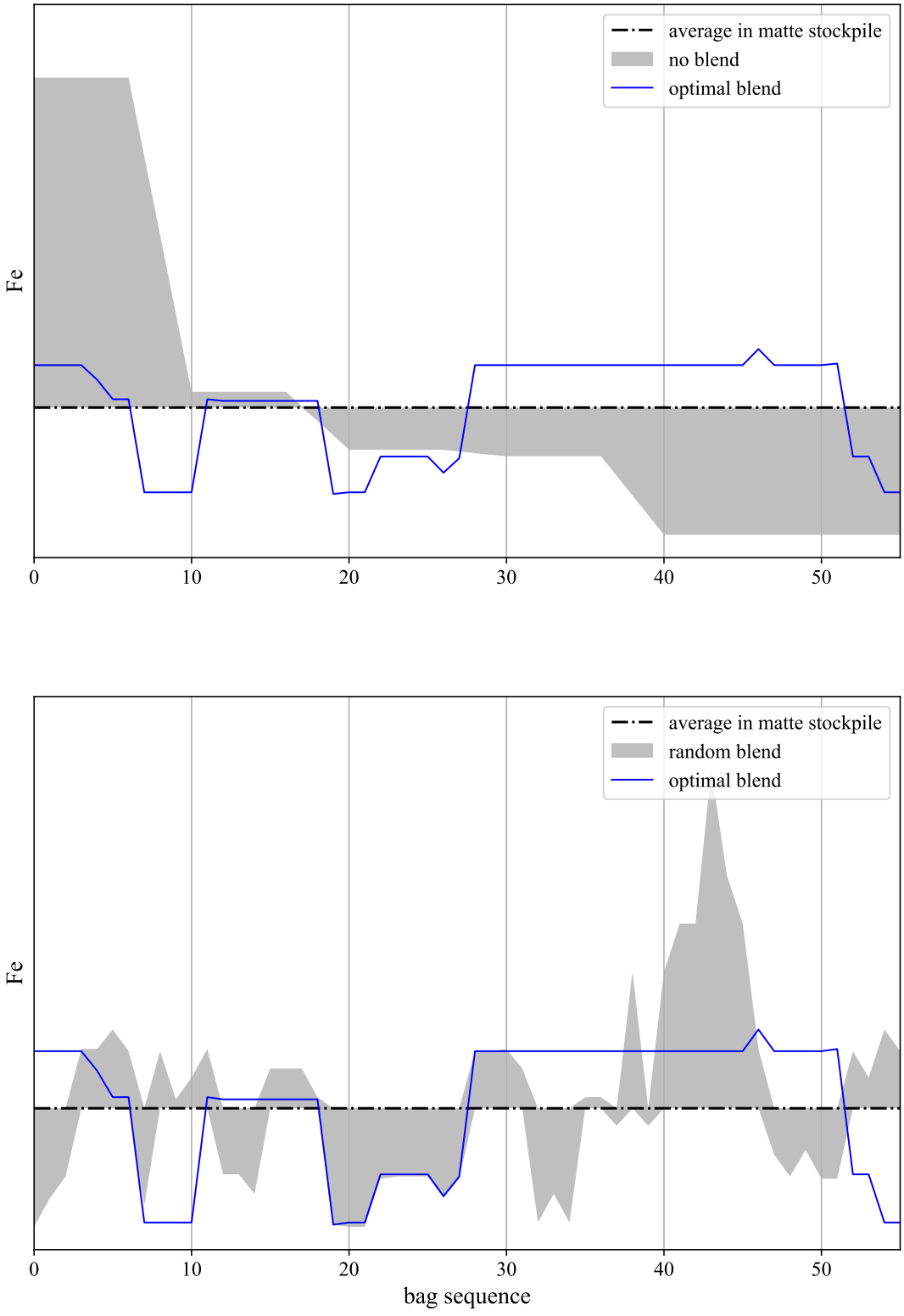

Figure 6.4. Four bag moving average of the Fe optimal blend achieved with the $(\mu + \lambda)$-ES compared to the unblended blow order (top) and randomised blow order (bottom).

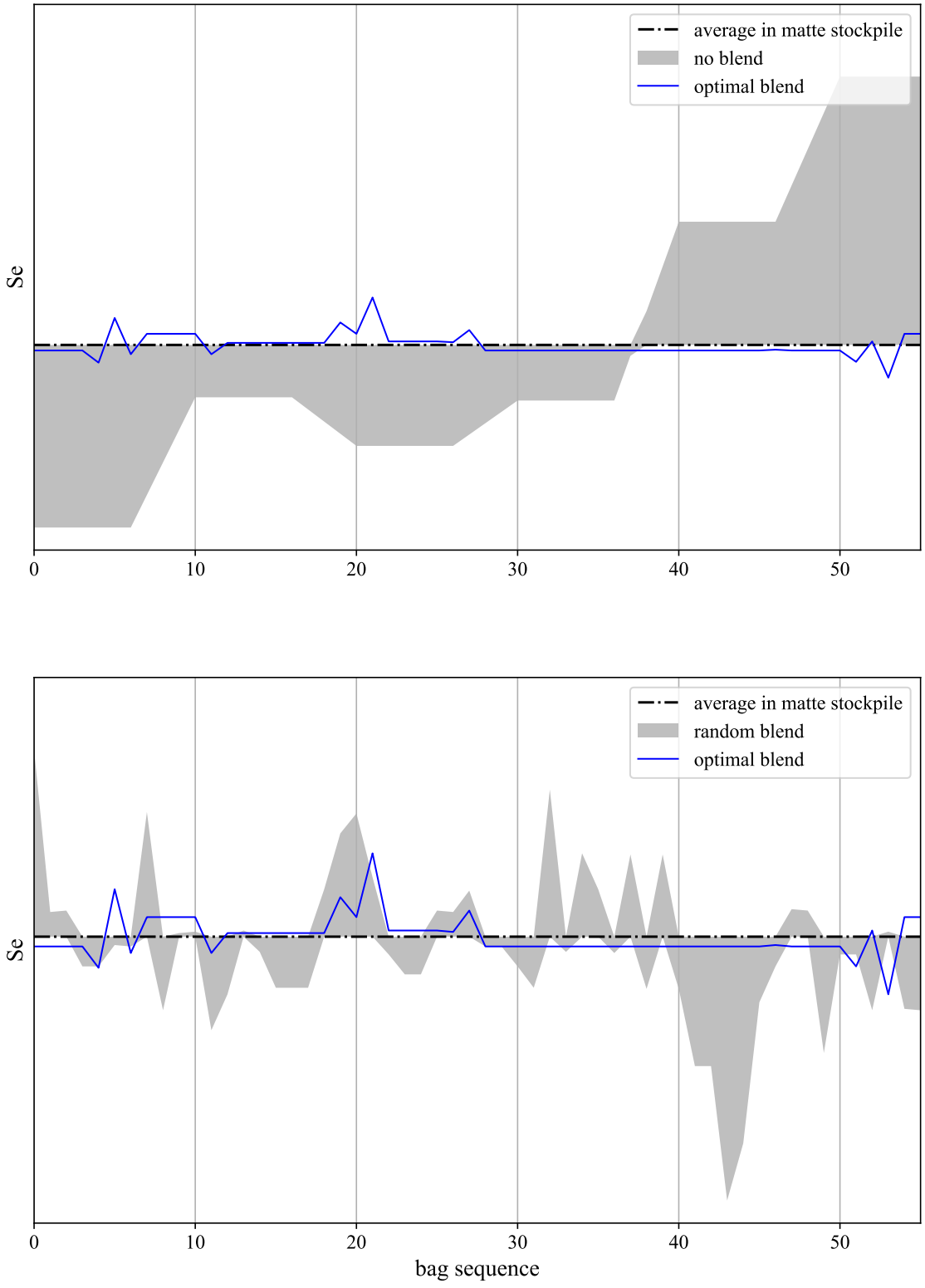

Figure 6.5. Four bag moving average of the Se optimal blend achieved with the $(\mu + \lambda)$-ES compared to the unblended blow order (top) and randomised blow order (bottom).

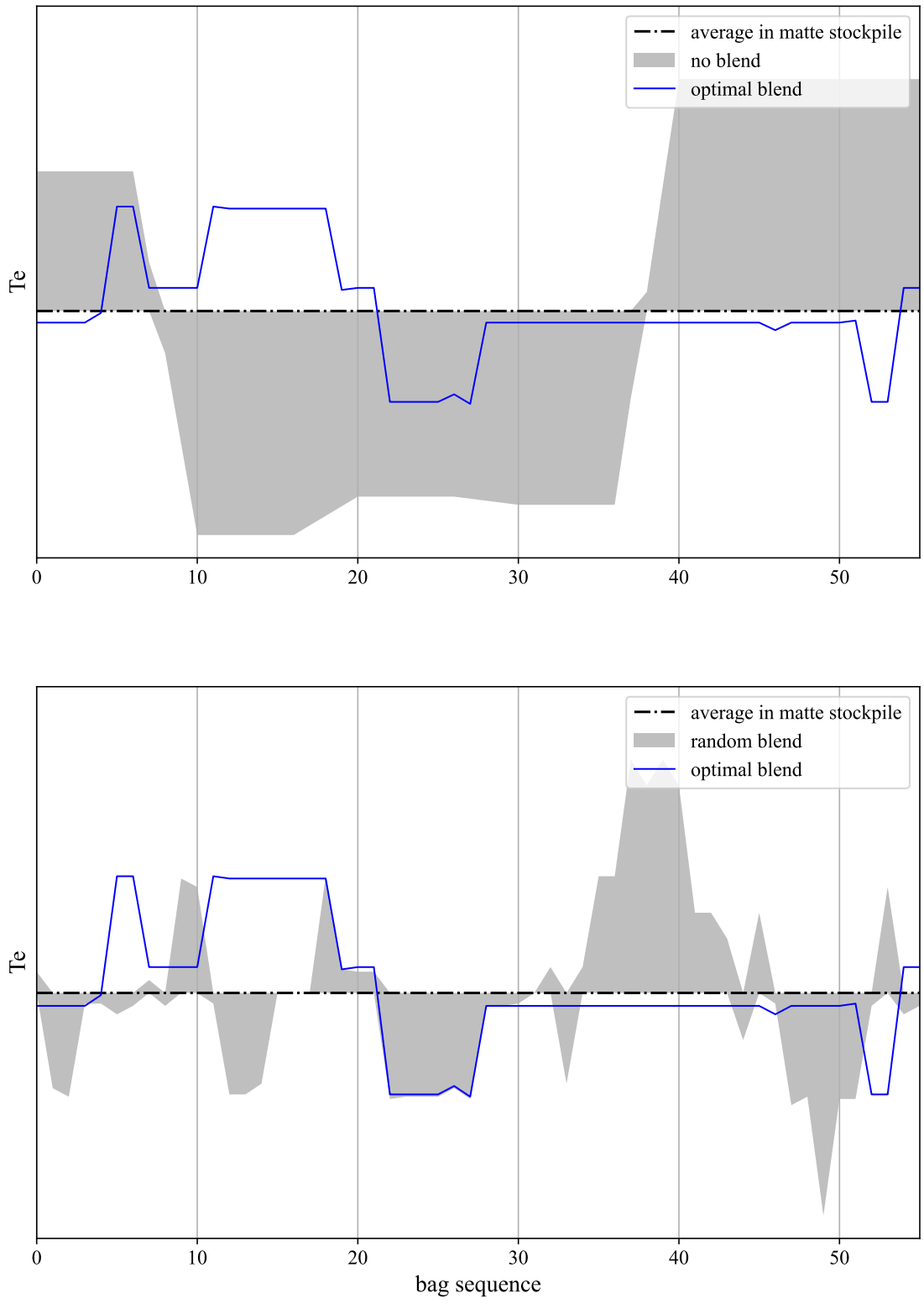

Figure 6.6. Four bag moving average of the Te optimal blend achieved with the $(\mu + \lambda)$-ES compared to the unblended blow order (top) and randomised blow order (bottom).

average concentration of the SiO_2 in the matte stock. Smaller deviations from the average are more appealing. The best individual in the final generation of the $(\mu + \lambda)$-ES improves 93.42% on the unblended strategy and 74.43% on the random blend strategy. Figures 6.4, 6.5, and 6.6 present visualisations of the blends achieved for the remainder of the contaminants. See Table 6.2 for a summary of the improvements obtained by the $(\mu + \lambda)$-ES over the unblended and random blend strategies.

Table 6.2. A summary of the performance improvement of the $(\mu + \lambda)$-ES compared to the unblended feed and randomised feed strategies.

Blend target	f($\boldsymbol{x}$)	SS_{SiO_2}	SS_{Fe}	SS_{Se}	SS_{Te}
Un-blended	91.19 %	93.42%	59.06%	96.89%	98.98%
Randomised	69.47 %	74.44%	25.54%	75.55%	37.31%

Note, that these blending improvements were assessed using the fitness function proposed in (5.1). Alternative definitions of fitness are also possible. For instance, while the $(\mu + \lambda)$-ES demonstrates significant improvements in reducing deviation from average contaminant concentration in a stockpile, as measured by the proposed fitness function, there are still occurrences of sudden increases in contaminant concentration, for example the spikes in SiO_2 concentration in Figure 6.3. An alternative fitness function that considers the rate of change could potentially reduce these contaminant concentration spikes. This can be explored in future work.

6.3 LEVEL AVERAGING CONTROL USING NMPC

The NMPC simulated in the previous section was implemented on the industrial plant using the GEKKO optimisation and machine learning library (Beal et al., 2018) in Python, using the interior point optimiser (IPOPT) algorithm (Wätcher and Biegler, 2006) to solve the nonlinear optimisation problem presented in (5.4) and (5.4). Other than the simulation study, the objective for the NMPC implemented on the plant was to maintain the surge tank level within 70 % and 90 %, with a target density of 1.45 t/m^3. The level range was chosen, expecting that the pressure controller on the output of the tank adjusts the pressure set point to maintain the tank level within this range. Therefore, to avoid pressure setpoint changes that would negatively effect cyclone efficiency, the same level range as used during simulation was chosen for the NMPC implemented on the plant. The target density was chosen as the nominal output density at the time.

Consider that for the steady-state operating point presented in Section 4.3.3, $\|\mathbf{B}\| \times \left\|\mathbf{B}^{-1}\right\| = 960 >> 1$. Hence at this operating point the system is ill-conditioned, which may result in excessively large adjustments in the manipulated inputs $\mathbf{u}$. To prioritise equipment health, the NMPC was constrained to not move the input flow to the surge tank by more than 20 m^3/min and the water addition to the surge tank by more than 50 m^3/min.

Custom modules were developed on an Allen-Bradley programmable logic controller (PLC) (Rockwell Automation, Inc., 2024) and a user interface on AVEVA Wonderware's (AVEVA, Inc., 2024) supervisory control and data acquisition (SCADA) system. These modules allowed, for example, switching between the baseline controller and the NMPC, and monitored communication health using a watchdog timer. A number of interlocks were also implemented on the PLC to disable the NMPC when conditions were not suitable. A key interlock was developed for when the input line would choke. If the surge tank was to remain under NMPC control with an input line choke, the tank density would plummet as the NMPC would demand an ever higher input flow of tailings to counter a dropping density while only water was being added.

Figure 6.7 presents a time series plot of 180-hours before and 60-hours after the NMPC was switched on. This dataset records the hourly-averages of the key surge tank measures. The baseline controller maintained the level between 60 % and 90 % by stepping the pressure target on the output line at fixed step sizes. Note, the pressure of the output line is maintained by adjusting the output flow rate q_o. The baseline controller maintained the surge tank density by adjusting the water addition to the tank.

The level under NMPC control has a lower variability, i.e. a lower standard deviation. Although the output flow has lower variability under NMPC control, there remains some variability. Noting that the output flow from the surge tank is adjusted by a baseline controller, i.e. is a disturbance to the NMPC, there remains an opportunity to review the baseline control strategy to not unnecessarily adjust this flow to compensate for density or level disturbances.

Table 6.3 presents a summary of the results using the permutation method for comparing two independent groups, as described in Wilcox (2003). For each key plant variable a permutation test was performed to determine if there is a statistically significant difference between its mean or standard deviation before and after the NMPC was put online. The null hypothesis h_0 of equal mean or equal standard deviation is rejected with 5 % confidence if the significance value is less than 0.05.

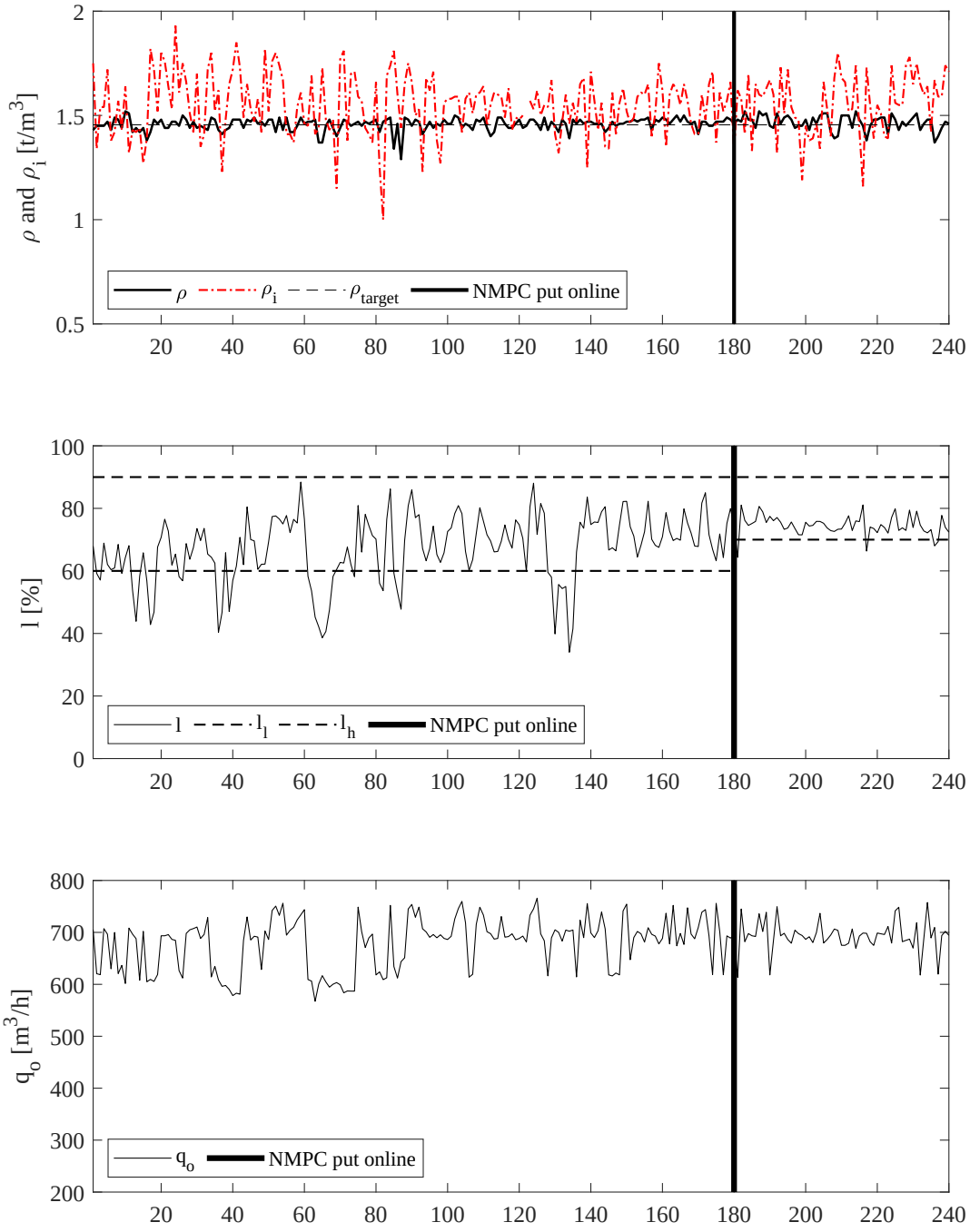

Figure 6.7. Time series of surge tank variables before and after the NMPC was put online.

Figures 6.8 to 6.13 present the individual permutation tests from Table 6.3. For each test in these figures a positive test statistic (red) would indicate that the mean or standard deviation has decreased after the NMPC was put online. Alternatively, a negative test statistic would indicate that the mean or standard deviation has increased after the NMPC was put online.

Table 6.3. A summary of the results, comparing the differences in mean and standard deviation before and after the NMPC was put online.

Process Variable	Mean Before, After	Accept or Reject h_0 : Equal Mean (Significance)
ρ_i	1.548, 1.560	accept (0.266)
ρ_p	1.478, 1.500	reject (0.002)
q_i	511.186, 524.903	accept (0.164)
q_p	674.531, 674.277	reject (0.022)
m_i	385.274, 423.058	reject (0.000)
m_p	454.584, 472.779	reject (0.001)
Process Variable	Standard Deviation Before, After	Accept or Reject h_0 : Equal Standard Deviation (Significance)
ρ_i	0.147, 0.145	accept (0.476)
ρ_p	0.058, 0.106	accept (0.117)
q_i	89.762, 94.094	accept (0.453)
q_p	16.833, 6.526	accept (0.284)
m_i	52.472, 56.061	accept (0.310)
m_p	42.146, 30.580	reject (0.015)

Figure 6.8 and Table 6.3 show that both the mean and standard deviation of the input density to the plant ρ_i is comparable for the periods before and after the NMPC is put online. There is no significant difference in the standard deviation of plant output density ρ_p, as shown in Figure 6.9, however, the mean plant output density has significantly increased while the NMPC was online. *A comparable mean plant input density with a significantly higher plant output density can only be explained by improved dewatering ability of the plant while the NMPC was online.*

Figures 6.10 and 6.11, and Table 6.3 show that while there is no significant difference in the mean input flow to the plant q_i, the mean output flow from the plant q_p is significantly lower while the NMPC was online. *This lower volumetric flow rate of tailings from the plant can also be explained by an increase in the dewatering ability of the plant with the NMPC online, considering that an increase in water recovered via the thickener overflow would imply less water reporting to the plant output.*

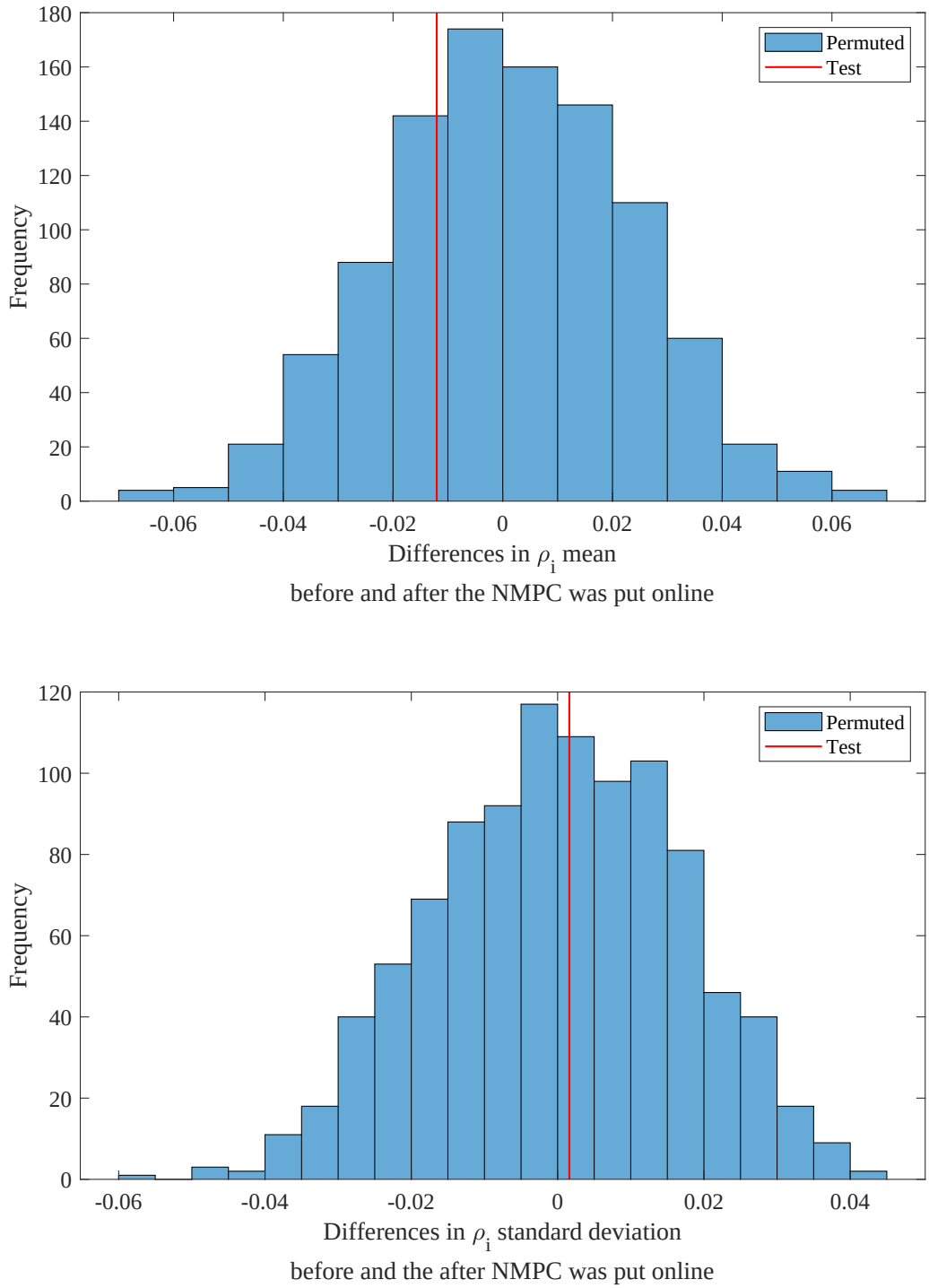

Figure 6.8. Permutation test results for the input density of the plant, recorded before and after the NMPC was put online.

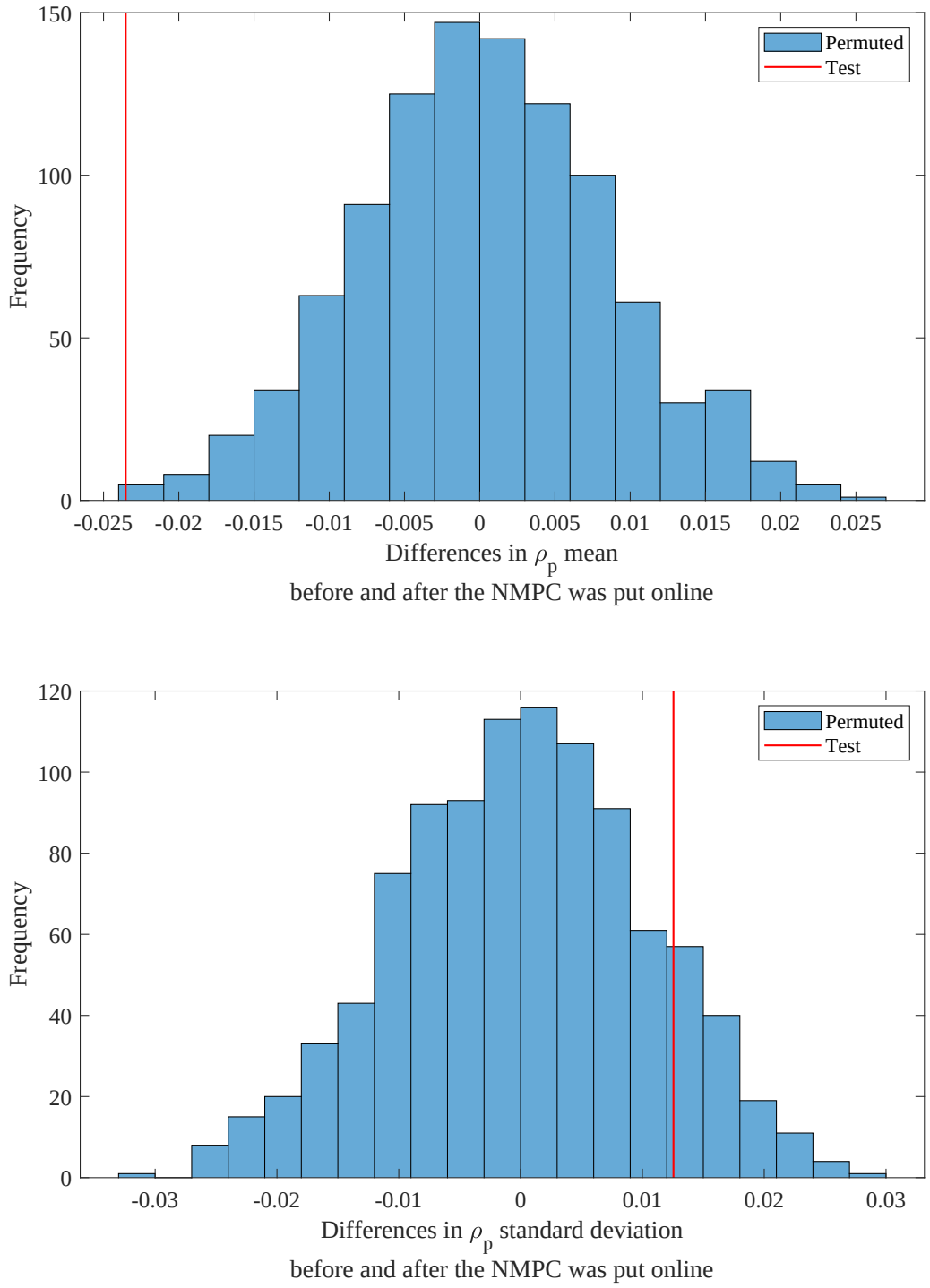

Figure 6.9. Permutation test results for the surge tank density, recorded before and after the NMPC was put online.

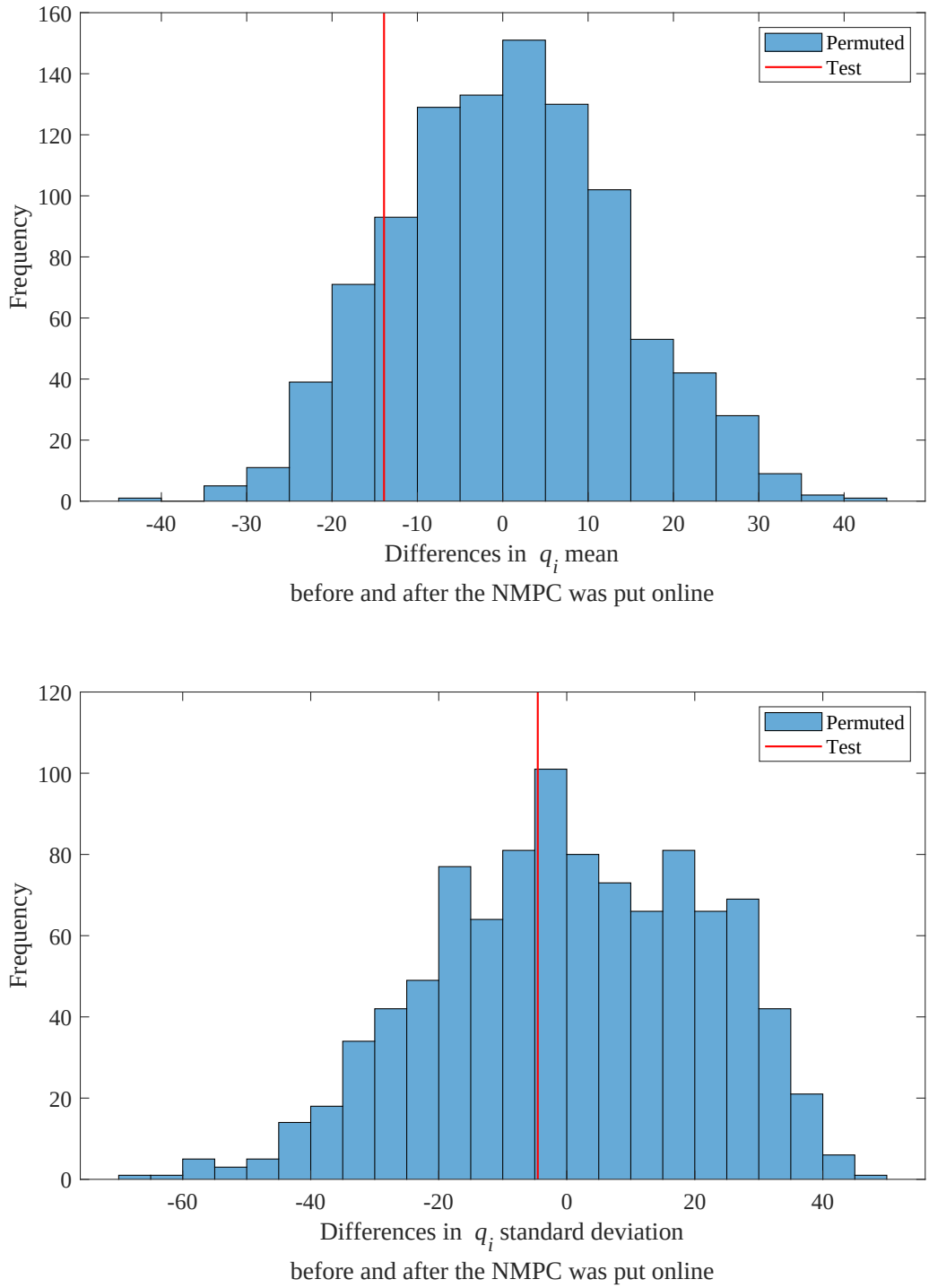

Figure 6.10. Permutation test results for the input flow to the plant, recorded before and after the NMPC was put online.

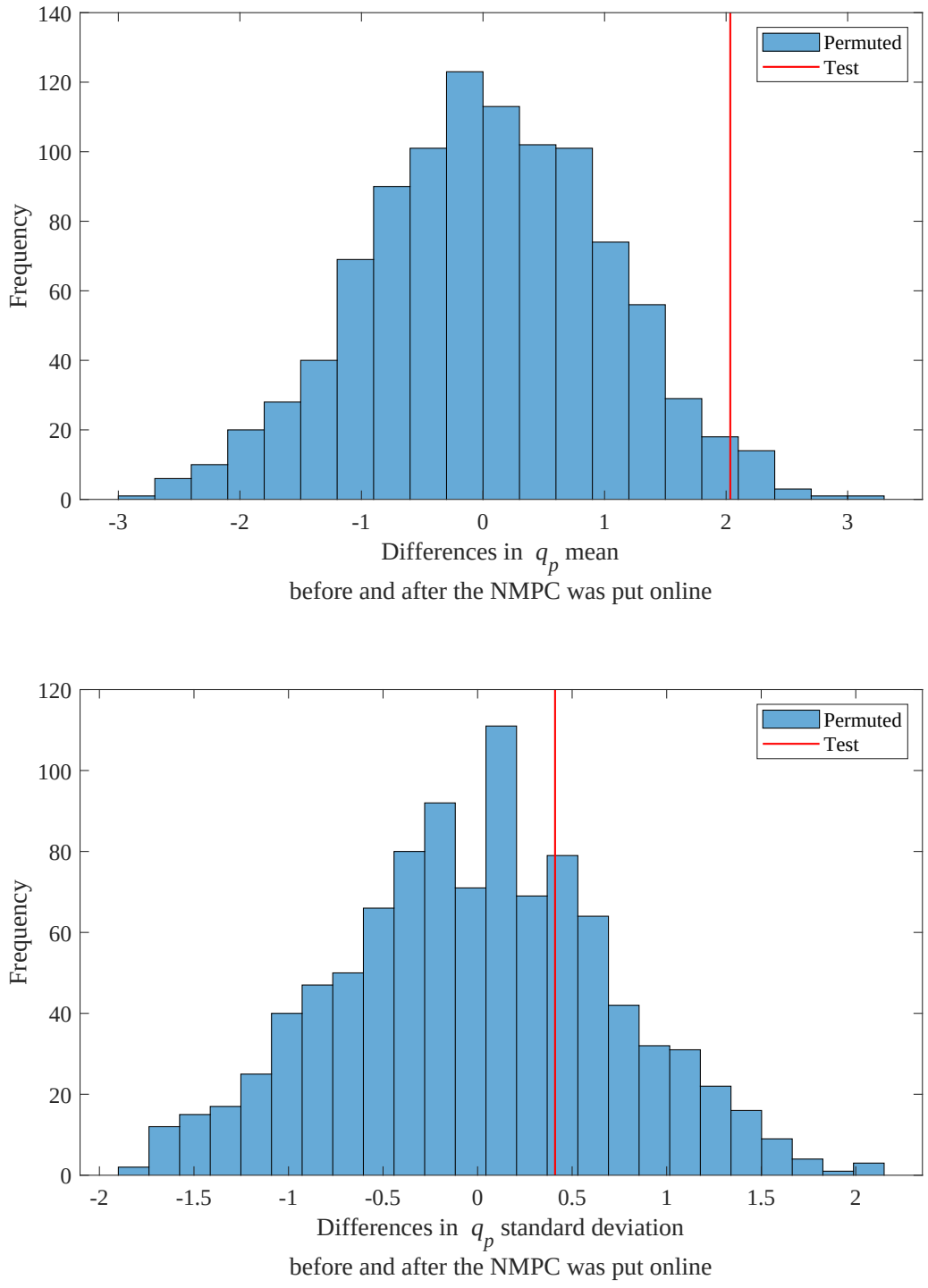

Figure 6.11. Permutation test results for the output flow to the plant, recorded before and after the NMPC was put online.

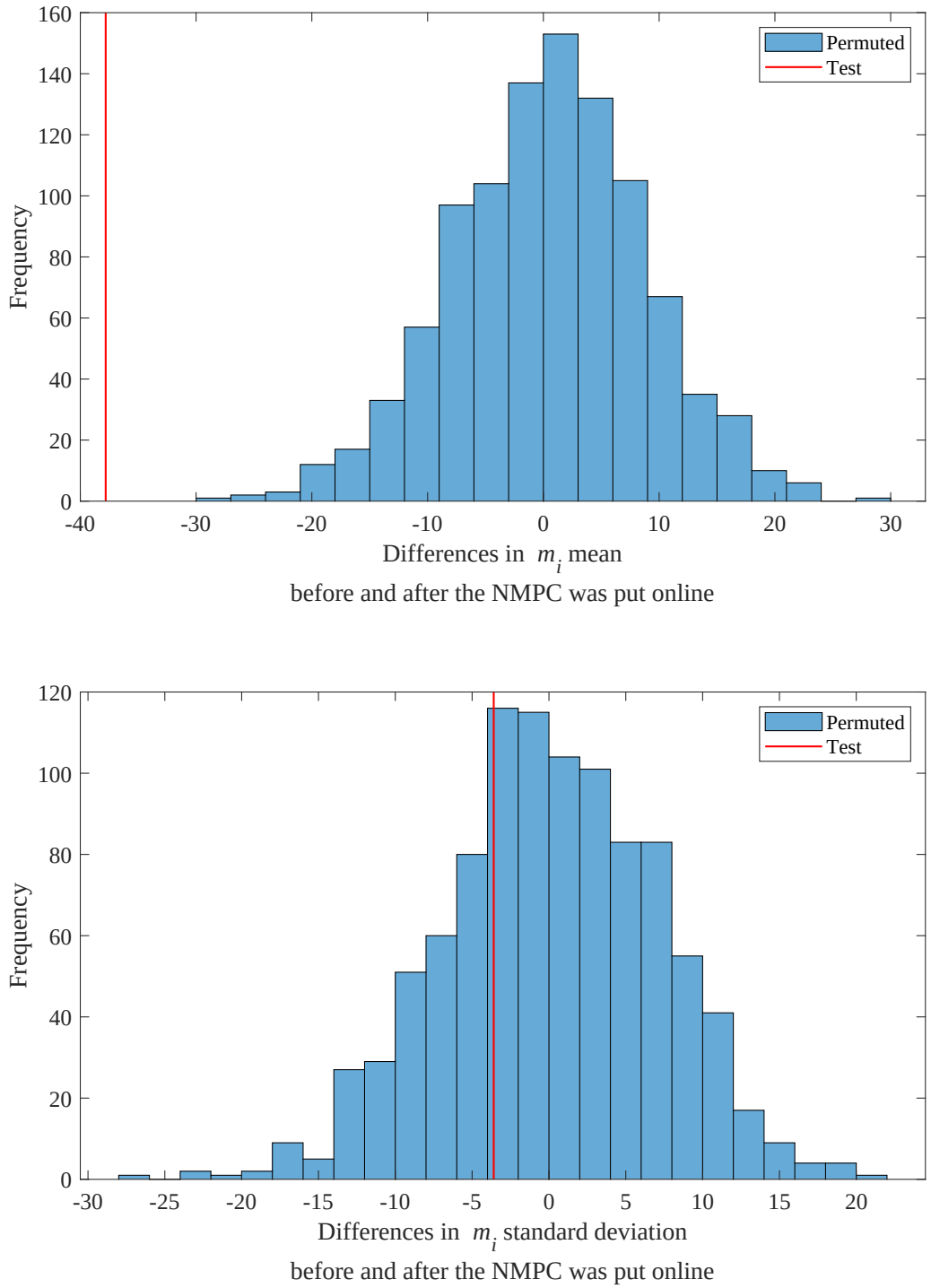

Figure 6.12. Permutation test results for the input mass flow of the plant, recorded before and after the NMPC was put online.

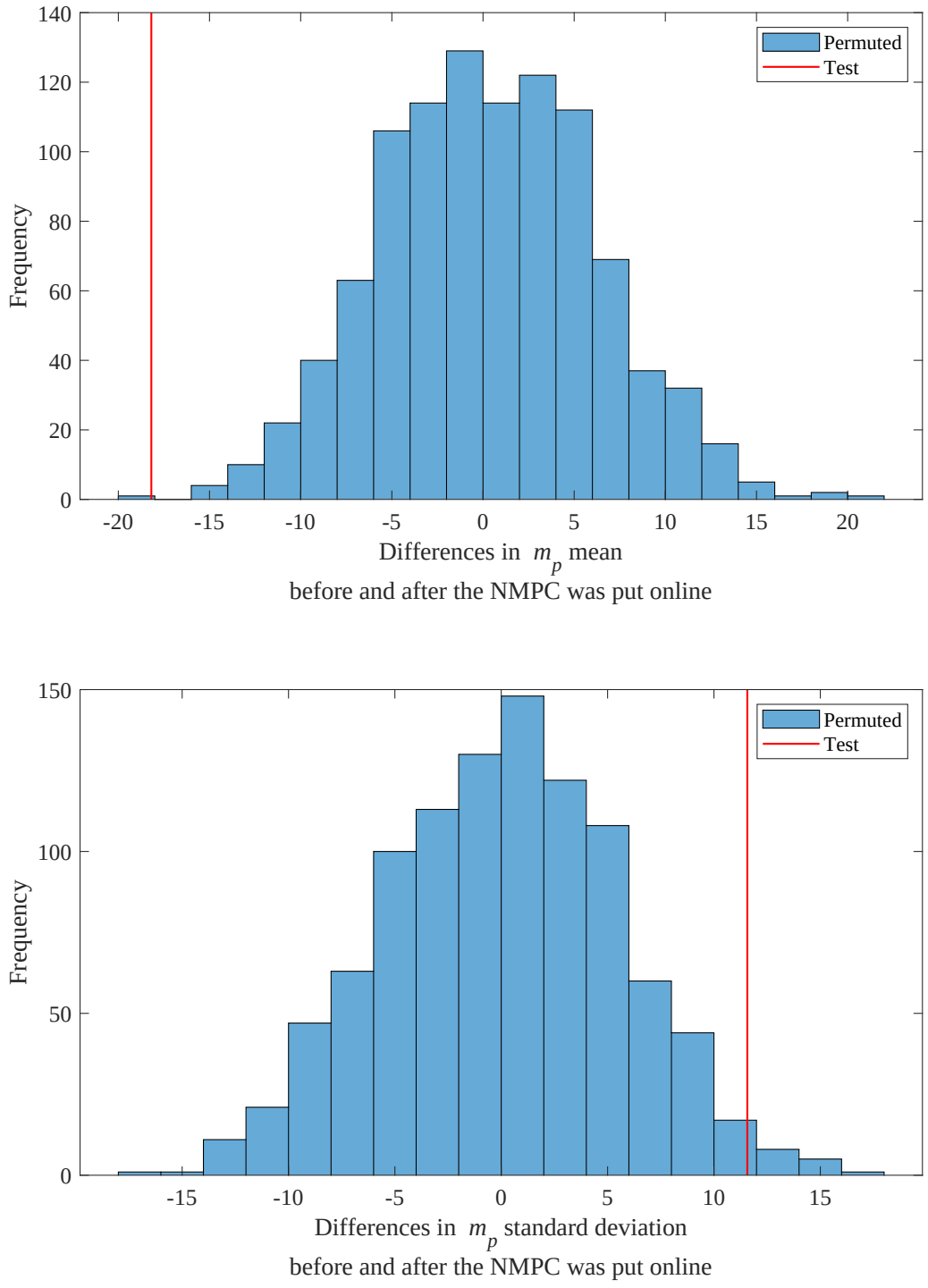

Figure 6.13. Permutation test results for the output mass flow of the plant, recorded before and after the NMPC was put online.

The concentration of solids by weight in a slurry c_s is calculated as follows (Michaelides et al., 2016):

$$c_s = 100\left(\frac{\frac{\rho_s}{\rho_{sl}} - \rho_s}{1 - \rho_s}\right), \tag{6.1}$$

with ρ_s the density of the solids and ρ_{sl} the density of the slurry. Plant operations assume a solids density of $\rho_s = 4.1$ t/m^3. By comparing the difference between the concentration of solids in the plant output before and after the NMPC is put online, *it is possible to show that an additional 0.063 ton water was recovered for every ton solids produced when the NMPC was online. This amounts to approximately 13 m^3/h, or 5 % of the water contained in the tailings product of the plant*.

Both the mean mass flow into and out of the plant, m_i and m_p, are significantly higher for the period when the NMPC was online, as shown in Figures 6.12 and 6.13, and Table 6.3. The standard deviation of the input mass flow was comparable, while the standard deviation for the output mass flow significantly lower while the NMPC was online. The variability of the mass flow from the plant is therefore improved, with a 27 % lower standard deviation, while the NMPC was online.

6.4 CHAPTER CONCLUSION

The chapter demonstrates the successful application of the $(\mu + \lambda)$-ES and NMPC optimisation and control methods developed in this thesis. Both methods were implemented using non-proprietary software packages available for Python.

The evolutionary algorithm showed significant improvements in the input blending of an industrial dataset, outperforming both unblended and random blend strategies. Similarly, the NMPC was implemented in an industrial tailings reprocessing circuit and results demonstrate its ability to improve both the stability of mass flow and water recovery in the circuit.

CHAPTER 7 CONCLUSIONS

7.1 SUMMARY

This thesis explores two optimisation and control solutions aimed at enhancing the consistency of material flow and composition into metallurgical operations. The first solution optimises the input blend to a BMR, while the second improves the surge control in hydromining based tailings reprocessing circuits. The central theme for this research establishes process optimisation and control as a key enabling discipline for advancing ESG objectives.

This chapter outlines the operational challenges investigated, motivations for the specific approaches used, and the process efficiency improvements achieved. A review is presented of the ESG considerations and objectives enhanced by these optimisation and control solutions, together with motivations for future research to further strengthen the findings of this thesis.

7.2 BMR INPUT BLENDING USING THE $(\mu + \lambda)$-ES

The overview of the BMR process presented in Section 2.2 describes the input blending challenge for the operations, aiming to minimise variations in mass flow of contaminants into the plant. These variations can be linked to downstream instabilities negatively impacting process efficiency and ESG objectives. This blending problem is considered a sequencing problem, with individual bags of different composition selected for loading into the hopper that feeds the mill. The size of the search space – the set of all possible sequences of bags – is vast, growing exponentially with each additional bag added to the stockpile in front of the operations.

The discrete nature of this problem, combined with the complexity of its search space, motivates the use of a heuristic optimisation approach, as described in Section 3.2. Section 4.2, argues for an EA as

the preferred optimisation approach, and models the blending objectives, laying the foundation for algorithm selection and design.

A $(\mu + \lambda)$-ES algorithm is developed in Section 5.2 and implemented in Section 6.2, optimising the input blend of an industrial dataset, and comparing results to baseline strategies. The $(\mu + \lambda)$-ES significantly outperforms the baseline strategies, achieving a 93.42% improvement over an unblended strategy and a 74.43% improvement over a randomised strategy.

7.3 LEVEL AVERAGING CONTROL USING NMPC

The overview of a chrome tailings reprocessing circuit that relies on hydromining for the recovery and transportation of tailings from a tailings dam is presented in Section 2.3. This reprocessing circuit includes a process known as BTT, which is tasked with dewatering and stabilising the incoming tailings. Due to the open-loop and largely unregulated nature of hydromining activities at the tailings dam, the feed to BTT is subject to significant disturbances in both flow and density. The BTT process depends on a surge tank to attenuate these incoming surges in density and flow. The efficiency of water and overall chrome recovery from the circuit is significantly influenced by this surge tank's ability to dampen incoming surges.

In the literature review in Section 3.3, level averaging control is identified as the established surge control strategy. However, the literature does not adequately address the multivariate problem of attenuating both flow and density surges. Existing studies primarily focus on rejecting disturbances in flow, assuming constant density when considering mass flow stability.

A rigorous model describing the dynamics of the surge tank was developed in Section 4.3 and validated in Section 4.3.1. Through simulation using this rigorous dynamic model, as demonstrated in Section 4.3.3, it was shown that the density disturbances typical to hydromining based tailings reprocessing drive a gain inversion in the density model of the surge tank. This motivated for an nonlinear surge control strategy.

An NMPC strategy was developed in Section 5.3, where, through simulation using an industrial dataset, the effectiveness of different control strategies was assessed. It was determined that allowing the tank level to fluctuate between specified lower and upper limits improves density surge attenuation compared to maintaining the tank level at the specified upper limit. This strategy of a fluctuating level

was demonstrated to be superior to a constant high-volume strategy, even though the dynamics of density are dampened by the reciprocal of the tank volume, as identified in the rigorous model.

The NMPC was implemented in an industrial tailings reprocessing circuit as presented in Section 6.3, where the results demonstrate a significant improvements in BTT process efficiencies. Specifically, under NMPC control, improvements in both mass flow stability and water recovery were observed.

7.4 ESG CONSIDERATIONS

ESG objectives benefiting from the process efficiency improvements achieved with the $(\mu + \lambda)$-ES for input blending and the NMPC for level averaging control, as discussed above, include:

- **Environmental Stewardship:**
  - **Improved hazardous reagent efficiency**: Improved blending of selenium and tellurium into the BMR benefits downstream stability of these contaminants. With sulfur dioxide used as a reagent for extraction of these contaminants, improved blending benefits the efficiency of sulfur dioxide usage. This decreases the potential for hazardous emissions from the operations.
  - **Enhanced water recovery**: The NMPC optimisation of the the tailings reprocessing circuit improves water recovery. This lowers the overall consumption of fresh water in the circuit, thereby minimising the environmental footprint of the operations.
  - **Energy efficiency**:Both optimised input blending and the dewatering of tailings contribute to energy efficiency improvements. Input blending lowers the risk of product contamination, reducing the likelihood of product rework and associated energy consumption. Dewatering of tailings reduces the solids content in the water supply to the hydromining activities. This lowers a recirculating load of solids in the circuit, reducing the energy consumed by pumps, which require more power to maintain desired flow rates when transporting mixtures with higher viscosity and densities.
- **Resource Efficiency:** Improving the blend of contaminants into the circuit reduces the need for rework due to contamination. As with first pass efficiency challenges, rework inevitably results in primary product losses to waste and secondary product streams, thereby negatively impacting primary resource efficiency. Improved stability of mass flow under NMPC control in the tailings

reprocessing circuit directly benefits efficiency and recoveries of downstream processes, where gravity separation that is sensitive to mass flow disturbances is used for classification. These resource efficiency improvements enhances the value extracted from each ton of ore, thereby reducing waste and the overall environmental degradation associated with the organisation's mining activities.

- **Social Impact and Community Engagement:** Improved input blending benefits the efficiency of sulfur dioxide usage and reduces hazardous emissions. This has direct benefits on the health and safety of workers and surrounding communities. By reducing the potential for hazardous emissions, operations demonstrate a commitment to minimising its social and environmental impact.
- **Governance and Compliance:** While reducing sulfur dioxide emissions directly assists with compliance to emissions' standards, these control and optimisation initiatives indirect benefits governance. Considering that governance represents the rules and processes by which operations are managed, investing in control and optimisation initiatives like these that focus on environmental and social benefits demonstrate a commitment to sustainability, and a governance culture that values long term resilience over short term gains.

In summary, the applications of $(\mu + \lambda)$-ES for input blending to the BMR and NMPC for level averaging control in tailings reprocessing illustrate a comprehensive approach to improving ESG performance across multiple dimensions. These optimisation and control initiatives not only enhance operational efficiency and reduce environmental impact, but also support broader ESG objectives by demonstrating a commitment to sustainable and responsible management practices.

7.5 FUTURE WORK

There are several opportunities for research to strengthen and build on the findings presented in this thesis. This section recommends future research topics aimed at enhancing both process efficiency and ESG objectives through process optimisation and control.

7.5.1 Automated storage and retrieval assisted input blend optimisation

The BMR input blending strategy assumes equal bag weights, as described in Section 5.2. This assumption was a necessary sacrifice in model accuracy to facilitate a more practical strategy that does not require any capital investment. It cannot be guaranteed that operations will have access to individual bags in the stockpile, however, access to individual blows is more likely. Consequently, the solution vector provided by the $(\mu + \lambda)$-ES specifies a sequence of blows, meaning that operations

should align with the algorithm's recommendations as long as any bag from a specified blow is fed into the plant.

Future research could explore enhancing the accuracy of the input blend model by abandoning the equal weight assumption and integrating an automated storage and retrieval system (AS/RS) (Karakaya et al., 2021). The inclusion of AS/RS would require a capital investment, as it relies on material handling equipment (MHE). Investing in MHE would necessitate a more detailed assessment of the return on investment for AS/RS supported input blend optimisation.

7.5.2 Enhanced NMPC density disturbance rejection using adaptive machine learning

The MPC formulation presented in (5.3) employs a crude approach to predicting the input disturbance values over the prediction horizon N_p by assuming disturbances remain constant. Alternatively, the MPC could assume that the gradient of the input disturbances remain constant of N_p.

Enhancing the accuracy of input disturbance prediction is expected to positively impact NMPC performance. Future research could investigate the use of machine learning (ML) for predicting input disturbances, with a focus on comparing the accuracy of ML based predictions against baseline strategies, such as the assumption of constant input disturbances or constant gradients of input disturbances. An adaptive ML approach (Vatankhah and Farrokhi, 2017) should be considered, given that the dynamics at the tailings dam are likely to change over time due to the varying characteristics of the tailings and the migration of operations to different areas of the dam.

7.5.3 Plant-wide optimisation and control for enhanced ESG

Both the BMR blending optimisation and the level averaging control problems represent local or unit optimisation and control studies within processing plants. These case studies focused on the optimisation and control of single processing steps–the blending of input to a BMR and the surge control into a tailings reprocessing circuit, respectively. While demonstrating benefits to overall process efficiency, including comprehensive ESG objectives, these studies primarily considered localised optimisation and control challenges.

Plant-wide control (Larsson and Skogestad, 2000; Skogestad, 2004) refers to the design and implementation of strategies and systems across the overall process, such as the entire chemical plant. The approach starts with a top-down analysis, which includes specifying economic and operational

objectives. Future research should explore integrating ESG considerations, specifically by reviewing existing plant-wide control strategies to enhance overall sustainability and efficiency.

A key consideration of the top-down analysis involves determining where the production rate should be set. Typically, control strategies set this rate at the input to the plant (Skogestad, 2004), resulting in the loss of a degree of freedom for internal processing steps within the plant. Consequently, internal flows may reach their constraints and become bottlenecks. This can lead to local process inefficiencies negatively impacting ESG, as the rate of incoming mass flow needs to be accommodated under constraint conditions.

Future research should consider plant-wide optimisation and control that emphasise ESG enhancement. For example, allowing the production rate to be set at constrained processes internal to the operations will would allow for an extra degree of freedom to improve the control of these constrained processes. This will lead to local process efficiency improvements, and comprehensive ESG benefits. The hypothesis is that allowing the production rate to be set at internal bottlenecks will not negatively impact overall production throughput, as improvements to the stability of internal processes should enhance plant-wide stability and throughput.

REFERENCES

Adetola, V., DeHaan, D., Guay, M., 2009. Adaptive model predictive control for constrained nonlinear systems. Systems and Control Letters 58, 320–326.

Alcalde, J., Kelm, U., Vergara, D., 2018. Historical assessment of metal recovery potential from old mine tailings: A study case for porphyry copper tailings, Chile. Minerals Engineering 127, 334–338.

Allgöwer, F., Findeisen, R., Nagy, Z., 2004. Nonlinear model predictive control: From theory to application. Journal of the Chinese Institute of Chemical Engineers 35, 299–315.

Amini, S.H., Vass, C., Shahabi, M., Noble, A., 2022. Optimisation of coal blending operations under uncertainty – robust optimization approach. International Journal of Coal Preparation and Utilisation 42, 30–50.

AVEVA, Inc., 2024. Wonderware | Operations and Performance Software Solutions. URL: `https://www.aveva.com/en/solutions/operations/wonderware/`. accessed on February 04 2024.

Bäck, T., 1996. Evolutionary algorithms in theory and practice: Evolution strategies, evolutionary programming, genetic algorithms. Oxford University Press.

Back, T., Fogel, D.B., Michalewicz, Z. (Eds.), 2000. Evolutionary computation 1: Basic algorithms and operators. Institute of Physics Publishing.

Beal, L.D.R., Hill, D.C., Martin, R.A., Hedengren, J.D., 2018. GEKKO optimization suite. Processes 6, 106.

Blickle, T., Thiele, L., 1995. A comparison of selection schemes used in genetic algortihms. Technical report from the Computer Engineering and Communication Networks Lab. Swiss Federal Institute of Technology. Gloriastrasse 35, 8092, Zurich, Switzerland.

Blomsma, F., Brennan, G., 2017. The emergence of circular economy: A new framing around prolonging resource productivity. Journal of Industrial Ecology 21, 603–614.

Bonami, P., Biegler, L.T., Conn, A.R., Cornuéjols, G., Grossmann, I.E., Laird, C.D., Lee, J., Lodi, A., Margot, F., Sawaya, N., Wächter, A., 2008. An algorithmic framework for convex mixed integer nonlinear programs. Discrete Optimization 5, 186–204.

Chanda, E.K.C., Dagdelen, K., 1995. Optimal blending of mine production using goal programming and interactive graphics systems. International Journal of Surface Mining, Reclamation and Environment 9, 203–208.

Coello Coello, C.A., 2002. Theoretical and numerical constraint-handling techniques used with evolutionary algorithms: A survey of the state of the art. Computer Methods in Applied Mechanics and Engineering 191, 1245–1287.

Coetzee, R., 2016. Platinum group metals behaviour during iron precipitation and goethite seeding in nickel sulphate solution. Masters thesis. University of Stellenbosch. Stellenbosch, South Africa.

Craig, I.K., 1997. On the role of the general control problem in engineering education. IFAC Proceedings Volumes 30, 201–204.

Craig, I.K., Henning, R.D.G., 2000. Evaluation of advanced industrial projects: A framework for determining economic benefit. Control Engineering Practice 8, 769–780.

Crisafulli, S., Peirce, R.D., 1999. Surge tank control in a cane raw sugar factory. Journal of Process Control 9, 33–39.

Curry, J.A., Ismay, M.J.L., Jameson, J.G., 2014. Mine operating costs and the potential impacts of energy and grinding. Minerals Engineering 56, 70–80.

Davis, L., 1985. Applying adaptive algorithms to epistatic domains, in: Proceedings of the International Joint Conference on Artificial Intelligence, IEEE Computer Society Press, Los Angeles. pp. 162–164.

Dontsov, E.V., Perice, A.P., 2014. A new technique for proppant schedule design. Hydraulic Fracturing Journal 1, 1–8.

Dorfling, C., 2012. Characterisation and dynamic modelling of the behaviour of platinum group metals in high pressure sulphuric acid/oxygen leaching systems. Ph.D. thesis. University of Stellenbosch. South Africa.

Eberhart, R., Shi, Y., 2001. Particle swarm optimization: Developments, applications and resources. Proceedings of the 2001 Congress on Evolutionary Computation 1, 81 – 86.

Eiben, A., Smit, S., 2011. Parameter tuning for configuring and analyzing evolutionary algorithms. Swarm and Evolutionary Computation 1, 19–31.

Eksteen, J.J., Van Beek, B., Bezuidenhout, G.A., 2011. Cracking a hard nut: An overview of Lonmin's operations directed at smelting of UG2-rich concentrate blends. Journal of the Southern African Institute of Mining and Metallurgy 111, 681 – 690.

Eom, M., Kim, B.I., 2023. Combinatorial benders decomposition for melted material blending systems considering transportation and scheduling. International Journal of Production Research 61, 3481–3503.

Falagán, C., Grail, B.M., Johnson, D.B., 2017. New approaches for extracting and recovering metals from mine tailings. Minerals Engineering 106, 71–78.

Fogel, L.J., Owens, M.J., Walsh, M.J., 1966. Artifical intelligence through simulated evolution. Wiley.

Fortin, F.A., De Rainville, F.M., A., G.M., Parizeau, M., Gagne, C., 2012. Deap: Evolutionary algorithms made easy. Journal of Machine Learning Research 13, 2171–2175.

Franzin, A., Stützle, T., 2019. Revisiting simulated annealing: A component-based analysis. Computers & Operations Research 104, 191–206.

Ghodrat, M., Qi, Z., Kuang, S.B., Ji, L., Yu, A.B., 2016. Computational investigation of the effect of particle density on the multiphase flows and performance of hydrocyclones. Minerals Engineering 90, 55–69.

Gous, G., Wiid, A., Le Roux, J., Craig, I., 2023. Advanced regulatory control techniques for improved averaging level control performance. Industrial & Engineering Chemistry Research 62, 15578–15587.

Gros, S., Mario, Z., Rian, Q., Bemporad, A., Moritz, D., 2020. From linear to nonlinear MPC: Bridging the gap via the real-time iteration. International Journal of Control 93, 62–80.

Hann, D., 2022. Copper tailings reprocessing. Materials and Geoenvironment 68, 7–16.

Hansen, N., Arnold, D.V., Auger, A., 2015. Handbook of Computational Intelligence. Springer. chapter Evolution Strategies. pp. 871–898.

Ilka, A., Veseleý, V., 2015. Gain-scheduled MPC design for nonlinear systems with input constraints. IFAC-PapersOnLine 48, 912–917.

Karakaya, E., Vinel, A., Smith, A.E., 2021. Relocations in container depots for different handling equipment types: Markov models. Computers & Industrial Engineering 157, 107311.

Kennedy, J., Eberhart, R., 1999. Discrete particle swarm optimization, illustrated by the traveling salesman problem, in: Corne, D., Dorigo, M., Glover, F. (Eds.), New Ideas in Optimization. McGraw-Hill, pp. 219 – 228.

Khan, K.D., Spurgeon, S.K., 2006. Robust MIMO water level control in interconnected twin-tanks using second-order sliding mode control. Control Engineering Practice 14, 375–386.

Kossoff, D., Dubbin, W.E., Alfredson, M., Edwards, S.J., Macklin, M.G., Hudson-Edwards, K.A., 2014. Mine tailings dams: Characteristics, failure, environmental impacts, and remediation. Applied Geochemistry 51, 229–245.

van Laarhoven, P., Aarts, E., 1987. Simulated annealing: Theory and applications. Kluwer Academic Publishers.

Lakerveld, R., Benyahia, B., Heider, P.L., Zhang, H., Braatz, R.D., Barton, P.I., 2013. Averaging level control to reduce off-spec material in a continuous pharmaceutical pilot plant. Processes 1, 330–348.

Lambooy, T., 2011. Corporate social responsibility: Sustainable water use. Journal of Cleaner Production 19, 852–866.

Larsson, T., Skogestad, S., 2000. Plantwide control - a review and a new design procedure. Modeling, Identification, and Control 21, 209–240.

Lee, M., Shin, J., 2009. Constrained optimal control of liquid level loops using a conventional proportional-integral controller. Chemical Engineering Communications 196, 729–745.

Liu, X., Wang, D., Yin, Y., Cheng, T., 2023. Robust optimization for the electric vehicle pickup and delivery problem with time windows and uncertain demands. Computers & Operations Research 151, 106–119.

Luyben, W.L., 2020. Liquid level control: Simplicity and complexity. Control Engineering Practice 103, 57–64.

Lèbre, E., Corder, G., Golev, A., 2017. The role of the mining industry in a circular economy: A framework for resource management at the mine site level. Journal of Industrial Ecology 21, 662–672.

Ma, H., Zhang, X., Li, S.E., Lin, Z., Lyu, Y., Zheng, S., 2021. Feasibility enhancement of constrained receding horizon control using generalized control barrier function. ArXiv arXiv:2102.13304.

Martin, T.E., McRoberts, E.C., 1999. Some considerations in the stability analysis of upstream tailings dams, in: Proceedings of the sixth international conference on tailings and mine waste, A.A Balkema Rotterdam, Rotterdam, Netherlands. pp. 287–302.

Marín, O.A., Kraslawski, A., Cisternas, L.A., 2022. Estimating processing cost for the recovery of valuable elements from mine tailings using dimensional analysis. Minerals Engineering 184, 107629.

Mazyavkina, N., Sviridov, S., Ivanov, S., Burnaev, E., 2021. Reinforcement learning for combinatorial optimization: A survey. Computers & Operations Research 134, 105400.

McCarthy, T.S., 2014. The impact of acid mine drainage in South Africa. South African Journal of Science 107, 7.

Meyer, E.J., Olivier, M.C., Matumba, L., Craig, I.K., 2019. Model predictive control and simulation, implementation and performance assessment of a coal comminution circuit. Minerals Engineering 144, 1–14.

Michaelides, E., Crowe, C.T., Schwarzkopf, J.D. (Eds.), 2016. Multiphase Flow Handbook. 2 ed., Taylor & Francis.

Mohammad Nezhad, A., Mahlooji, H., 2011. A revised particle swarm optimization based discrete lagrange multipliers method for nonlinear programming problems. Computers & Operations Research 38, 1164–1174.

Moskalyk, R.R., Alfantazi, A.M., 2002. Nickel sulphide smelting and electrorefining practice: A review. Mineral Processing and Extractive Metallurgy Review 23, 141–180.

Muir, D.M., Ho, E., 2006. Process review and electrochemistry of nickel sulphides and nickel mattes in acidic sulphate and chloride media. Mineral Processing and Extractive Metallurgy 115, 57–65.

Murad, S.A., 2017. Environment, social, and governance (ESG) criteria and preferences of managers. Cogent Busness & Management 4, 1340820.

Nemhauser, G.L., Wolsey, L.A., 1999. Integer and Combinatorial Optimization. John Wiley & Sons, New York, NY.

Ntengwe, F., Witika, L.K., 2011. Optimization of the operating density and particle size distribution of the cyclone overflow to enhance the recovery of flotation of copper sulphide and oxide minerals. Journal of the South African Institute of Mining and Metallurgy 111, 295–300.

Olivier, L.E., Craig, I.K., 2015. Development and application of a model-plant mismatch expression for linear time-invariant systems. Journal of Process Control 32, 77–86.

Ortega, R., Van Der Schaft, A., Mareels, I., Maschke, B., 2001. Putting energy back in control. IEEE Control Systems Magazine 21, 18–33.

Park, I., Tabelin, C.B., Jeon, S., Li, X., Seno, K., Ito, M., Hiroyoshi, N., 2019. A review of recent strategies for acid mine drainage prevention and mine tailings recycling. Chemosphere 219, 588–606.

Proakis, J.G., Manolakis, D.K., 2007. Digital signal processing: Principles, algorithms, and applications. 4 ed., Prentice-Hall.

Qin, S.J., Badgwell, T.A., 2003. A survey of industrial model predictive control technology. Control Engineering Practice 11, 733–764.

Rahmaniani, R., Crainic, T. J. Gendreau, M., Rei, W., 2017. The benders decomposition algorithm: A literature review. European Journal of Operational Research 259, 801–817.

Ramos-Figueroa, O., Quiroz-Castellanos, M., Mezura-Montes, E., Schütze, O., 2020. Metaheuristics to solve grouping problems: A review and a case study. Swarm and Evolutionary Computation 53, 100643.

Reyes-Lúa, A., Backi, C.J., Skogestad, S., 2018. Improved PI control for a surge tank satisfying level constraints. IFAC-PapersOnLine 54, 835–840.

Roche, C., Thygesen, K., Baker, E., 2017. Mine tailings storage: Safety is no accident. UN Environment, GRID-Arendal .

Rockwell Automation, Inc., 2024. Programmable controllers | allen-bradley. URL: https://www.rockwellautomation.com/en-us/products/hardware/allen-bradley/programmable-controllers.html. accessed on February 04 2024.

Rokebrand, L.L., 2022. Towards an access economy model for industrial process control. Masters of Engineering. University of Pretoria. South Africa. Department of Electrical, Electronic and Computer Engineering.

Rokebrand, L.L., Burchell, J.J., Olivier, L.E., Craig, I.K., 2020. Competing advanced process control via an industrial automation cloud platform. ArXiv arXiv:2011.13184.

Rokebrand, L.L., Burchell, J.J., Olivier, L.E., Craig, I.K., 2021. Towards an access economy model for industrial process control: A bulk tailings treatment plant case study. IFAC-PapersOnLine 54, 121–126.

Rosander, P., Isaksson, A.J., Löfberg, J., Forsman, K., 2011. Robust averaging level control. Technical report from the department of Automatic Control. Linköpings Universitet. Department of Electrical Engineering, Linköpings Universitet, Linköping, Sweden. Submitted to AIChE Annual Meeting 2011.

Rosander, P., Isaksson, A.J., Löfberg, J., Forsman, K., 2012. Practical control of surge tanks suffering from frequent inlet flow upsets. IFAC Proceedings Volumes 45, 258–263.

Rosenqvist, T., 2004. Principles of Extractive Metallurgy. 2 ed., Tapir Academic Press, Trondheim, Norway.

Rugenstein, E.K., Kupferschmid, M., 2004. Active set strategies in an ellipsoid algorithm for nonlinear programming. Computers & Operations Research 31, 941–962.

Russell, A., 2020. Online spiral grade control. Journal of the Southern African Institute of Mining and Metallurgy 120, 113 – 119.

Sanchis, R., Romero, J.A., Martin, J.M., 2011. A new approach to averaging level control. Control Engineering Practice 19, 1037–1043.

Santamarina, J.C., Torres-Cruz, L.A., Bachus, R.C., 2019. Why coal ash and tailings dam disasters occur: Knowledge gaps and management shortcomings contribute to catastrophic dam failures. Science 364, 526–528.

Sbarbaro, D., Ortega, R., 2007. Averaging level control: An approach based on mass balance. Journal of Process Control 17, 621–629.

Schewefel, H.P., 1995. Evolution and Optimum Seeking. Wiley.

Sepúlveda, G.F., Álvarez, P.J., Bedoya, J.B., 2020. Stochastic optimization in mine planning scheduling. Computers & Operations Research 115, 104823.

Singh, V., Biswas, A., Tripathy, S.K., Chatterjee, S., Charkerborthy, T.K., 2016. Smart ore blending methodology for ferromanganese production process. Ironmaking and Steelmaking 43, 481–487.

Skogestad, S., 2004. Control structure design for complete chemical plants. Computers & Chemical Engineering 28, 219–234.

Skogestad, S., Postlethwaite, I., 2005. Multivariable feedback control: Analysis and design. 2nd ed., Wiley-Interscience.

Thyse, E., Akdogan, G., Eksteen, J.J., 2011. The effect of changes in iron-endpoint during Peirce-Smith converting on PGE-containing nickel converter matte mineralization. Minerals Engineering 24, 688–697.

Umadevi, T., Kumar, A., Umashanker, A., Sah, R., Marutiram, K., 2021. Performance evaluation of a laboratory floatex density separator and its comparison with a spiral concentrator. Mineral Processing and Extractive Metallurgy 130, 118–125.

Vanderbei, R.J., 2014. Linear programming: Foundations and extensions. 4 ed., Springer, New York, NY.

Vatankhah, B., Farrokhi, M., 2017. Nonlinear model-predictive control with disturbance rejection property using adaptive neural networks. Journal of the Franklin Institute 354, 5201–5220.

Vinel, A., Krokhmal, P.A., 2017. Mixed integer programming with a class of nonlinear convex constraints. Discrete Optimization 24, 66–86.

Wang, C., Harbottle, D., Liu, Q., Xu, Z., 2014. Current state of fine mineral tailings treatment: A critical review on theory and practice. Minerals Engineering 58, 113–131.

Wätcher, A., Biegler, L.T., 2006. On the implementation of a primal-dual interior point filter line search algorithm for large-scale nonlinear programming. Mathematical Programming 106, 25–57.

Wiid, A.J., le Roux, J.D., Craig, I.K., 2021. Pressure buffering control to reduce pollution and improve flow stability in industrial gas headers. Control Engineering Practice 115, 104904.

Wilcox, R.R., 2003. Applying Contemporary Statistical Techniques. Academic Press, San Diego, California.

Xu, D.M., Zhan, C.L., Liu, H.X., Lin, H.Z., 2019. A critical review of environmental implications, recycling strategies, and ecological remediation for mine tailings. Environmental Science and Pollution Research 27, 35657–35669.

Yang, C., Gui, W., Kong, L., Wang, Y., 2009. Modeling and optimal-setting control of blending process in a metallurgical industry. Computers & Chemical Engineering 33, 1289–1297.

Zeng, X., Zhang, X., Zhang, Z., Liu, Y., Wang, C., 2021. A review of sustainable technologies for the management of mine tailings. Journal of Cleaner Production 286, 125363.

Zheng, J., Zhong, J., Chen, M., He, K., 2023. A reinforced hybrid genetic algorithm for the traveling salesman problem. Computers & Operations Research 157, 106249.